

BIOACTIVE COMPOUNDS FROM *DIOSPYROS GRACILIS* STEM



A Thesis Submitted in Partial Fulfillment of the Requirements  
for the Degree of Master of Science in Pharmaceutical Sciences and Technology

Faculty of Pharmaceutical Sciences

Chulalongkorn University

Academic Year 2023

สารที่มีฤทธิ์ทางชีวภาพจากลำต้นมะเกลือกา



วิทยานิพนธ์นี้เป็นส่วนหนึ่งของการศึกษาตามหลักสูตรปริญญาวิทยาศาสตรมหาบัณฑิต  
สาขาวิชาเภสัชศาสตร์และเทคโนโลยี  
คณะเภสัชศาสตร์ จุฬาลงกรณ์มหาวิทยาลัย  
ปีการศึกษา 2566



สมณัฐกิจ วุฒิกิจ : สารที่มีฤทธิ์ทางชีวภาพจากลำต้นมะเกลือกา. ( BIOACTIVE  
COMPOUNDS FROM *DIOSPYROS GRACILIS* STEM) อ.ที่ปรึกษาหลัก : ผศ. ภญ.ดร.  
วิชชุดา ธนกิจเจริญวัฒน์

ในการศึกษานี้สามารถแยกไตรเทอร์พีนอยด์หกชนิดจากลำต้นของมะเกลือกา (*Diospyros gracilis* H.R.Fletcher วงศ์ Ebenaceae) โดยประกอบด้วยไตรเทอร์พีนอยด์ประเภท friedelane 2 ชนิด คือ friedelin และ epifriedelanol และประเภท lupane 3 ชนิด คือ betulin, betulinic acid, และ betulinaldehyde การพิสูจน์โครงสร้างทางเคมีของสารเหล่านี้ทำโดยวิเคราะห์ข้อมูลทางสเปกโทรสโกปีของสาร (IR, NMR และ DART-TOF MS) ร่วมกับการเปรียบเทียบกับข้อมูลที่มีการรายงานไว้ก่อนหน้านี้ ในการศึกษาฤทธิ์เป็นพิษต่อเซลล์มะเร็งเฉพาะเลี้ยง สาร lupeol, betulin และ betulinic acid แสดงฤทธิ์เป็นพิษต่อเซลล์มะเร็งสมอง glioblastoma ชนิด U87 (ค่า  $IC_{50}$  เท่ากับ 13.16, 15.39 และ 8.31 ไมโครโมลาร์ ตามลำดับ) และเซลล์มะเร็งเต้านมชนิด MDA-MB231 (ค่า  $IC_{50}$  เท่ากับ 34.41, 74.49 และ 43.88 ไมโครโมลาร์ ตามลำดับ) นอกจากนี้พบว่าสาร lupeol กับ betulinic acid มีผลทำให้การสร้าง interleukin 2 โดย Jurkat T cells ซึ่งถูกกระตุ้นด้วย anti-CD3/anti-CD28 antibodies ลดลงที่ความเข้มข้นที่ไม่เป็นพิษต่อเซลล์ จึงมีความเป็นไปได้ว่าสารทั้งสองมีฤทธิ์ยับยั้งการกระตุ้นการทำงานของ T-cell ที่เกิดผ่านกลไกซึ่งเกี่ยวข้องกับ CD3 และ CD28

จุฬาลงกรณ์มหาวิทยาลัย  
CHULALONGKORN UNIVERSITY

สาขาวิชา	เภสัชศาสตร์และเทคโนโลยี	ลายมือชื่อนิสิต .....
ปีการศึกษา	2566	ลายมือชื่อ อ.ที่ปรึกษาหลัก .....





## ACKNOWLEDGEMENTS

I would like to express my deepest gratitude to my thesis advisor, Assistant Professor Witchuda Thanakijcharoenpath, Ph.D., for her wisdom, unwavering support, insightful suggestions, and constant encouragement during this research. Her unparalleled expertise, keen insights, and tireless dedication have greatly influenced my work, for which I am eternally grateful.

I would like to thank all the members of the thesis committee for their valuable suggestions and comments.

My sincere thanks also go to Dr. Nonthaneth Nalinratana, who kindly performed biological assays for this research work.

I would like to extend my heartfelt thanks to Dr. Nonthalert Lertnitikul for his generous assistance with the NMR Spectra. His tireless efforts have been a continual source of inspiration for me.

I am deeply thankful for the supply of plant material from Suan Luang Rama IX Royal Botanical Garden.

I am especially grateful for the members of the laboratory who have supported me throughout this research work.

Finally, I express my profound gratitude to my parents. Their ceaseless love is so meaningful, contributing to my success.

Somnatthakit Wuttikit

## TABLE OF CONTENTS

	Page
.....	iii
ABSTRACT (THAI).....	iii
.....	iv
ABSTRACT (ENGLISH).....	iv
ACKNOWLEDGEMENTS.....	v
TABLE OF CONTENTS.....	vi
LIST OF TABLES.....	viii
LIST OF FIGURES.....	x
LIST OF SCHEMES.....	xiii
LIST OF ABBREVIATIONS AND SYMBOLS.....	xiv
CHAPTER I.....	1
INTRODUCTION.....	1
CHAPTER II.....	7
HISTORICAL.....	7
1. Chemical Constituents of <i>Diospyros</i> Plants.....	7
2. Biological and Pharmacological Activities of <i>Diospyros</i> Plants.....	51
CHAPTER III.....	53
EXPERIMENTAL.....	53
1. Source of Plant Material.....	53
2. General Techniques.....	53
3. Extraction and Isolation.....	55

4. Physical and Spectral Data of Isolated Compounds .....	63
5. Determination of Biological Activities .....	66
CHAPTER IV .....	68
RESULTS AND DISCUSSION .....	68
1. Identification of Isolated Compounds .....	68
1.1 Compound DG01 (friedelin).....	68
1.2 Compound DG02 (epifriedelanol).....	74
1.3 Compound DG03 (lupeol).....	80
1.4 Compound DG04 (betulin).....	86
1.5 Compound DG05 (betulinic acid).....	92
1.6 Compound DG06 (betulinaldehyde).....	103
2. Biological Activities of Isolated Compounds .....	110
2.1 Cytotoxic Activity .....	110
2.2 Inhibitory Activity on T Cell Activation.....	112
CHAPTER V .....	115
CONCLUSION.....	115
REFERENCES .....	116
VITA.....	126

## LIST OF TABLES

	Page
<b>Table 1.</b> Distribution of naphthoquinones and naphthalene derivatives in the genus <i>Diospyros</i> .....	9
<b>Table 2.</b> Distribution of triterpenoids in the genus <i>Diospyros</i> .....	31
<b>Table 3.</b> Biological and pharmacological activities of extracts from <i>Diospyros</i> species .....	52
<b>Table 4.</b> Combined fractions from the EtOAc extract.....	57
<b>Table 5.</b> Combined fractions from E6.....	58
<b>Table 6.</b> Combined fractions from E6A.....	58
<b>Table 7.</b> Combined fractions from E11.....	60
<b>Table 8.</b> Combined fractions from E4.....	60
<b>Table 9.</b> Combined fractions from E5.....	61
<b>Table 10.</b> Combined fractions from E(4C5B).....	61
<b>Table 11.</b> <sup>1</sup> H (400 MHz) and <sup>13</sup> C (100 MHz) NMR assignments of compound DG01 and friedelin (in CDCl <sub>3</sub> ).....	70
<b>Table 12.</b> <sup>1</sup> H (400 MHz) and <sup>13</sup> C (100 MHz) NMR assignments of compound DG02 and epifriedelanol (in CDCl <sub>3</sub> ) .....	76
<b>Table 13.</b> <sup>1</sup> H (400 MHz) and <sup>13</sup> C (100 MHz) NMR assignments of compound DG03 and lupeol (in CDCl <sub>3</sub> ).....	82
<b>Table 14.</b> <sup>1</sup> H (400 MHz) and <sup>13</sup> C (100 MHz) NMR assignments of compound DG04 and betulin (in CDCl <sub>3</sub> ).....	88
<b>Table 15.</b> <sup>1</sup> H (400 MHz) and <sup>13</sup> C (100 MHz) NMR assignments of compound DG05 and betulinic acid (in CDCl <sub>3</sub> ).....	94

<b>Table 16.</b> $^1\text{H}$ (400 MHz) and $^{13}\text{C}$ (100 MHz) NMR assignments of compound DG06 and betulinaldehyde (in $\text{CDCl}_3$ ).....	105
<b>Table 17.</b> Cytotoxic activity of compounds DG01-DG05 .....	112



## LIST OF FIGURES

	Page
Figure 1. <i>Diospyros gracilis</i> H.R.Fletcher.....	6
Figure 2. IR spectrum of compound DG01.....	71
Figure 3a. <sup>1</sup> H NMR (400 MHz) spectrum of compound DG01 (in CDCl <sub>3</sub> ) .....	72
Figure 3b. <sup>1</sup> H NMR (400 MHz) spectrum of compound DG01 (in CDCl <sub>3</sub> ) (expanded). .....	72
Figure 4a. <sup>13</sup> C NMR (100 MHz) spectrum of compound DG01 (in CDCl <sub>3</sub> ) .....	73
Figure 4b. <sup>13</sup> C NMR (100 MHz) spectrum of compound DG01 (in CDCl <sub>3</sub> ) (expanded). .....	73
Figure 5. DART-TOF Mass spectrum of compound DG01.....	74
Figure 6. IR spectrum of compound DG02.....	77
Figure 7a. <sup>1</sup> H NMR (400 MHz) spectrum of compound DG02 (in CDCl <sub>3</sub> ) .....	78
Figure 7b. <sup>1</sup> H NMR (400 MHz) spectrum of compound DG02 (in CDCl <sub>3</sub> ) (expanded). .....	78
Figure 8a. <sup>13</sup> C NMR (100 MHz) spectrum of compound DG02 (in CDCl <sub>3</sub> ).....	79
Figure 8b. <sup>13</sup> C NMR (100 MHz) spectrum of compound DG02 (in CDCl <sub>3</sub> ) (expanded). .....	79
Figure 9. DART-TOF Mass spectrum of compound DG02.....	80
Figure 10. IR spectrum of compound DG03.....	83
Figure 11a. <sup>1</sup> H NMR (400 MHz) spectrum of compound DG03 (in CDCl <sub>3</sub> ) .....	84

<b>Figure 11b.</b> $^1\text{H}$ NMR (400 MHz) spectrum of compound DG03 (in $\text{CDCl}_3$ ) (expanded). .....	84
<b>Figure 12a.</b> $^{13}\text{C}$ NMR (100 MHz) spectrum of compound DG03 (in $\text{CDCl}_3$ ) .....	85
<b>Figure 12b.</b> $^{13}\text{C}$ NMR (100 MHz) spectrum of compound DG03 (in $\text{CDCl}_3$ ) (expanded). .....	85
<b>Figure 13.</b> DART-TOF Mass spectrum of compound DG03.....	86
<b>Figure 14.</b> IR spectrum of compound DG04.....	89
<b>Figure 15a.</b> $^1\text{H}$ NMR (400 MHz) spectrum of compound DG04 (in $\text{CDCl}_3$ ).....	90
<b>Figure 15b.</b> $^1\text{H}$ NMR (400 MHz) spectrum of compound DG04 (in $\text{CDCl}_3$ ) (expanded). .....	90
<b>Figure 16a.</b> $^{13}\text{C}$ NMR (100 MHz) spectrum of compound DG04 (in $\text{CDCl}_3$ ) .....	91
<b>Figure 16b.</b> $^{13}\text{C}$ NMR (100 MHz) spectrum of compound DG04 (in $\text{CDCl}_3$ ) (expanded). .....	91
<b>Figure 17.</b> DART-TOF Mass spectrum of compound DG04.....	92
<b>Figure 18.</b> HMBC and NOESY Correlations of DG05.....	96
<b>Figure 19.</b> IR spectrum of compound DG05.....	96
<b>Figure 20a.</b> $^1\text{H}$ NMR (400 MHz) spectrum of compound DG05 (in $\text{CDCl}_3$ ).....	97
<b>Figure 20b.</b> $^1\text{H}$ NMR (400 MHz) spectrum of compound DG05 (in $\text{CDCl}_3$ ) (expanded). .....	97
<b>Figure 21.</b> $^1\text{H}$ - $^1\text{H}$ NOESY spectrum of compound DG05.....	98
<b>Figure 22a.</b> $^{13}\text{C}$ NMR (100 MHz) spectrum of compound DG05 (in $\text{CDCl}_3$ ).....	99
<b>Figure 22b.</b> $^{13}\text{C}$ NMR (100 MHz) spectrum of compound DG05 (in $\text{CDCl}_3$ ) (expanded). .....	99



<b>Figure 23.</b> HSQC spectrum of compound DG05.....	100
<b>Figure 24a.</b> HMBC spectrum of compound DG05.....	101
<b>Figure 24b.</b> HMBC spectrum of compound DG05 (expanded).....	102
<b>Figure 24c.</b> HMBC spectrum of compound DG05 (expanded).....	102
<b>Figure 25.</b> DART-TOF Mass spectrum of compound DG05.....	103
<b>Figure 26.</b> IR spectrum of compound DG06.....	106
<b>Figure 27a.</b> $^1\text{H}$ NMR (400 MHz) spectrum of compound DG06 (in $\text{CDCl}_3$ ).....	107
<b>Figure 27b.</b> $^1\text{H}$ NMR (400 MHz) spectrum of compound DG06 (in $\text{CDCl}_3$ ) (expanded). .....	107
<b>Figure 28a.</b> $^{13}\text{C}$ NMR (100 MHz) spectrum of compound DG06 (in $\text{CDCl}_3$ ).....	108
<b>Figure 28b.</b> $^{13}\text{C}$ NMR (100 MHz) spectrum of compound DG06 (in $\text{CDCl}_3$ ) (expanded). .....	108
<b>Figure 29.</b> Cytotoxicity of tested compounds on glioblastoma U87 cells.....	110
<b>Figure 30.</b> Cytotoxicity of tested compounds on breast cancer MDA-MB231 cells... จุฬาลงกรณ์มหาวิทยาลัย CHULALONGKORN UNIVERSITY	111
<b>Figure 31.</b> Cytotoxicity of tested compounds on normal endothelial EA.hy926 cells.. .....	111
<b>Figure 32.</b> Cytotoxicity of tested compounds on Jurkat T cells.....	113
<b>Figure 33.</b> Effects of tested compounds on Jurkat T cells stimulated with anti- CD3/CD28 antibodies.....	114

## LIST OF SCHEMES

	<i>Page</i>
Scheme 1. Extraction of <i>D. gracilis</i> stem .....	56
Scheme 2. Isolation of the EtOAc extract .....	63



## LIST OF ABBREVIATIONS AND SYMBOLS

$\alpha$	=	Alpha
$\beta$	=	Beta
<i>br d</i>	=	Broad doublet (for NMR spectra)
<i>br s</i>	=	Broad singlet (for NMR spectra)
BuOH	=	Butanol
°C	=	Degree celsius
CC	=	Column chromatography
CD	=	Cluster of differentiation
CDCl <sub>3</sub>	=	Deuterated chloroform
CH <sub>2</sub> Cl <sub>2</sub>	=	Dichloromethane
cm	=	Centimeter
cm <sup>-1</sup>	=	Reciprocal centimeter (unit of wave number)
<sup>13</sup> C NMR	=	Carbon-13 nuclear magnetic resonance
2D NMR	=	Two-dimensional nuclear magnetic resonance
DART	=	Direct analysis in real time
<i>d</i>	=	Doublet (for NMR spectra)
<i>dd</i>	=	Doublet of doublets (for NMR spectra)
<i>ddd</i>	=	Doublet of doublets of doublets (for NMR spectra)
DMSO	=	Dimethylsulfoxide
$\delta$	=	Chemical shift (in part per million unit)
EtOAc	=	Ethyl acetate
g	=	Gram
HMBC	=	Heteronuclear multiple bond Correlation
<sup>1</sup> H NMR	=	Proton nuclear magnetic resonance
HSQC	=	Heteronuclear single quantum coherence
Hz	=	Hertz

IC <sub>50</sub>	=	Half maximal inhibitory concentration
IL	=	Interleukin
IR	=	Infrared spectroscopy
<i>J</i>	=	Coupling constant
Kg	=	Kilogram
L	=	Liter
<i>m</i>	=	Multiplet (for NMR spectra)
MeOH	=	Methanol
mg	=	Milligram
mL	=	Milliliter
μL	=	Microliter
μM	=	Micromolar
MS	=	Mass spectroscopy
MW	=	Molecular weight
<i>m/z</i>	=	Mass to charge ratio
nm	=	Nanometer
NMR	=	Nuclear magnetic resonance spectroscopy
NOESY	=	Nuclear overhauser effect spectroscopy
<b>v</b> <sub>max</sub>	=	Wave number at maximal absorption
ppm	=	Part per million
<i>q</i>	=	Quartet (for NMR spectra)
<i>s</i>	=	Singlet (for NMR spectra)
TLC	=	Thin layer chromatography
TOF	=	Time of flight
UV	=	Ultraviolet

## CHAPTER I

### INTRODUCTION

The *Diospyros* genus is the largest genus in the Ebenaceae family, comprising over 700 species. Most are distributed in the tropics, while only a few extend into the subtropics (Phengklai, 1981; POWO, 2023). These plants are trees or shrubs, which are dioecious, occasionally monoecious, or polygamous, and mostly unarmed. All parts of the plants often turn black when dry. The leaves are distichous, mostly reflexed and penninerved. The inflorescences are cymose or fasciculate, and axillary or ramiflorous, (rarely cauliflorous); solitary flowers can be found. The flowers are actinomorphic. The calyx is more or less deeply lobed, persistent and usually accrescent in fruit; lobes are valvate or imbricate in bud. The corolla is gamopetalous and caducous; its segments appear twisted in the bud. The androecium consists of 6 to many stamens, which can be free or paired, on the base of the corolla tube, or in bundles on the receptacle. The anthers are basifixed and bilocular, dehiscing longitudinally. Male flowers typically contain a rudimentary ovary. Staminodes are commonly present in female flowers. The ovary is superior. The number of styles ranges from one to five. The fruits are indehiscent and can be fleshy, dry, or woody, containing 1 to many seeds. The endosperm can be ruminant or smooth (Phengklai, 1981).

*Diospyros* species found in Thailand include the following: (Pooma and Suddee, 2014; POWO, 2023)

1. *D. andamanica* (Kurz) Bakh.; พลับอันดา (phlap anda)
2. *D. apiculata* Hiern; มะพลับไชนก (ma phlap khai nok)
3. *D. areolata* King & Gamble; มะพลับ (ma phlap)
4. *D. bambuseti* H.R.Fletcher; มะเกลืออรัญญ (ma kluea aran)
5. *D. bejaudii* Lecomte; พลับดง (phlap dong)

6. *D. blancoi* A.DC.; มะริด (ma rit)
7. *D. borneensis* Hiern; ขี้หนู (khi nu)
8. *D. brandisiana* Kurz; ดำ (dam)
9. *D. buxifolia* (Blume) Hiern; สั่งท่า (sang tham)
10. *D. castanea* (Craib) H.R.Fletcher; ตะโกพนม (tako phanom)
11. *D. cauliflora* Blume; เห้าแสนปม (thao saen pom)
12. *D. coetanea* H.R.Fletcher; ลำตากวาย (lam ta khwai)
13. *D. collinsiae* Craib; พลับยอดดำ (phlap yot dam)
14. *D. confertiflora* (Hiern) Bakh.; ลูกห้วนก (luk hua nok)
15. *D. curranii* Merr.; รั๊กดำ (rak dam)
16. *D. dasyphylla* Kurz; จันเข่า (chan khao)
17. *D. decandra* Lour.; จัน (chan)
18. *D. defectrix* H.R.Fletcher; พญารากดำ (phaya rak dam)
19. *D. dictyoneura* Hiern; ดงน้ำ (dong nam)
20. *D. diepenhorstii* Miq.; เนียน (nian)
21. *D. dumetorum* W.W.Sm.; มะเกลืออ่อน (ma kluea noi)
22. *D. dussaudii* Lecomte
23. *D. ehretioides* Wall. ex G.Don; ตับเต่าตัน (tap tao ton)
24. *D. ferrea* (Willd.) Bakh.; ลำบิต (lam bit)
25. *D. filipendula* Pierre ex Lecomte; ลำบิตดง (lam bit dong)
26. *D. frutescens* Blume; พลับกล้วย (phlap kluai)
27. *D. fulvopilosa* H.R.Fletcher; เนียน (nian)
28. *D. glandulosa* Lace; กล้วยฤๅษี (kluai ruesi)
29. *D. gracilis* H.R.Fletcher; มะเกลือกา (ma kluea ka)
30. *D. hasseltii* Zoll.; ตะโกจัน (tako chan)
31. *D. insidiosa* Bakh.; จันเข่า (chan khao)
32. *D. kaki* Thunb.; พลับจีน (phlap chin)
33. *D. kerrii* Craib; มะพลับดง (ma phlap dong)

34. *D. kurzii* Hiern; พลับม่าน (phlap man)
35. *D. lanceifolia* Roxb.; พลับหัวแข็ง (phlap hua khaeng)
36. *D. latisepala* Ridl.; เทพพนม (thep phanom)
37. *D. littorea* (R.Br.) Kosterm.; ชี้นู (khi nu)
38. *D. longipilosa* Phengklai; มะพลับขน (ma phlap khon)
39. *D. malabarica* (Desr.) Kostel.; ตะโกสวน (tako suan)
40. *D. martabanica* C.B.Clarke; พลับไข่เต่า (phlap khai tao)
41. *D. mollis* Griff.; มะเกลือ (ma kluea)
42. *D. montana* Roxb.; ตานดำ (tan dam)
43. *D. oblonga* Wall. ex G.Don; โม่รี (mori)
44. *D. pendula* Hasselt ex Hassk.; อินป่า (in pa)
45. *D. phengklaii* Duangjai, Sinbumr. & Suddee; มะพลับเฟ็งคล้าย (ma phlap pheng klai)
46. *D. phuketensis* Phengklai; พลับภูเก็ต (phlap phuket)
47. *D. phuwuaensis* Duangjai, Rueangr. & Suddee; มะพลับภูวูว (ma phlap phu wua)
48. *D. pilosiuscula* G.Don; หางหนู (hang nu)
49. *D. pyrrhocarpa* Miq.; เนียน (nian)
50. *D. ranongensis* Phengklai; พลับระนอง (phlap ranong)
51. *D. rhodocalyx* Kurz; ตะโกนา (tako na)
52. *D. savannarum* Kosterm.
53. *D. scalariformis* H.R.Fletcher; พลับทองขาว (phlap thong khao)
54. *D. schmidtii* Craib
55. *D. scortechinii* King & Gamble; ไข่นก (khai nok)
56. *D. sumatrana* Miq.; ลักเคยลักเกลือ (lak khoei lak kluea)
57. *D. thaiensis* Phengklai; มะพลับเล็บนาง (ma phlap lep nang)
58. *D. toposia* Buch.-Ham.; ข้าวเม่าเหล็ก (khao mao lek)
59. *D. transitoria* Bakh.; มะพลับทอง (ma phlap thong)
60. *D. trianthos* Phengklai; สามเกลอ (sam kloe)
61. *D. truncata* Zoll. & Moritzi; พลับน้อย (phlap noi)

62. *D. undulata* Wall. ex G.Don; พลับเขา (phlap khao)
63. *D. variegata* Kurz; พญารากดำ (phaya rak dam)
64. *D. venosa* Wall. ex A.DC.; จันทำ (chan dam)
65. *D. wallichii* King & Gamble; ตำตะโก (dam tako)
66. *D. winitii* H.R.Fletcher; มะพลับเจ้าคุณ (ma phlap chao khun)

Several *Diospyros* species have commercial importance and economic value. For instance, *D. kaki*, commonly known as persimmon, is highly popular in Asia due to its delicious ripe fruit. Additionally, Ceylon ebony (*D. ebenum*) and East Indian ebony (*D. melanoxylon*) are utilized in construction work (Rauf *et al.*, 2017). Ma klue (*D. mollis*) and Chan (*D. decandra*) are *Diospyros* species in Thailand which have been ethnomedicinally used as an anthelmintic and emmenagogue, respectively (Utsunomiya *et al.*, 1998). *Diospyros* plants have diverse uses in folk medicine and contain interesting chemical constituents.

The major compounds found in the genus *Diospyros* are triterpenoids and naphthoquinones which have been shown to possess various biological activities, such as cytotoxic, anti-inflammatory and immunomodulating activities. Several triterpenoids have been reported for their interesting antitumor and anti-inflammatory effects. One of the remarkable compounds is betulinic acid, which has been extensively studied for its potential in anticancer drug development (Jiang *et al.*, 2021). Examples of triterpenoids with anti-inflammatory property include lupeol, ursolic acid and oleanolic acid (Dzubak *et al.*, 2006). A number of naphthoquinones were found to exhibit cytotoxic and anti-inflammatory activities, for example,  $\beta$ -lapachone and plumbagin with cytotoxic activity and shikonin with anti-inflammatory activity (Aminin and Polonik, 2020; Rahman *et al.*, 2022). Plumbagin were also found to exert an immunosuppressive effect on human T-cell acute lymphoblastic leukemia MOLT-4 cells (Bae *et al.*, 2016).



*Diospyros gracilis* H.R.Fletcher, commonly known as "Ma kluea ka " or "Ka cha" in Thai, is an evergreen tree that can grow up to 5 meters tall. The leaves are lanceolate or oblong-lanceolate, 3-10 cm long and 1-3 cm wide, glabrous on both sides, with 8-10 pairs of secondary veins. The leaf base is cuneate, and the leaf apex is acuminate with bult tip. The flowers are unisexual. Male flowers are 4-merous, borne in a cymose inflorescence, and have broadly campanulate calyx, 2-3 mm long, urn-shaped corolla, 5-7 mm long, and 14-18 stamens with glabrous anthers. Female flowers are solitary, 4-merous, larger than the male flowers, and have two styles and a globose, 4-loculate ovary covered with coarse hairs. The fruit is a globose berry with a persistent calyx, 1.5-2 by 2-2.5 cm. The seeds have smooth endosperm (Phengkjai, 1981).

*D. gracilis* is distributed throughout central Thailand and its fruits are utilized for dyeing net and clothes. Its wood is used in various woodworking applications (Phengkjai, 1981). This plant is a native species in Thailand that has never been previously studied on phytochemicals and bioactivity. The objective of this research is to isolate and identify chemical constituents from the stem of *D. gracilis*, and to examine the bioactivity of isolated compounds. The plant may serve as a potential source of compounds with interesting bioactivities, which could lead to further investigations for drug development.



A.



B.



C.



D.

Figure 1. *Diospyros gracilis* H.R.Fletcher

A. Tree    B. Leaves    C. Pollinated flowers    D. Fruits

## CHAPTER II

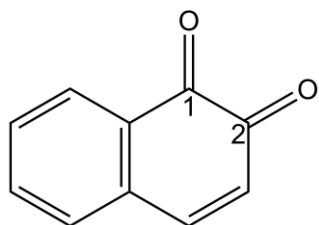
### HISTORICAL

#### 1. Chemical Constituents of *Diospyros* Plants

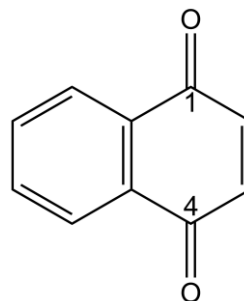
A variety of *Diospyros* species have been extensively studied for their phytochemical composition, revealing a diverse array of compounds. Chemical constituents found in *Diospyros* plants are naphthoquinones, naphthalene derivatives, triterpenoids, steroids, flavonoids, coumarins, tannins, and others. Notably, naphthoquinones and triterpenoids are widely distributed and considered as major components within the *Diospyros* genus.

##### 1.1 Naphthoquinones

The *Diospyros* genus is an abundant reservoir of 1,4-naphthoquinones, in contrast to a minimal presence of 1,2-naphthoquinones. This prominence of 1,4-naphthoquinones can serve as a chemotaxonomic identifier for this genus. 1,4-Naphthoquinones found in *Diospyros* plants exist as monomeric or oligomeric structures. Most of them are derivatives of plumbagin and 7-methyljuglone. The oligomers are formed by the combination of individual units, and can exist as dimers, trimers, or tetramers. These quinones exhibit various pharmacological activities, including antioxidant, antimicrobial, anti-inflammatory, and anticancer. In contrast, 1,2-naphthoquinones are not prevalent in *Diospyros* plants as compared to their 1,4-naphthoquinone counterparts. However, they still contribute to the overall chemical diversity within the genus and may possess interesting biological activities. The occurrence of naphthoquinones and naphthalene derivatives in *Diospyros* plants, reported in the literature from the year 2012 to present, is shown in **Table 1**.



1,2-naphthoquinone



1,4-naphthoquinone



จุฬาลงกรณ์มหาวิทยาลัย  
CHULALONGKORN UNIVERSITY

**Table 1.** Distribution of naphthoquinones and naphthalene derivatives in the genus *Diospyros*

Compounds	Species	References	
1. Naphthoquinones			
plumbagin (1)	<i>D. anisandra</i>	Uc-Cachón <i>et al.</i> , 2014	
	<i>D. bipindensis</i>	Cesari <i>et al.</i> , 2013	
	<i>D. canaliculata</i>	Lenta <i>et al.</i> , 2015	
	<i>D. ehretioides</i>	Wosawat <i>et al.</i> , 2021	
	<i>D. gracilipes</i>	Rasamison <i>et al.</i> , 2016	
	<i>D. lotus</i>	Rauf <i>et al.</i> , 2015, 2020	
	<i>D. maritima</i>	Higa <i>et al.</i> , 2017	
	<i>D. oocarpa</i>	Dev and Rajarajeshwari, 2013	
	<i>D. shimbaensis</i>	Aronsson <i>et al.</i> , 2016	
	<i>D. undulata</i>	Suchaichit <i>et al.</i> , 2018, 2021	
	3-methylplumbagin (2)	<i>D. maritima</i>	Higa <i>et al.</i> , 2017
	3-(2-hydroxyethyl) plumbagin (3)	<i>D. maritima</i>	Higa <i>et al.</i> , 2017
3-bromoplumbagin (4)	<i>D. maritima</i>	Higa <i>et al.</i> , 2017	
3-chloroplumbagin (5)	<i>D. maritima</i>	Higa <i>et al.</i> , 2017	
droserone (6)	<i>D. anisandra</i>	Uc-Cachón <i>et al.</i> , 2014	
	<i>D. maritima</i>	Higa <i>et al.</i> , 2017	
6-(1-ethoxyethyl) plumbagin (7)	<i>D. maritima</i>	Higa <i>et al.</i> , 2017	
3-(5-oxohexyl) plumbagin (8)	<i>D. undulata</i>	Suchaichit <i>et al.</i> , 2021	
5-methoxy-2-methyl-1,4-naphthoquinone (9)	<i>D. burmanica</i>	Mori-Yasumoto <i>et al.</i> , 2012	
5,8-dimethoxy-2-methyl-1,4-naphthoquinone (10)	<i>D. burmanica</i>	Mori-Yasumoto <i>et al.</i> , 2012	
3-hydroxy-5-methoxy-2-methyl-1,4-naphthoquinone (11)	<i>D. burmanica</i>	Mori-Yasumoto <i>et al.</i> , 2012	
2-hydroxymethyl-5-methoxy-1,4-naphthoquinone (12)	<i>D. undulata</i>	Suchaichit <i>et al.</i> , 2018	

**Table 1.** Distribution of naphthoquinones and naphthalene derivatives in the genus *Diospyros* (continued)

Compounds	Species	.
7-methyljuglone (13)	<i>D. lotus</i>	Uddin <i>et al.</i> , 2014
	<i>D. maritima</i>	Higa <i>et al.</i> , 2017
3-methoxy-7-methyljuglone (14)	<i>D. zenkeri</i>	Feusso <i>et al.</i> , 2019
$\beta$ -dihydroplumbagin (15)	<i>D. maritima</i>	Higa <i>et al.</i> , 2017
7-methyl- $\beta$ -dihydrojuglone (16)	<i>D. maritima</i>	Higa <i>et al.</i> , 2017
2,3-epoxyplumbagin (17)	<i>D. maritima</i>	Higa <i>et al.</i> , 2017
2,3-epoxy-7-methyljuglone (18)	<i>D. maritima</i>	Higa <i>et al.</i> , 2017
7-hydroxy-8-methoxy-2-methyl-1,4-naphthoquinone (19)	<i>D. burmanica</i>	Mori-Yasumoto <i>et al.</i> , 2012
canaliculatin (20)	<i>D. bipindensis</i>	Cesari <i>et al.</i> , 2013
	<i>D. canaliculata</i>	Lenta <i>et al.</i> , 2015
canaliculin (21)	<i>D. canaliculata</i>	Lenta <i>et al.</i> , 2015
ismailin (22)	<i>D. bipindensis</i>	Cesari <i>et al.</i> , 2013
	<i>D. canaliculata</i>	Lenta <i>et al.</i> , 2015
makluoside B (23)	<i>D. mollis</i>	Suwama <i>et al.</i> , 2018
3,3'-biplumbagin (24)	<i>D. anisandra</i>	Uc-Cachón <i>et al.</i> , 2014
	<i>D. ehretioides</i>	Wosawat <i>et al.</i> , 2021
	<i>D. maritima</i>	Higa <i>et al.</i> , 2017
	<i>D. shimbaensis</i>	Aronsson <i>et al.</i> , 2016
	<i>D. undulata</i>	Suchaichit <i>et al.</i> , 2018, 2021
7,7'-biplumbagin (25)	<i>D. undulata</i>	Suchaichit <i>et al.</i> , 2018, 2021
burmanin A (26)	<i>D. burmanica</i>	Mori-Yasumoto <i>et al.</i> , 2012
burmanin B (27)	<i>D. burmanica</i>	Mori-Yasumoto <i>et al.</i> , 2012
burmanin C (28)	<i>D. burmanica</i>	Mori-Yasumoto <i>et al.</i> , 2012
chitranone (29)	<i>D. anisandra</i>	Uc-Cachón <i>et al.</i> , 2014
	<i>D. maritima</i>	Higa <i>et al.</i> , 2017
2,7'-dimethyl-2',3-bijuglone (30)	<i>D. maritima</i>	Higa <i>et al.</i> , 2017

**Table 1.** Distribution of naphthoquinones and naphthalene derivatives in the genus *Diospyros* (continued)

Compounds	Species	Reference
2,7'-dimethyl-3,3'-bijuglone (31)	<i>D. maritima</i>	Higa <i>et al.</i> , 2017
mamegakinone (32)	<i>D. maritima</i>	Higa <i>et al.</i> , 2017
di-naphthodiospyrol A (33)	<i>D. lotus</i>	Aljohny <i>et al.</i> , 2021; Bawazeer and Rauf, 2021
di-naphthodiospyrol B (34)	<i>D. lotus</i>	Aljohny <i>et al.</i> , 2021; Bawazeer and Rauf, 2021
di-naphthodiospyrol C (35)	<i>D. lotus</i>	Aljohny <i>et al.</i> , 2021; Bawazeer and Rauf, 2021
di-naphthodiospyrol D (36)	<i>D. lotus</i>	Aljohny <i>et al.</i> , 2021; Bawazeer and Rauf, 2021
di-naphthodiospyrol E (37)	<i>D. lotus</i>	Aljohny <i>et al.</i> , 2021; Bawazeer and Rauf, 2021
di-naphthodiospyrol F (38)	<i>D. lotus</i>	Aljohny <i>et al.</i> , 2021; Bawazeer and Rauf, 2021
di-naphthodiospyrol G (39)	<i>D. lotus</i>	Aljohny <i>et al.</i> , 2021; Bawazeer and Rauf, 2021
diospyrin (40)	<i>D. lotus</i>	Uddin <i>et al.</i> , 2014; Bawazeer and Rauf, 2021
	<i>D. melanoxylon</i>	Sharma <i>et al.</i> , 2018
	<i>D. montana</i>	Sharma, 2017
	<i>D. oocarpa</i>	Dev and Rajarajeshwari, 2013
8-hydroxydiospyrin (41)	<i>D. lotus</i>	Uddin <i>et al.</i> , 2014; Bawazeer and Rauf, 2021
diospyrin-2'-(2-epoxy-3-methyl-butanoate) (42)	<i>D. montana</i>	Sharma, 2017
diospyrin-2'-(2-hydroxy-propanoate) (43)	<i>D. montana</i>	Sharma, 2017
diospyrin-3'-(2-hydroxy-propanoate) (44)	<i>D. montana</i>	Sharma, 2017

**Table 1.** Distribution of naphthoquinones and naphthalene derivatives in the genus *Diospyros* (continued)

Compounds	Species	Reference
ehretione (45)	<i>D. maritima</i>	Higa <i>et al.</i> , 2017
elliptinone (46)	<i>D. anisandra</i>	Uc-Cachón <i>et al.</i> , 2014
	<i>D. gracilipes</i>	Rasamison <i>et al.</i> , 2016
	<i>D. maritima</i>	Higa <i>et al.</i> , 2017
3,8'-biplumbagin (47)	<i>D. maritima</i>	Higa <i>et al.</i> , 2017
2,7'-dimethyl-6,8'-bijuglone (48)	<i>D. maritima</i>	Higa <i>et al.</i> , 2017
maritinone (49)	<i>D. anisandra</i>	Uc-Cachón <i>et al.</i> , 2014
	<i>D. ehretioides</i>	Wosawat <i>et al.</i> , 2021
	<i>D. maritima</i>	Higa <i>et al.</i> , 2017
	<i>D. undulata</i>	Suchaichit <i>et al.</i> , 2018, 2021
isodiospyrin (50)	<i>D. ehretioides</i>	Wosawat <i>et al.</i> , 2021
	<i>D. fleuryana</i>	Ha <i>et al.</i> , 2020
	<i>D. undulata</i>	Suchaichit <i>et al.</i> , 2018, 2021
8'-hydroxyisodiospyrin (51)	<i>D. fleuryana</i>	Ha <i>et al.</i> , 2020
	<i>D. oocarpa</i>	Dev and Rajarajeshwari, 2013
neodiospyrin (52)	<i>D. maritima</i>	Higa <i>et al.</i> , 2017
isozeylanone (53)	<i>D. maritima</i>	Higa <i>et al.</i> , 2017
methylene-3,3'-biplumbagin (54)	<i>D. maritima</i>	Higa <i>et al.</i> , 2017
ethylidene-3,3'-biplumbagin (55)	<i>D. maritima</i>	Higa <i>et al.</i> , 2017
ethylidene-3,6'-biplumbagin (56)	<i>D. maritima</i>	Higa <i>et al.</i> , 2017
ethylidene-6,6'-biplumbagin (57)	<i>D. maritima</i>	Higa <i>et al.</i> , 2017
2',7'-dimethyl-3,6'-ethylidenebijuglone (58)	<i>D. maritima</i>	Higa <i>et al.</i> , 2017
7,7'-dimethyl-3,3'-ethylidenebijuglone (59)	<i>D. maritima</i>	Higa <i>et al.</i> , 2017
8,8'-oxo-biplumbagin (60)	<i>D. shimbaensis</i>	Aronsson <i>et al.</i> , 2016
zeylanone epoxide (61)	<i>D. anisandra</i>	Uc-Cachón <i>et al.</i> , 2014

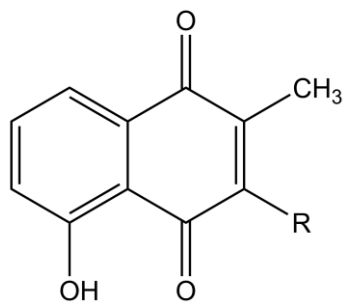


**Table 1.** Distribution of naphthoquinones and naphthalene derivatives in the genus *Diospyros* (continued)

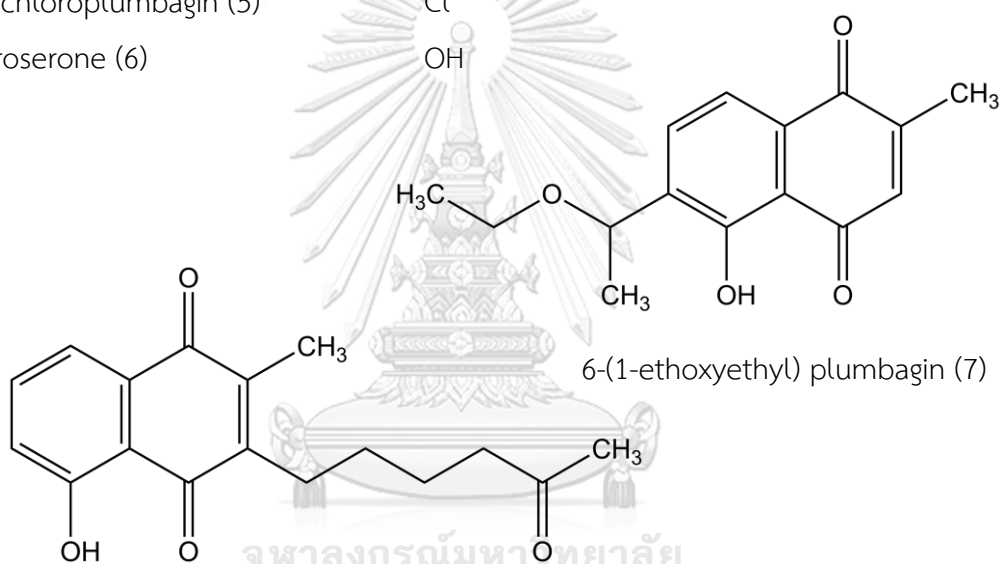
Compounds	Species	Reference
isoxyllopyrin (62)	<i>D. maritima</i>	Higa <i>et al.</i> , 2017
2. Naphthalene derivatives		
8-methoxy-3-methyl-1-naphthalenol (63)	<i>D. burmanica</i>	Mori-Yasumoto <i>et al.</i> , 2012
2,8-dimethoxy-3-methyl-1-naphthalenol (64)	<i>D. burmanica</i>	Mori-Yasumoto <i>et al.</i> , 2012
4,8-dimethoxy-3-methyl-1-naphthalenol (65)	<i>D. burmanica</i>	Mori-Yasumoto <i>et al.</i> , 2012
5,8-dimethoxy-3-methyl-1-naphthalenol (66)	<i>D. burmanica</i>	Mori-Yasumoto <i>et al.</i> , 2012
4-hydroxy-5-methoxy-2-naphthaldehyde (67)	<i>D. burmanica</i>	Mori-Yasumoto <i>et al.</i> , 2012
4-hydroxy-3,5-dimethoxy-2-naphthaldehyde (68)	<i>D. oocarpa</i>	Dev and Rajarajeshwari, 2013
5-hydroxy-4-methoxy-2-naphthaldehyde (69)	<i>D. oocarpa</i>	Dev and Rajarajeshwari, 2013
(1,4,5-trimethoxynaphthalen-2-yl)methyl acetate (70)	<i>D. ehretioides</i>	Wosawat <i>et al.</i> , 2021
7-methyl-1-methoxy-5-hydroxy-naphthalene-4- <i>O</i> -[[5''- <i>O</i> -galloyl- $\beta$ -D-apiofuranosyl-(1'→6')]- $\beta$ -D-glucopyranoside (71)	<i>D. subreana</i>	Boué <i>et al.</i> , 2018
diospyrol 8- <i>O</i> -(6 $\beta$ -D-apiofuranosyl- $\beta$ -D-glucopyranosyl)-8'- <i>O</i> - $\beta$ -D-glucopyranoside (72)	<i>D. mollis</i>	Suwama <i>et al.</i> , 2018
diospyrol 8,8'-di- <i>O</i> -(6 $\beta$ -D-apiofuranosyl- $\beta$ -D-glucopyranoside) (73)	<i>D. mollis</i>	Suwama <i>et al.</i> , 2018

**Table 1.** Distribution of naphthoquinones and naphthalene derivatives in the genus *Diospyros* (continued)

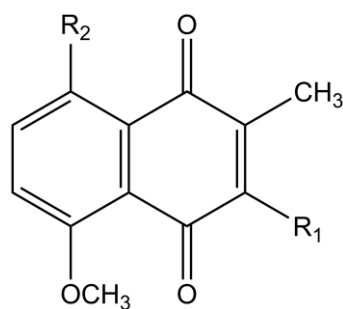
Compounds	Species	Reference
makluoside A (74)	<i>D. mollis</i>	Suwama <i>et al.</i> , 2018
makluoside C (75)	<i>D. mollis</i>	Suwama <i>et al.</i> , 2018
makluoside D (76)	<i>D. mollis</i>	Suwama <i>et al.</i> , 2018
makluoside E (77)	<i>D. mollis</i>	Suwama <i>et al.</i> , 2018
fragranone (78)	<i>D. fragrans</i>	Tameye <i>et al.</i> , 2022
<i>cis</i> -isoshinanolone (79)	<i>D. anisandra</i>	Uc-Cachón <i>et al.</i> , 2014
<i>cis</i> -isoshinanolone (79)	<i>D. ehretioides</i>	Wosawat <i>et al.</i> , 2021
	<i>D. shimbaensis</i>	Aronsson <i>et al.</i> , 2016
	<i>D. undulata</i>	Suchaichit <i>et al.</i> , 2018, 2021
<i>trans</i> -isoshinanolone (80)	<i>D. ehretioides</i>	Wosawat <i>et al.</i> , 2021
	<i>D. shimbaensis</i>	Aronsson <i>et al.</i> , 2016
<i>cis</i> -isoshinanolone-4-acetate (81)	<i>D. undulata</i>	Suchaichit <i>et al.</i> , 2018, 2021
3,4-dihydro-4 $\beta$ -hydroxy-5,6-dimethoxy-2 $\alpha$ -methyl-1(2H)-naphthalenone (82)	<i>D. undulata</i>	Suchaichit <i>et al.</i> , 2018



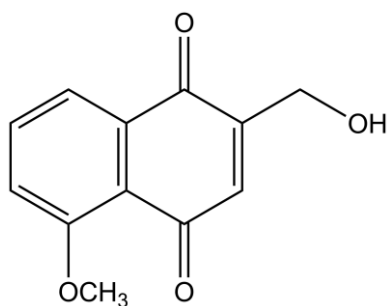
	R
plumbagin (1)	H
3-methylplumbagin (2)	CH <sub>3</sub>
3-(2-hydroxyethyl) plumbagin (3)	CH <sub>2</sub> CH <sub>2</sub> OH
3-bromoplumbagin (4)	Br
3-chloroplumbagin (5)	Cl
droserone (6)	OH



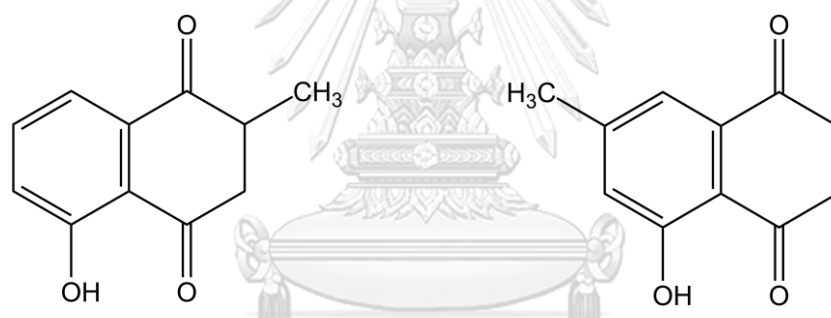
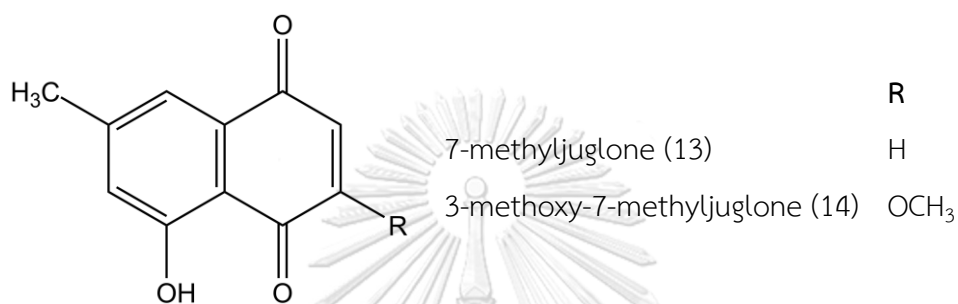
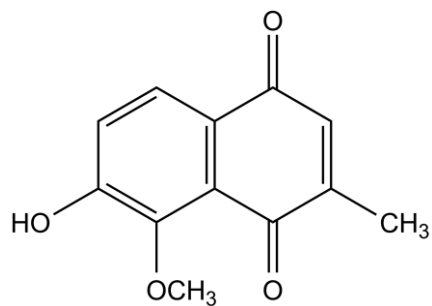
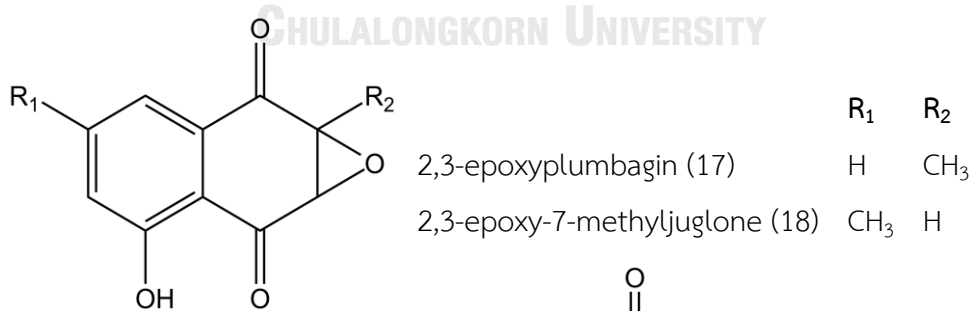
3-(5-oxohexyl) plumbagin (8)



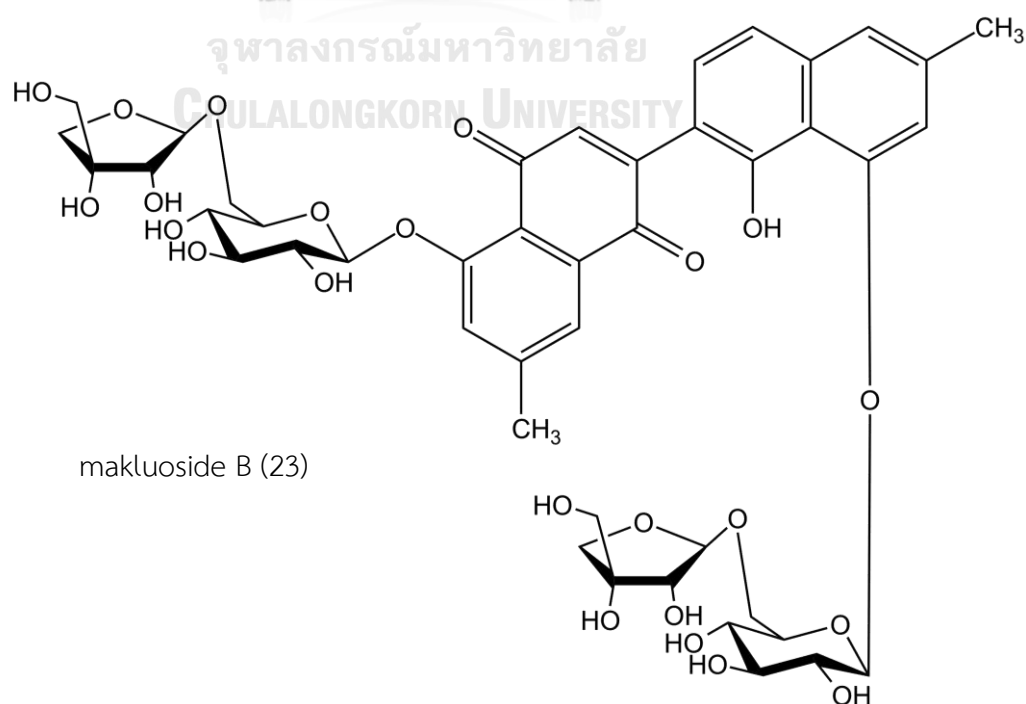
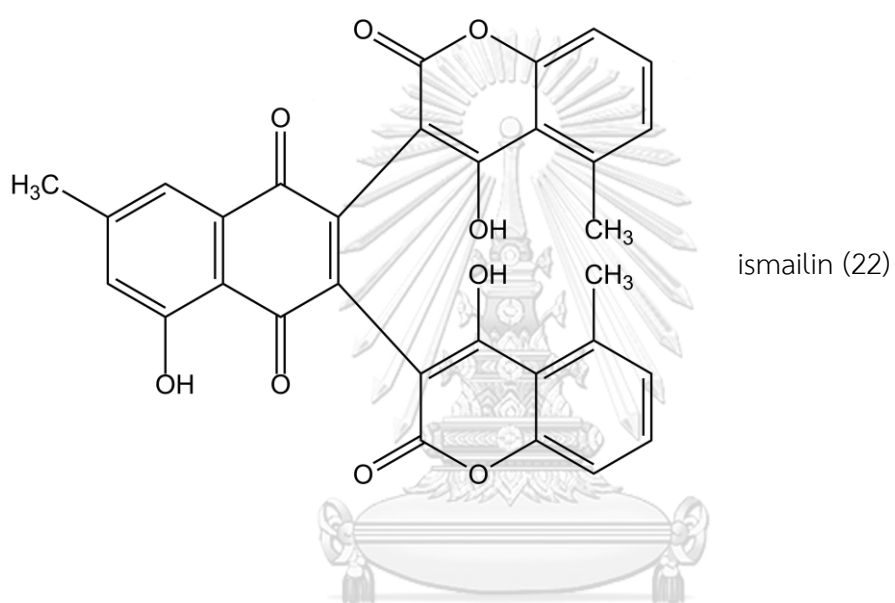
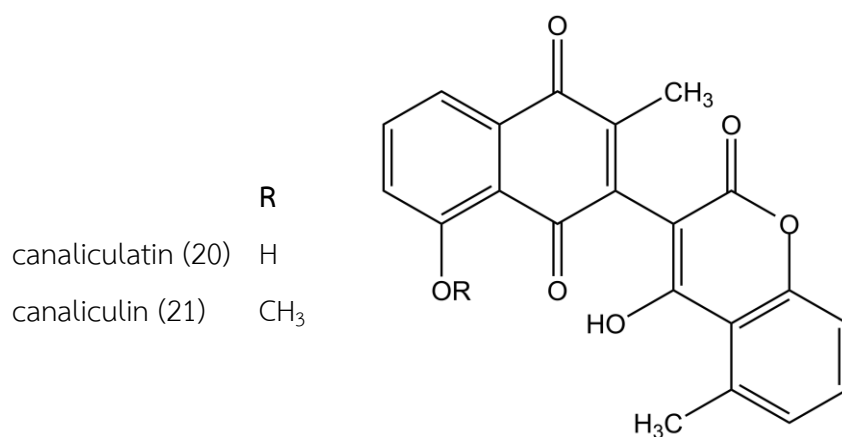
	R <sub>1</sub>	R <sub>2</sub>
5-methoxy-2-methyl-1,4-naphthoquinone (9)	H	H
5,8-dimethoxy-2-methyl-1,4-naphthoquinone (10)	H	OCH <sub>3</sub>
3-hydroxy-5-methoxy-2-methyl-1,4-naphthoquinone (11)	OH	H

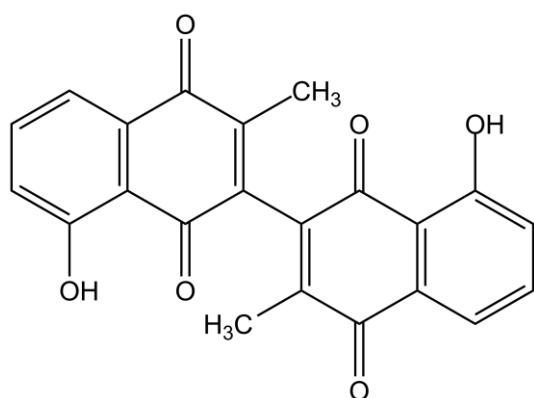


2-hydroxymethyl-5-methoxy-1,4-naphthoquinone (12)

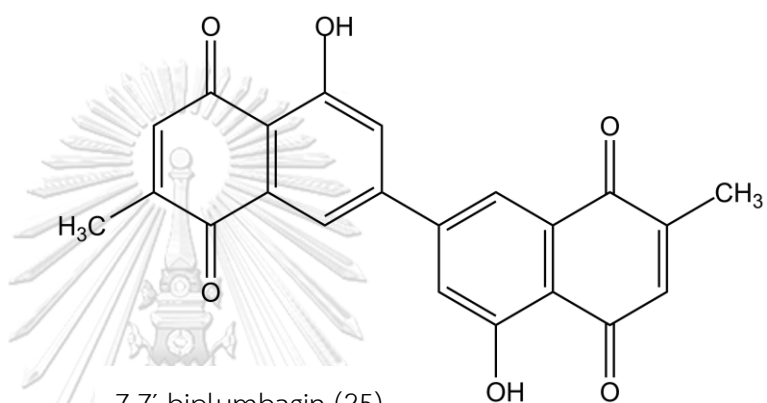
 $\beta$ -dihydroplumbagin (15)      7-methyl- $\beta$ -dihydrojuglone (16)

7-hydroxy-8-methoxy-2-methyl-1,4-naphthoquinone (19)

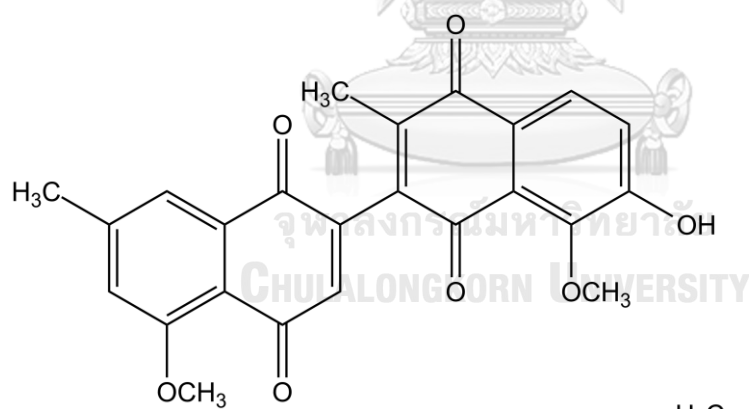




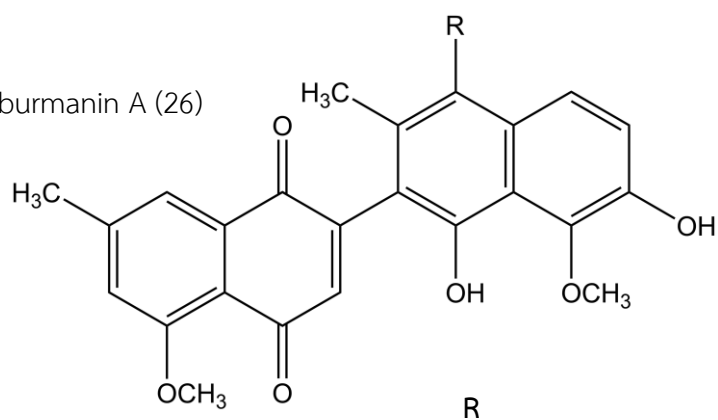
3,3'-biplumbagin (24)



7,7'-biplumbagin (25)

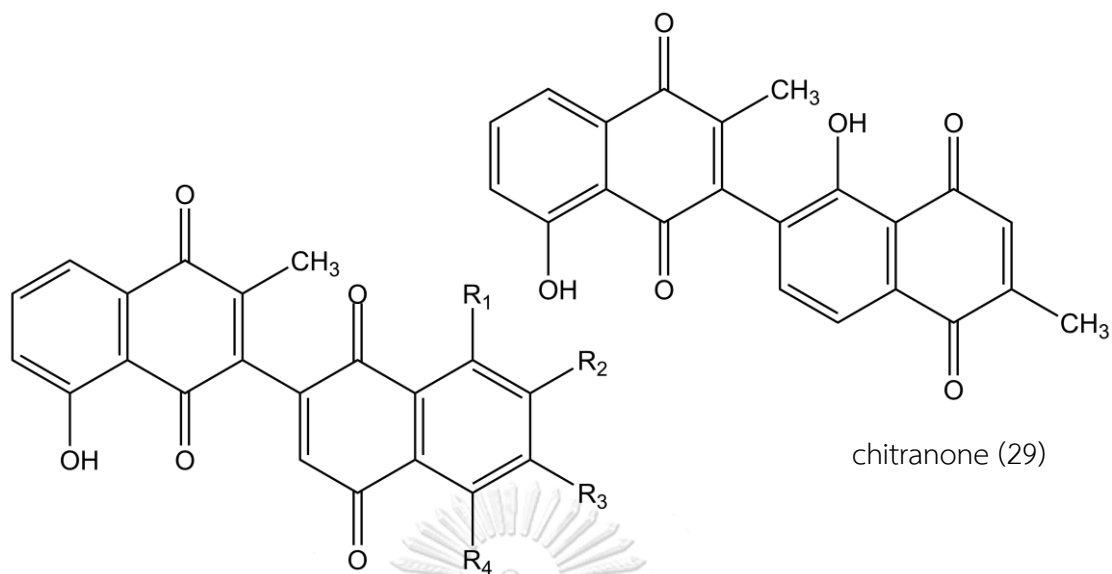


burmanin A (26)



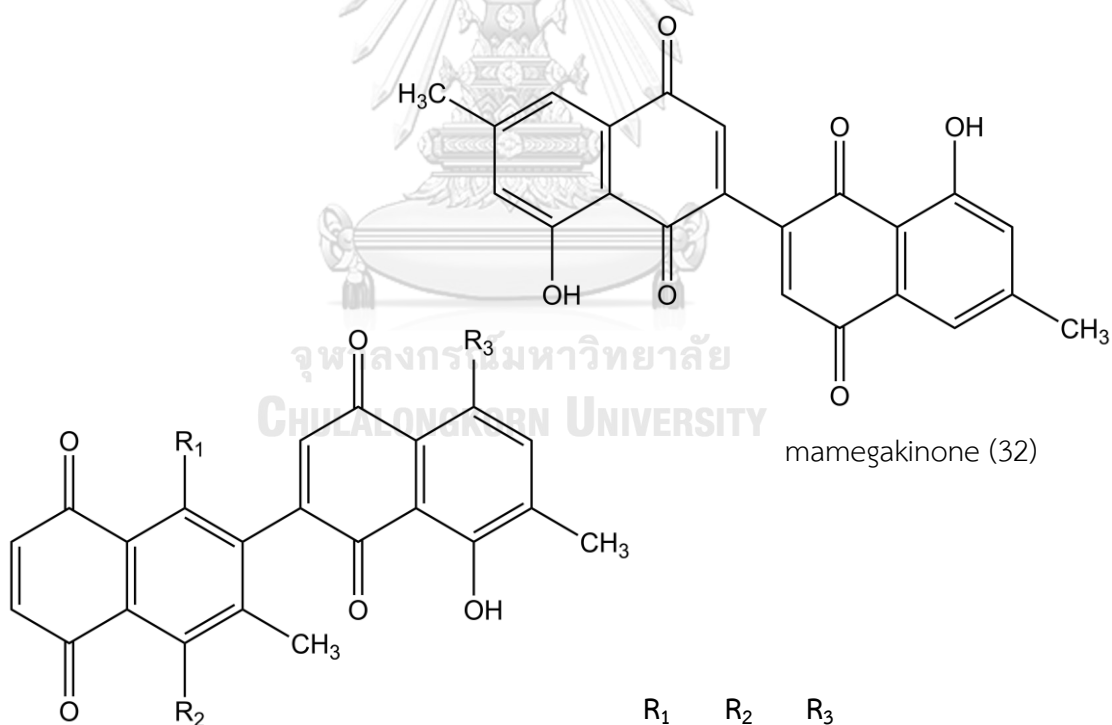
burmanin B (27) H

burmanin C (28) OCH<sub>3</sub>



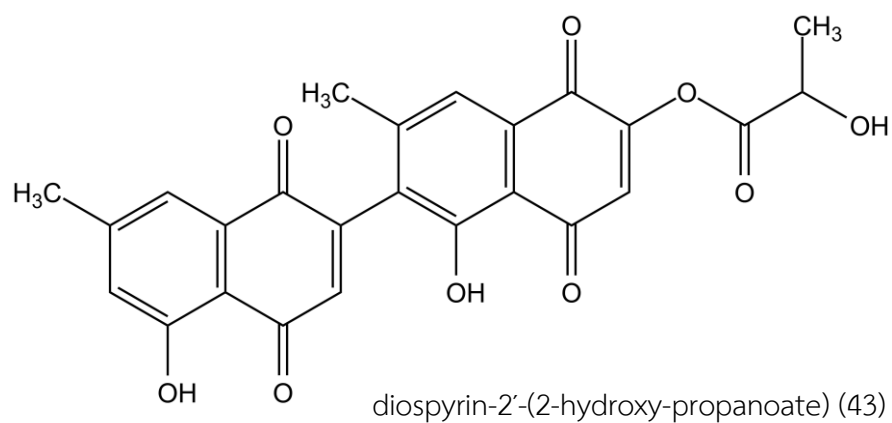
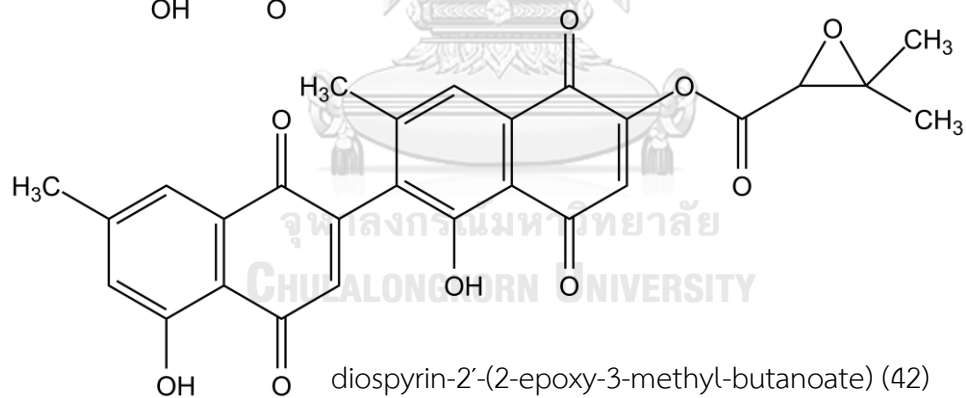
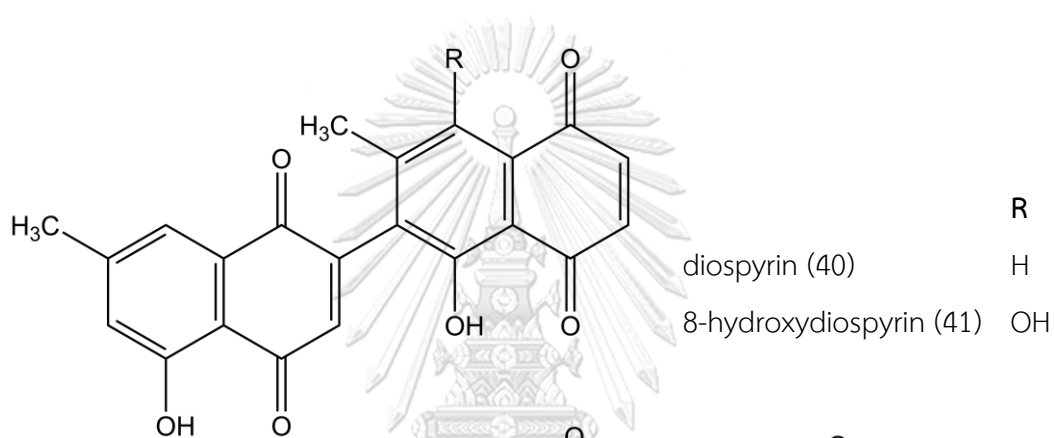
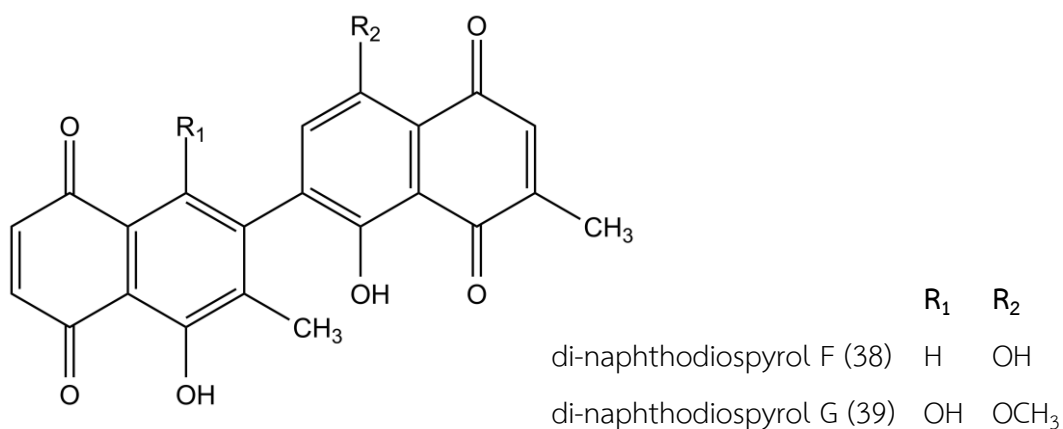
chitranone (29)

	R <sub>1</sub>	R <sub>2</sub>	R <sub>3</sub>	R <sub>4</sub>
2,7'-dimethyl-2',3'-bijuglone (30)	H	CH <sub>3</sub>	H	OH
2,7'-dimethyl-3,3'-bijuglone (31)	OH	H	CH <sub>3</sub>	H

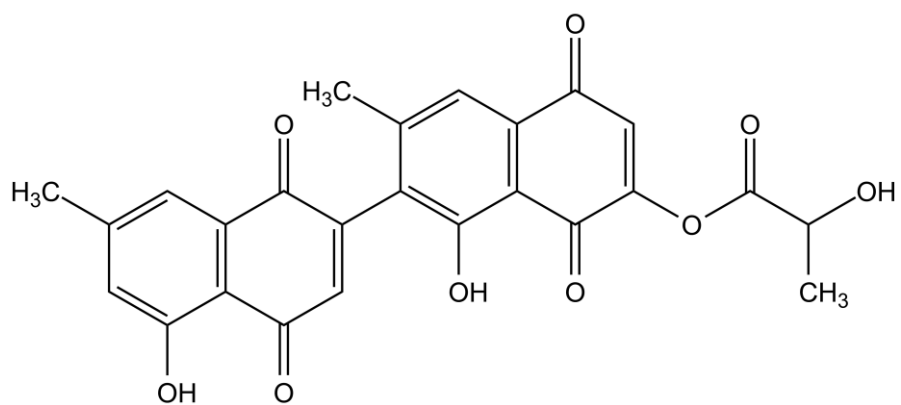


mamegakinone (32)

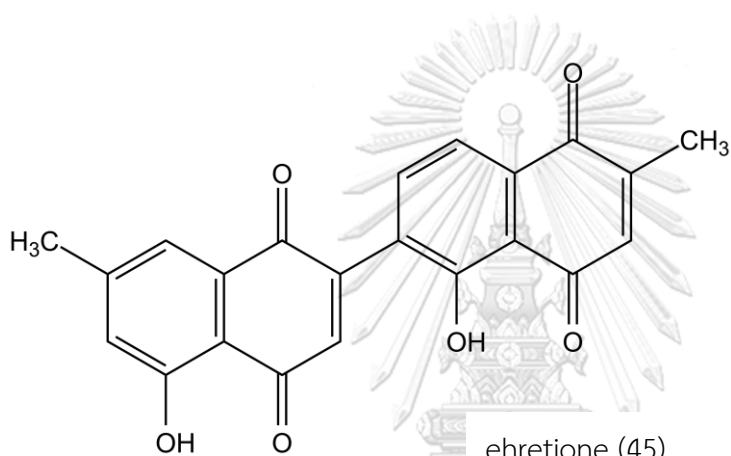
	R <sub>1</sub>	R <sub>2</sub>	R <sub>3</sub>
di-naphthodiospyrol A (33)	H	OCH <sub>3</sub>	OH
di-naphthodiospyrol B (34)	OH	H	OH
di-naphthodiospyrol C (35)	H	H	OH
di-naphthodiospyrol D (36)	OCH <sub>3</sub>	OCH <sub>3</sub>	OH
di-naphthodiospyrol E (37)	OH	OH	OCH <sub>3</sub>



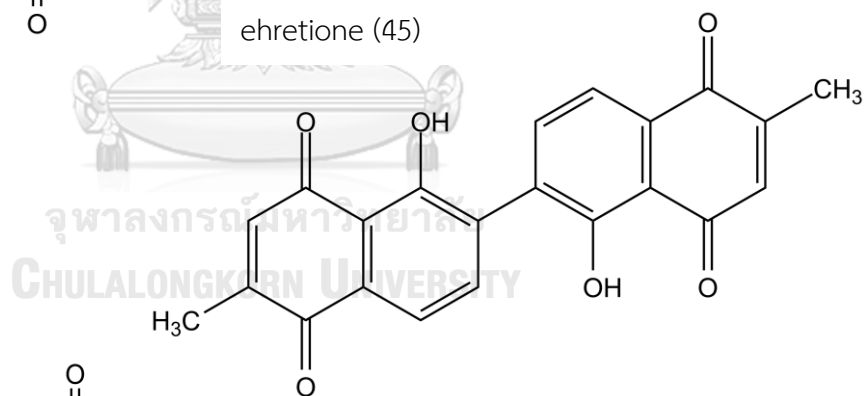




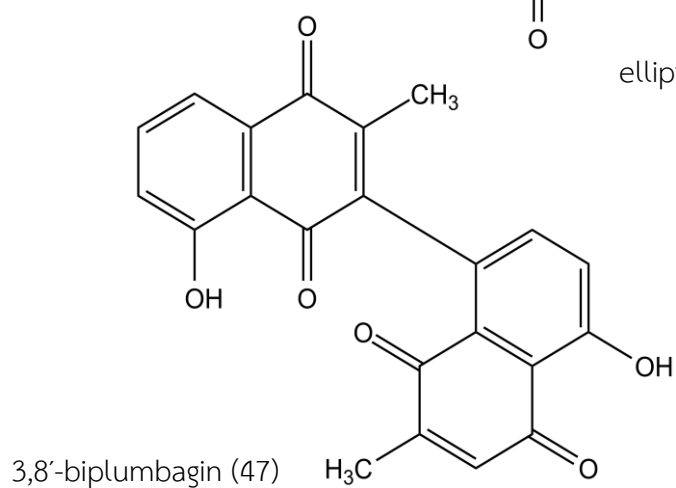
diospyrin-3'-(2-hydroxy-propanoate) (44)



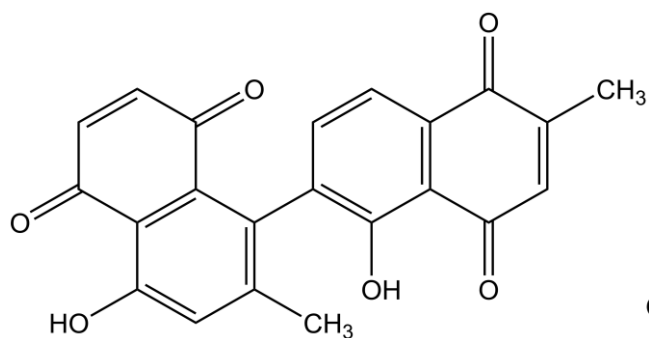
ehretione (45)



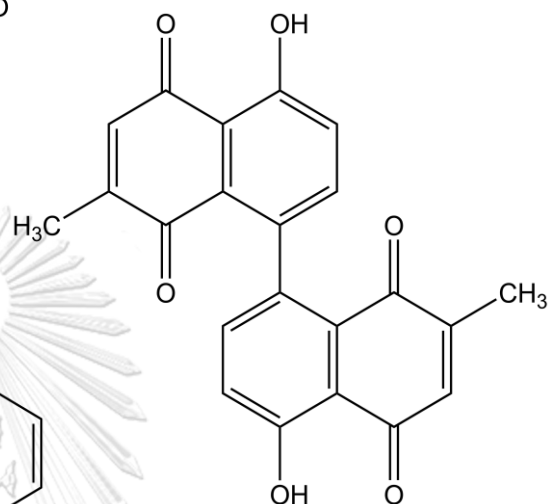
elliptinone (46)



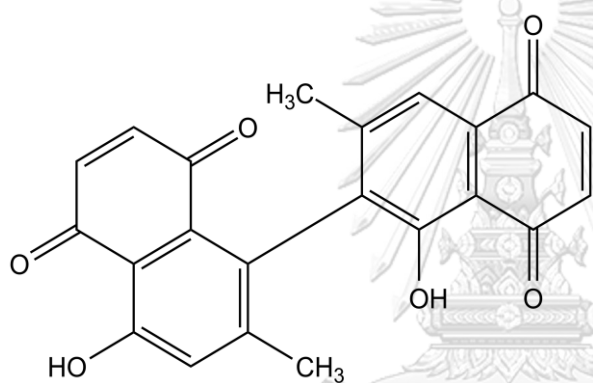
3,8'-biplumbagin (47)



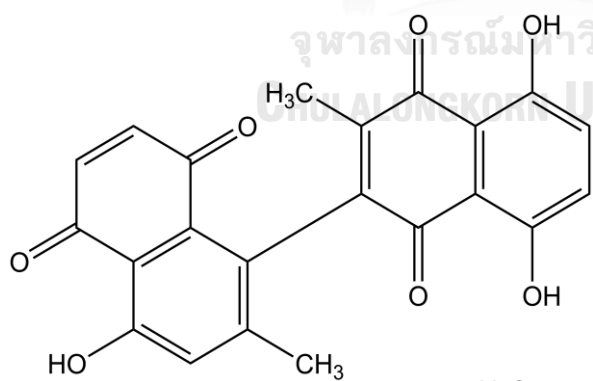
2,7-dimethyl-6,8'-bijuglone (48)



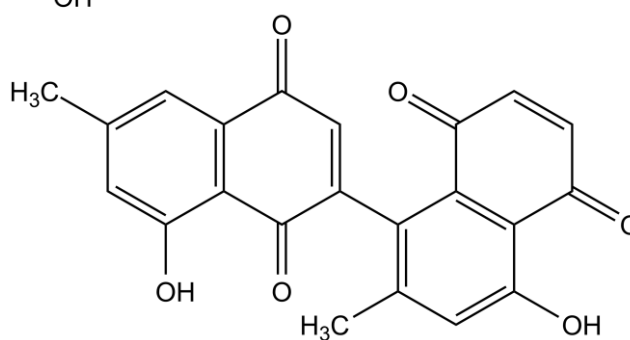
maritnone (49)



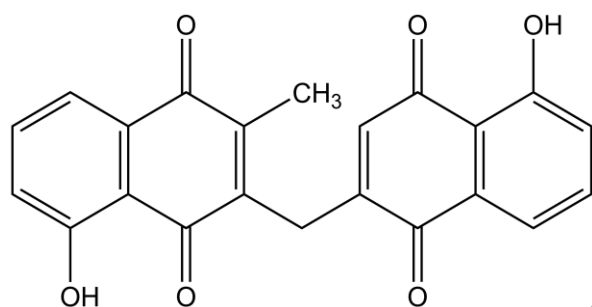
isodiospyrin (50)



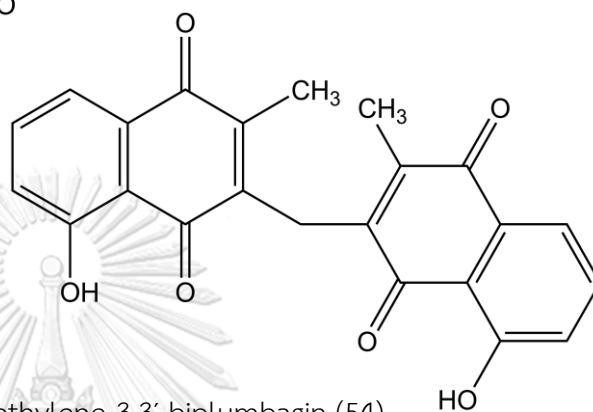
8'-hydroxyisodiospyrin (51)



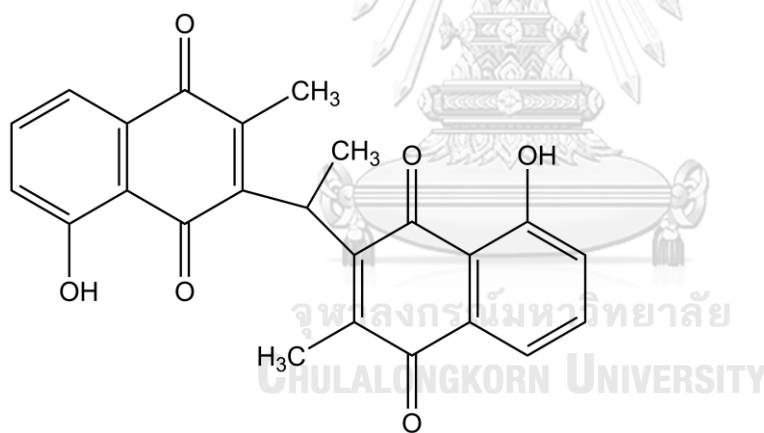
neodiospyrin (52)



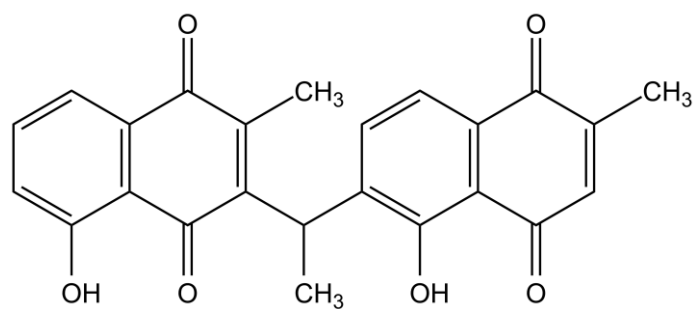
isozeylanone (53)



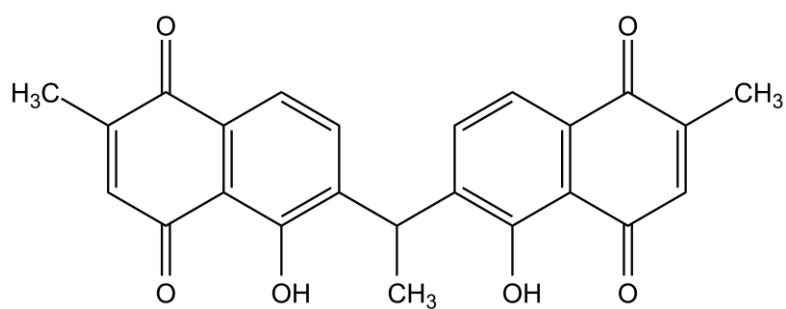
methylene-3,3'-biplumbagin (54)



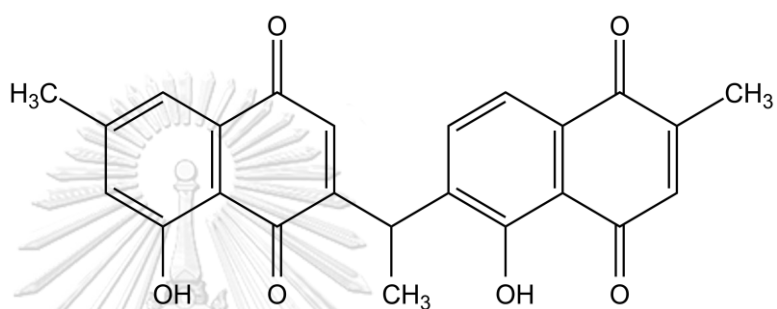
ethylidene-3,3'-biplumbagin (55)



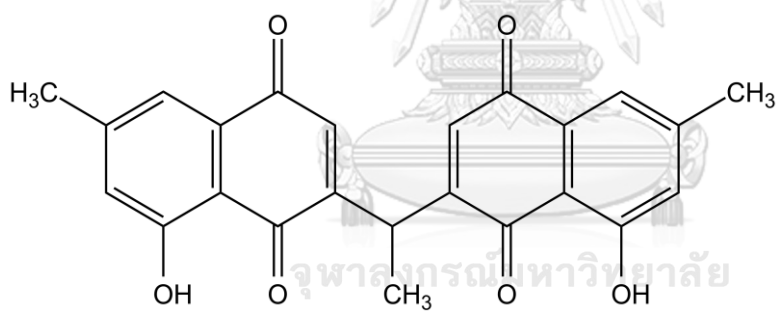
ethylidene-3,6'-biplumbagin (56)



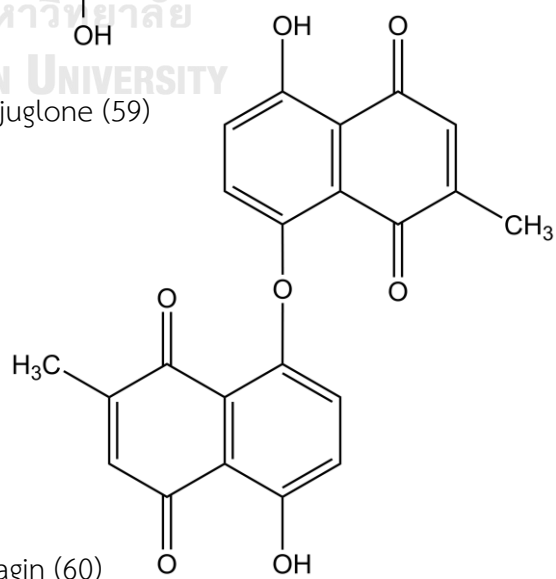
ethylidene-6,6'-biplumbagin (57)



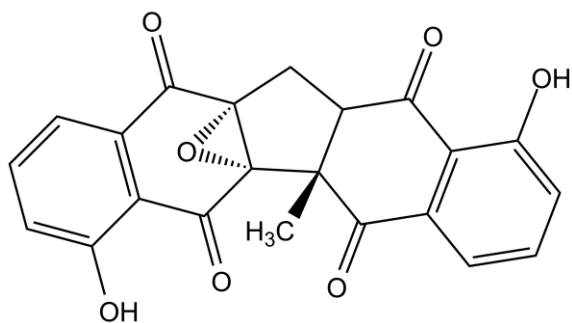
2',7-dimethyl-3,6'-ethylidenebijuglone (58)



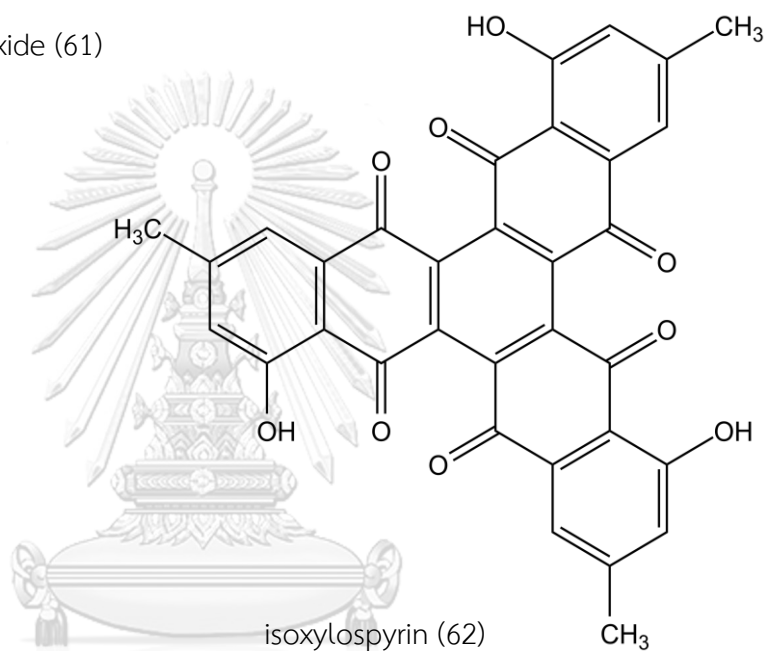
7,7'-dimethyl-3,3'-ethylidenebijuglone (59)



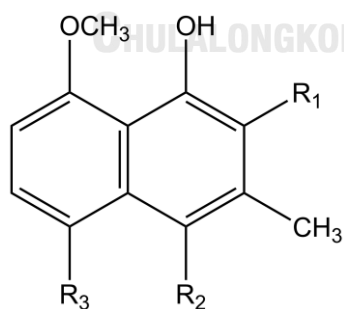
8,8'-oxo-biplumbagin (60)



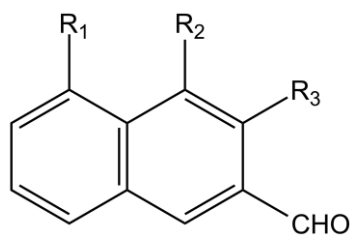
zeylanone epoxide (61)



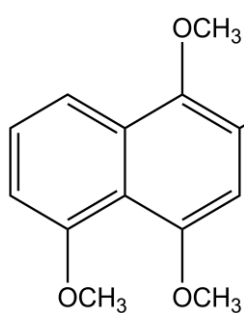
isoxyllopyrin (62)



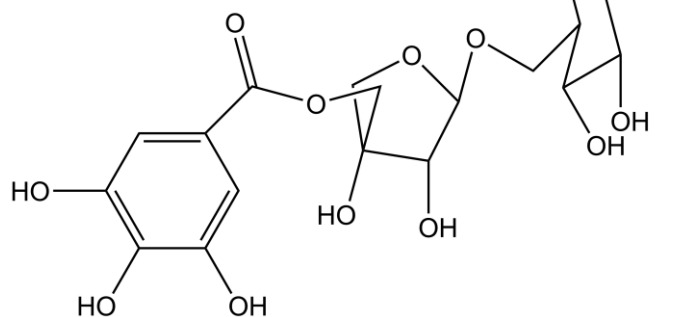
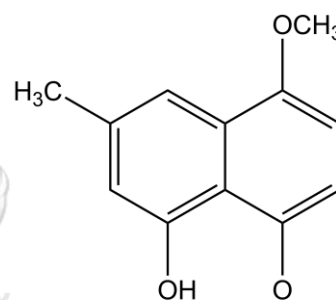
	R <sub>1</sub>	R <sub>2</sub>	R <sub>3</sub>
8-methoxy-3-methyl-1-naphthalenol (63)	H	H	H
2,8-dimethoxy-3-methyl-1-naphthalenol (64)	OCH <sub>3</sub>	H	H
4,8-dimethoxy-3-methyl-1-naphthalenol (65)	H	OCH <sub>3</sub>	H
5,8-dimethoxy-3-methyl-1-naphthalenol (66)	H	H	OCH <sub>3</sub>



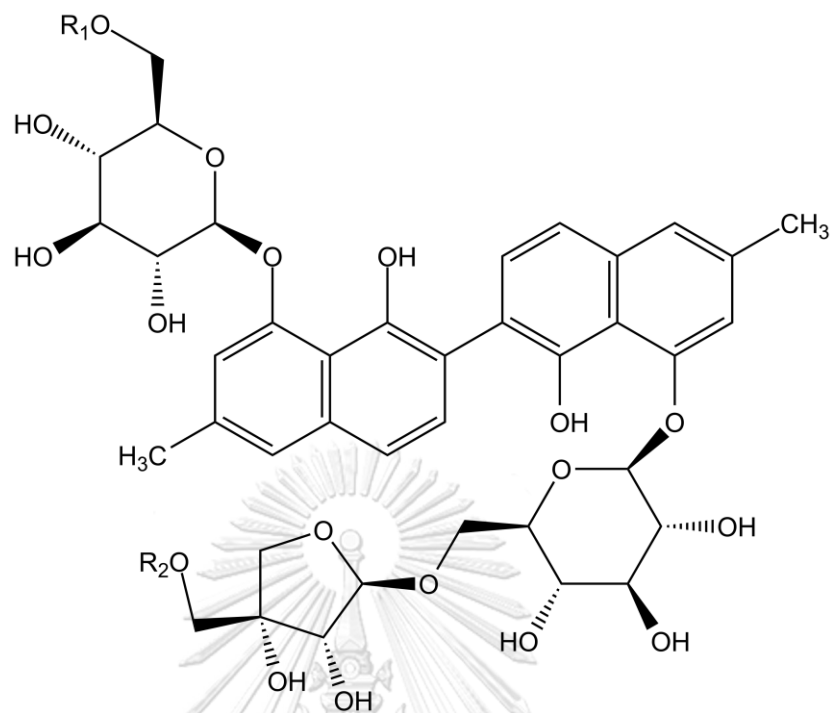
	$R_1$	$R_2$	$R_3$
4-hydroxy-5-methoxy-2-naphthaldehyde (67)	$\text{OCH}_3$	$\text{OH}$	$\text{H}$
4-hydroxy-3,5-dimethoxy-2-naphthaldehyde (68)	$\text{OCH}_3$	$\text{OH}$	$\text{OCH}_3$
5-hydroxy-4-methoxy-2-naphthaldehyde (69)	$\text{OH}$	$\text{OCH}_3$	$\text{H}$



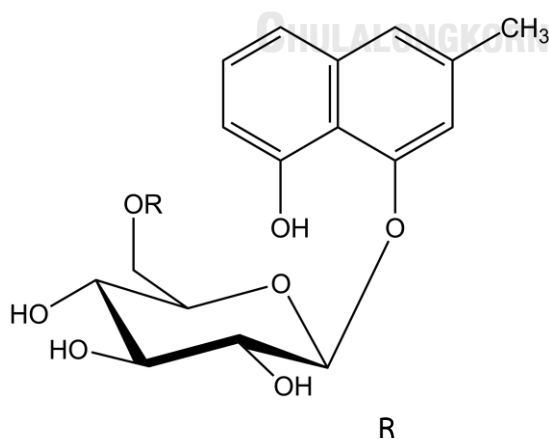
(1,4,5-trimethoxynaphthalen-2-yl) methyl acetate (70)



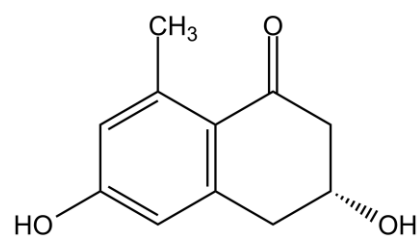
7-methyl-1-methoxy-5-dihydroxy-naphthalene-4-O-[(5''-O-galloyl- $\beta$ -D-apiofuranosyl-(1'  $\rightarrow$  6'))- $\beta$ -D-glucopyranoside (71)



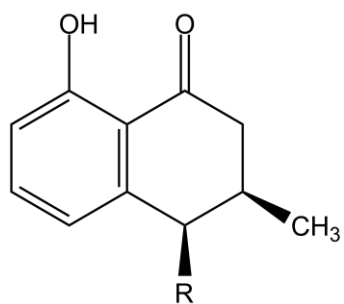
	$R_1$	$R_2$
diospyrol 8-O-(6- $\beta$ -D-apiofuranosyl- $\beta$ -D-glucopyranosyl)-8'-O- $\beta$ -D-glucopyranoside (72)	H	H
diospyrol 8,8'-di-O-(6- $\beta$ -D-apiofuranosyl- $\beta$ -D-glucopyranoside) (73)	apiofuranosyl	H
makluoside A (74)	apiofuranosyl	xylopyranosyl



	R
makluoside C (75)	H
makluoside D (76)	xylopyranosyl
makluoside E (77)	apiofuranosyl



fragranone (78)



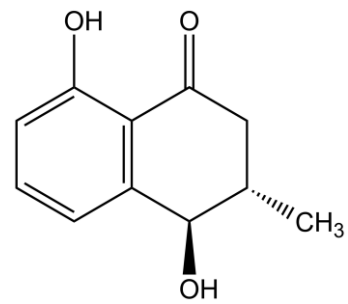
*cis*-isoshinanolone (79)

R

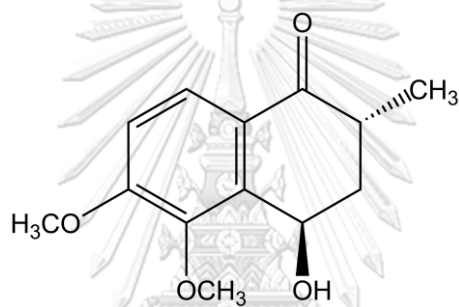
OH

*cis*-isoshinanolone-4-acetate (81)

OAc



*trans*-isoshinanolone (80)

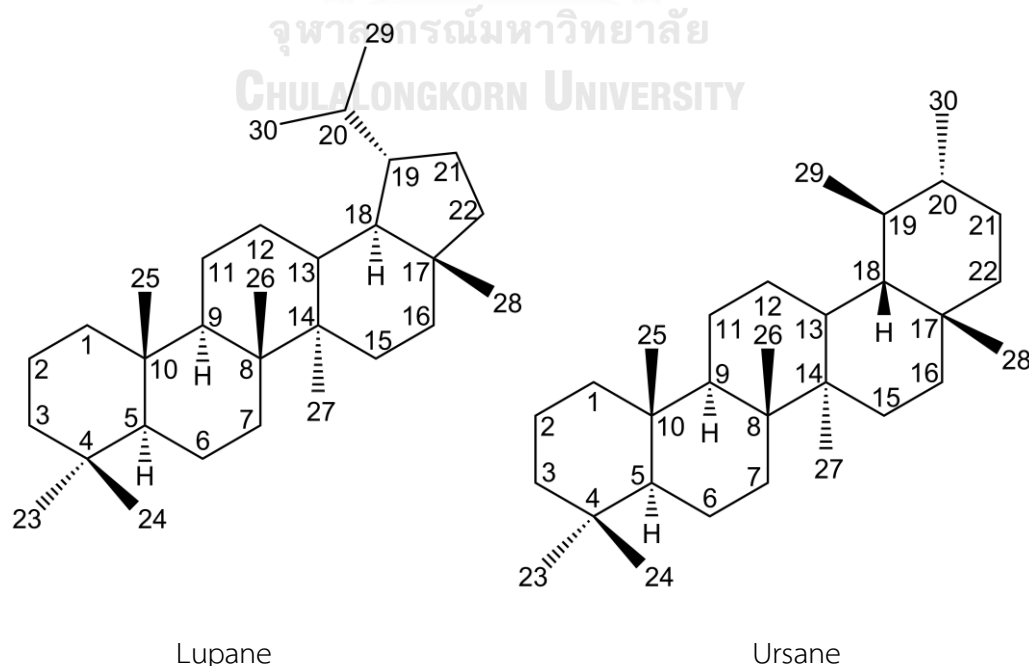


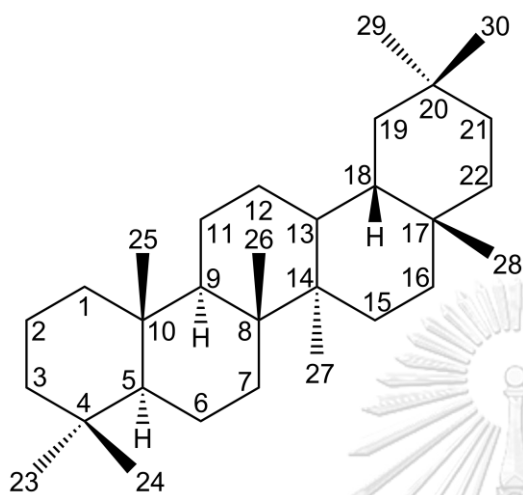
3,4-dihydro-4 $\beta$ -hydroxy-5,6-dimethoxy-2 $\alpha$ -methyl-1(2H)-naphthalenone (82)



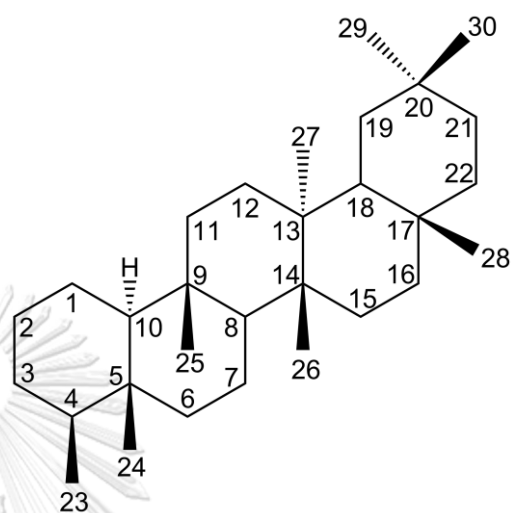
## 1.2 Triterpenoids

Triterpenoids are a class of natural compounds characterized by their core structure constructed from six isoprene units. *Diospyros* plants, known for their significant content of triterpenoids, have captured scientific attention due to their diverse and beneficial pharmacological properties. These plants are known to contain different types of triterpenoids, such as lupane, ursane, oleanane, friedelane, taraxerane and cycloartane. Each type exhibits interesting biological activities. For example, betulinic acid, a lupane-type triterpenoid, has shown various biological activities such as anti-cancer, anti-malarial, anti-inflammatory, and anti-viral (Ali-Seyed *et al.*, 2016). The ursane-type ursolic acid displayed anti-inflammatory, hepatoprotective, cardioprotective, anti-tumor, and neuroprotective effects (Pironi *et al.*, 2018), while the oleanane-type oleanolic acid has shown interesting biological activities such as hepatoprotective, anti-tumor, anti-inflammatory and anti-obesity (Feng *et al.*, 2020). The distribution of triterpenoids in the genus *Diospyros*, summarized from reported data in the literature from the year 2012 to present, is shown in **Table 2**.

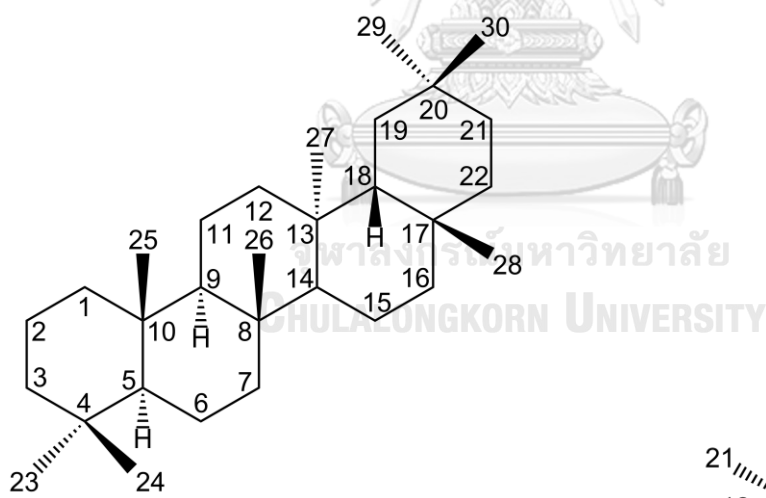




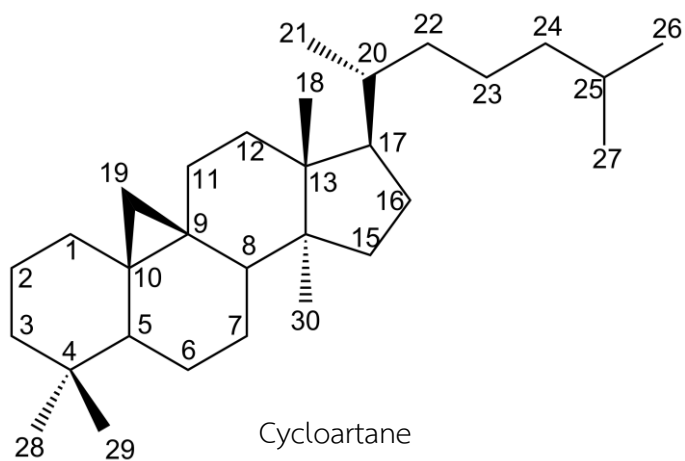
Oleanane



Friedelane



Taraxerane



Cycloartane

**Table 2.** Distribution of triterpenoids in the genus *Diospyros*

Compounds	Species	References
1. Acyclic type		
squalene (83)	<i>D. virginiana</i>	Priya <i>et al.</i> , 2014
2. Cycloartane type		
cycloart-24-en-3 $\beta$ ,26-diol (84)	<i>D. mannii</i>	Feusso <i>et al.</i> , 2017
(24 <i>E</i> )-3-hydroxycycloart-24-en-26-al (85)	<i>D. mannii</i>	Feusso <i>et al.</i> , 2017
mangiferolic acid (86)	<i>D. mannii</i>	Feusso <i>et al.</i> , 2017
3 $\beta$ ,23-dihydroxy-cycloart-24 <i>E</i> -en-26-oic acid (87)	<i>D. mannii</i>	Feusso <i>et al.</i> , 2017
conocarpol (88)	<i>D. conocarpa</i>	Feusso <i>et al.</i> , 2016
(24 <i>E</i> )-cycloart-24-en-26-ol-3-one (89)	<i>D. mannii</i>	Feusso <i>et al.</i> , 2017
(24 <i>E</i> )-3-oxocycloart-24-en-26-al (90)	<i>D. mannii</i>	Feusso <i>et al.</i> , 2017
mangiferonic acid (91)	<i>D. mannii</i>	Feusso <i>et al.</i> , 2017
3. Norcycloartane type		
4,4,14-trimethyl-9,19-cyclocholane-3 $\beta$ ,24-diol (92)	<i>D. mannii</i>	Feusso <i>et al.</i> , 2017
4. Friedelane type		
friedelinol (93)	<i>D. filipendula</i>	Wisetsai <i>et al.</i> , 2021
friedelin (94)	<i>D. collinsae</i>	Bumroong and Thanakijcharoenpath, 2016
	<i>D. filipendula</i>	Wisetsai <i>et al.</i> , 2021
	<i>D. undulata</i>	Suchaichit <i>et al.</i> , 2018, 2021
5. Friedo-oleanane type		
3 $\beta$ -hydroxy-D:B-friedo-olean-5-ene (95)	<i>D. burmanica</i>	Choi <i>et al.</i> , 2015
6. Lupane type		
lupeol (96)	<i>D. burmanica</i>	Choi <i>et al.</i> , 2015
	<i>D. collinsae</i>	Bumroong and Thanakijcharoenpath, 2016

**Table 2.** Distribution of triterpenoids in the genus *Diospyros* (continued)

Compounds	Species	References
lupeol (96)	<i>D. conocarpa</i>	Feusso <i>et al.</i> , 2016
	<i>D. ehretioides</i>	Wosawat <i>et al.</i> , 2021
	<i>D. fragrans</i>	Tameye <i>et al.</i> , 2022
	<i>D. gillettii</i>	Tameye <i>et al.</i> , 2020
	<i>D. gracilescens</i>	Njanpa <i>et al.</i> , 2021
	<i>D. longiflora</i>	Dongmo <i>et al.</i> , 2018
	<i>D. lotus</i>	Uddin <i>et al.</i> , 2014
	<i>D. melanoxylon</i>	Sharma <i>et al.</i> , 2018
	<i>D. mollis</i>	Suwama <i>et al.</i> , 2018
	<i>D. oocarpa</i>	Dev and Rajarajeshwari, 2013
	<i>D. soubreana</i>	Blanchard <i>et al.</i> , 2018
	<i>D. undulata</i>	Suchaichit <i>et al.</i> , 2021
	<i>D. zenkeri</i>	Feusso <i>et al.</i> , 2019
lupeol acetate (97)	<i>D. soubreana</i>	Blanchard <i>et al.</i> , 2018
lupeol caffeate (98)	<i>D. mollis</i>	Suwama <i>et al.</i> , 2018
betulin (99)	<i>D. canaliculata</i>	Lenta <i>et al.</i> , 2015
	<i>D. carbonaria</i>	Peyrat <i>et al.</i> , 2017
	<i>D. collinsae</i>	Bumroong and Thanakijcharoenpath, 2016
	<i>D. conocarpa</i>	Feusso <i>et al.</i> , 2016
	<i>D. discolor</i>	Somat <i>et al.</i> , 2020
	<i>D. ehretioides</i>	Wosawat <i>et al.</i> , 2021
	<i>D. gillettii</i>	Tameye <i>et al.</i> , 2020
	<i>D. gracilescens</i>	Njanpa <i>et al.</i> , 2021
	<i>D. iturensis</i>	Feusso <i>et al.</i> , 2020
	<i>D. longiflora</i>	Dongmo <i>et al.</i> , 2018
	<i>D. mannii</i>	Feusso <i>et al.</i> , 2017
	<i>D. melanoxylon</i>	Sharma <i>et al.</i> , 2018

**Table 2.** Distribution of triterpenoids in the genus *Diospyros* (continued)

Compounds	Species	References
betulin (99)	<i>D. mollis</i>	Suwama <i>et al.</i> , 2018
	<i>D. undulata</i>	Suchaichit <i>et al.</i> , 2018, 2021
	<i>D. zenkeri</i>	Feusso <i>et al.</i> , 2019
28-O-acetylbetulin (100)	<i>D. ehretioides</i>	Wosawat <i>et al.</i> , 2021
	<i>D. undulata</i>	Suchaichit <i>et al.</i> , 2018
betulinaldehyde (101)	<i>D. glans</i>	Peyrat <i>et al.</i> , 2016
	<i>D. oocarpa</i>	Dev and Rajarajeshwari, 2013
betulinic acid (102)	<i>D. bipindensis</i>	Cesari <i>et al.</i> , 2013
	<i>D. canaliculata</i>	Lenta <i>et al.</i> , 2015
	<i>D. carbonaria</i>	Peyrat <i>et al.</i> , 2017
	<i>D. collinsae</i>	Bumroong and Thanakijcharoenpath, 2016
	<i>D. conocarpa</i>	Feusso <i>et al.</i> , 2016
	<i>D. discolor</i>	Somat <i>et al.</i> , 2020
	<i>D. ehretioides</i>	Wosawat <i>et al.</i> , 2021
	<i>D. filipendula</i>	Wisetsai <i>et al.</i> , 2021
	<i>D. fragrans</i>	Tameye <i>et al.</i> , 2022
	<i>D. gillettii</i>	Tameye <i>et al.</i> , 2020
	<i>D. glans</i>	Peyrat <i>et al.</i> , 2016
	<i>D. gracilescens</i>	Njanpa <i>et al.</i> , 2021
	<i>D. iturensis</i>	Feusso <i>et al.</i> , 2020
	<i>D. kaki</i>	Kim <i>et al.</i> , 2016
	<i>D. longiflora</i>	Dongmo <i>et al.</i> , 2018
	<i>D. lotus</i>	Uddin <i>et al.</i> , 2014
	<i>D. mannii</i>	Feusso <i>et al.</i> , 2017
	<i>D. melanoxylon</i>	Sharma <i>et al.</i> , 2018
	<i>D. mollis</i>	Suwama <i>et al.</i> , 2018
	<i>D. soubreana</i>	Blanchard <i>et al.</i> , 2018

**Table 2.** Distribution of triterpenoids in the genus *Diospyros* (continued)

Compounds	Species	References
betulinic acid (102)	<i>D. undulata</i>	Suchaichit <i>et al.</i> , 2018, 2021
	<i>D. zenkeri</i>	Feusso <i>et al.</i> , 2019
3- <i>O</i> - <i>trans</i> -caffeoylbetulinic acid (103)	<i>D. ehretioides</i>	Wosawat <i>et al.</i> , 2021
alphaltolic acid (104)	<i>D. mannii</i>	Feusso <i>et al.</i> , 2017
3- <i>O</i> - <i>cis</i> - <i>p</i> -coumaroylalphaltolic acid (105)	<i>D. carbonaria</i>	Peyrat <i>et al.</i> , 2017
3- <i>O</i> - <i>trans</i> - <i>p</i> -coumaroylalphaltolic acid (106)	<i>D. carbonaria</i>	Peyrat <i>et al.</i> , 2017
	<i>D. filipendula</i>	Wisetsai <i>et al.</i> , 2021
eucalyptic acid (107)	<i>D. carbonaria</i>	Peyrat <i>et al.</i> , 2017
lupenone (108)	<i>D. gracilipes</i>	Rasamison <i>et al.</i> , 2016
	<i>D. mollis</i>	Suwama <i>et al.</i> , 2018
betulonaldehyde (109)	<i>D. filipendula</i>	Wisetsai <i>et al.</i> , 2021
methyl lup-20(29)-en-3-on-28-oate (110)	<i>D. burmanica</i>	Choi <i>et al.</i> , 2015
<i>O</i> - <i>trans</i> - <i>p</i> -coumaroylcyclicodiscic acid (111)	<i>D. mannii</i>	Feusso <i>et al.</i> , 2017
(3 $\beta$ )-3,23-dihydroxylup-20(29)-en-28-oic acid (112)	<i>D. glans</i>	Peyrat <i>et al.</i> , 2016
(3 $\beta$ )-3,23-dihydroxylup-12,20(29)-dien-28-oic acid (113)	<i>D. glans</i>	Peyrat <i>et al.</i> , 2016
3 $\beta$ ,28,30-lup-20(29)-ene triol (114)	<i>D. zenkeri</i>	Feusso <i>et al.</i> , 2019
lup-20 (29)-ene-3 $\alpha$ ,6 $\beta$ -diol (115)	<i>D. melanoxylon</i>	Sharma <i>et al.</i> , 2018
messagenin (116)	<i>D. zenkeri</i>	Feusso <i>et al.</i> , 2019
7. Oleanane type		
$\beta$ -amyrin (117)	<i>D. burmanica</i>	Choi <i>et al.</i> , 2015
	<i>D. iturensis</i>	Feusso <i>et al.</i> , 2020
	<i>D. soubreana</i>	Blanchard <i>et al.</i> , 2018
$\beta$ -amyrin acetate (118)	<i>D. fragrans</i>	Tameye <i>et al.</i> , 2022

**Table 2.** Distribution of triterpenoids in the genus *Diospyros* (continued)

Compounds	Species	References
oleanolic acid (119)	<i>D. fragrans</i>	Tameye <i>et al.</i> , 2022
	<i>D. kaki</i>	Zhang <i>et al.</i> , 2018
	<i>D. melanoxylon</i>	Sharma <i>et al.</i> , 2018
hederagenin (120)	<i>D. fragrans</i>	Tameye <i>et al.</i> , 2022
	<i>D. mannii</i>	Feusso <i>et al.</i> , 2017
$\beta$ -amyrenone (121)	<i>D. iturensis</i>	Feusso <i>et al.</i> , 2020
aridanin (122)	<i>D. conocarpa</i>	Feusso <i>et al.</i> , 2016
kakisaponin VII (123)	<i>D. kaki</i>	Zhang <i>et al.</i> , 2018
ryobunin C (124)	<i>D. kaki</i>	Zhang <i>et al.</i> , 2018
2 $\alpha$ , 3 $\alpha$ , 19 $\alpha$ , 24- tetrahydroxyolea-12-en-28-oic acid- $\beta$ -D-glucopyranosyl ester (125)	<i>D. kaki</i>	Zhang <i>et al.</i> , 2018
kakisaponin IV (126)	<i>D. kaki</i>	Zhang <i>et al.</i> , 2018
8. Taraxerane type		
3 $\beta$ -taraxerol (127)	<i>D. filipendula</i>	Wisetsai <i>et al.</i> , 2021
	<i>D. gracilipes</i>	Rasamison <i>et al.</i> , 2016
taraxeryl acetate (128)	<i>D. filipendula</i>	Wisetsai <i>et al.</i> , 2021
3 $\beta$ - <i>E</i> -coumaroyltaraxerol (129)	<i>D. gracilipes</i>	Rasamison <i>et al.</i> , 2016
3 $\alpha$ -taraxerol (130)	<i>D. gracilipes</i>	Rasamison <i>et al.</i> , 2016
9. Ursane type		
$\alpha$ -amyrin (131)	<i>D. burmanica</i>	Choi <i>et al.</i> , 2015
	<i>D. soubreana</i>	Blanchard <i>et al.</i> , 2018
uvaol (132)	<i>D. fragrans</i>	Tameye <i>et al.</i> , 2022
	<i>D. iturensis</i>	Feusso <i>et al.</i> , 2020
ursolic acid (133)	<i>D. discolor</i>	Somat <i>et al.</i> , 2020
	<i>D. fragrans</i>	Tameye <i>et al.</i> , 2022
	<i>D. gillettii</i>	Tameye <i>et al.</i> , 2020

**Table 2.** Distribution of triterpenoids in the genus *Diospyros* (continued)

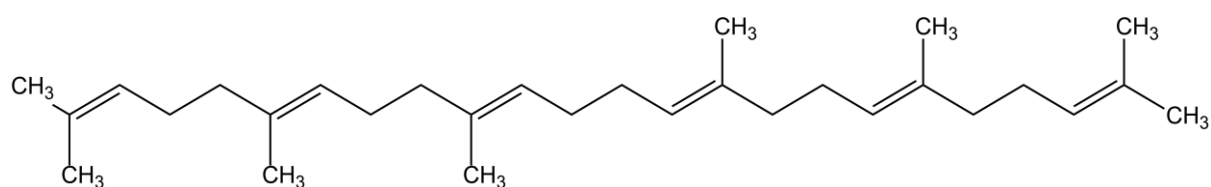
Compounds	Species	References
ursolic acid (133)	<i>D. gracilipes</i>	Rasamison <i>et al.</i> , 2016
	<i>D. iturensis</i>	Feusso <i>et al.</i> , 2020
	<i>D. melanoxylon</i>	Sharma <i>et al.</i> , 2018
	<i>D. zenkeri</i>	Feusso <i>et al.</i> , 2019
(3 $\beta$ )-3-(acetyloxy)-urs-12-en-28-oic acid (134)	<i>D. glans</i>	Peyrat <i>et al.</i> , 2016
corosolic acid (135)	<i>D. fragrans</i>	Tameye <i>et al.</i> , 2022
	<i>D. gillettii</i>	Tameye <i>et al.</i> , 2020
	<i>D. gracilipes</i>	Rasamison <i>et al.</i> , 2016
	<i>D. iturensis</i>	Feusso <i>et al.</i> , 2020
	<i>D. kaki</i>	Kim <i>et al.</i> , 2016
$\alpha$ -amyrenone (136)	<i>D. iturensis</i>	Feusso <i>et al.</i> , 2020
13,28-epoxyurs-11-ene-3,28-dione (137)	<i>D. glans</i>	Peyrat <i>et al.</i> , 2016
myrtifolic acid (138)	<i>D. fragrans</i>	Tameye <i>et al.</i> , 2022
11-oxo-acetyl ursolic acid (139)	<i>D. glans</i>	Peyrat <i>et al.</i> , 2016
actinidic acid (140)	<i>D. iturensis</i>	Feusso <i>et al.</i> , 2020
kakisaponin A (141)	<i>D. kaki</i>	Zhang <i>et al.</i> , 2018
2 $\alpha$ , 3 $\alpha$ , 19 $\alpha$ , 23-tetrahydroxyurs-12-en-28-oic acid-O- $\beta$ -D-glucopyranosyl ester (142)	<i>D. kaki</i>	Zhang <i>et al.</i> , 2018
2 $\alpha$ , 3 $\alpha$ , 19 $\alpha$ , 24-tetrahydroxyurs-12-en-28-oic acid-28-O- $\beta$ -D-glucopyranosyl ester (143)	<i>D. kaki</i>	Zhang <i>et al.</i> , 2018
rotungenic acid 28-O- $\alpha$ -L-rhamnopyranosyl-(1 $\rightarrow$ 2)- $\beta$ -D-glucopyranoside (144)	<i>D. kaki</i>	Zhang <i>et al.</i> , 2018
niga-ichigoside F <sub>1</sub> (145)	<i>D. kaki</i>	Zhang <i>et al.</i> , 2018



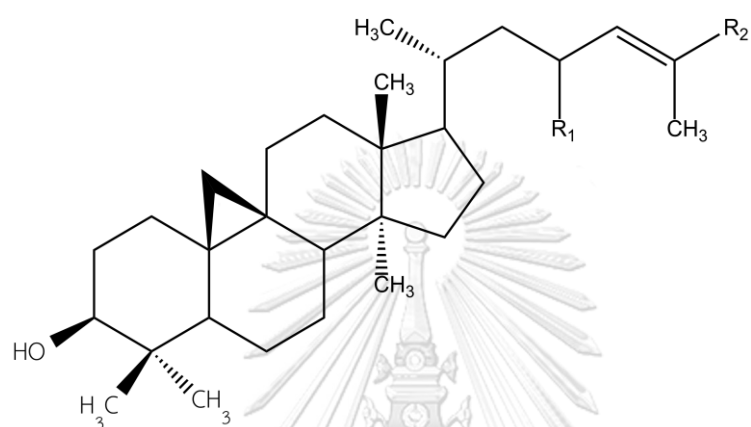
**Table 2.** Distribution of triterpenoids in the genus *Diospyros* (continued)

Compounds	Species	References
28- <i>O</i> - $\alpha$ -L-rhamnopyranosyl(1 $\rightarrow$ 2)- $\beta$ -D-glucopyranoside tormentic acid ester (146)	<i>D. kaki</i>	Zhang <i>et al.</i> , 2018
vismiaefolic acid (147)	<i>D. fragrans</i>	Tameye <i>et al.</i> , 2022
kakisaponin VI (148)	<i>D. kaki</i>	Zhang <i>et al.</i> , 2018
kakisaponin I (149)	<i>D. kaki</i>	Zhang <i>et al.</i> , 2018
kakisaponin III (150)	<i>D. kaki</i>	Zhang <i>et al.</i> , 2018
kakisaponin V (151)	<i>D. kaki</i>	Zhang <i>et al.</i> , 2018
kakisaponin B (152)	<i>D. kaki</i>	Zhang <i>et al.</i> , 2018
kakisaponin II (153)	<i>D. kaki</i>	Zhang <i>et al.</i> , 2018





squalene (83)

cycloart-24-en-3 $\beta$ ,26-diol (84)

R <sub>1</sub>	R <sub>2</sub>
H	CH <sub>2</sub> OH

(24*E*)-3-hydroxycycloart-24-en-26-al (85)

H	CHO
---	-----

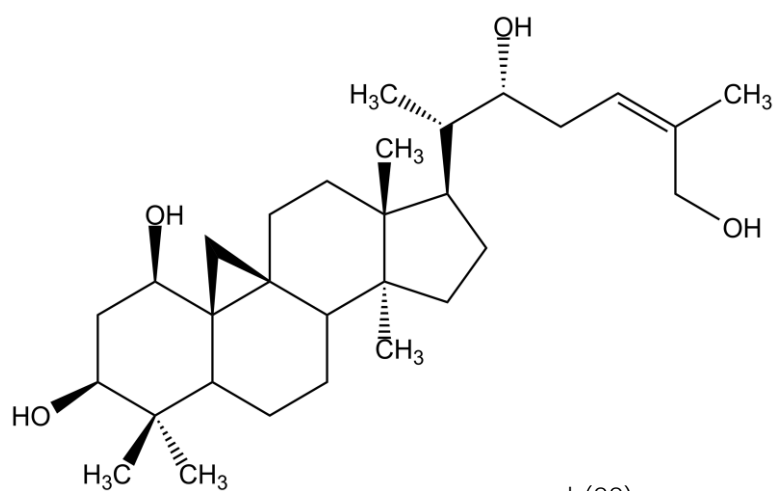
mangiferolic acid (86)

H	COOH
---	------

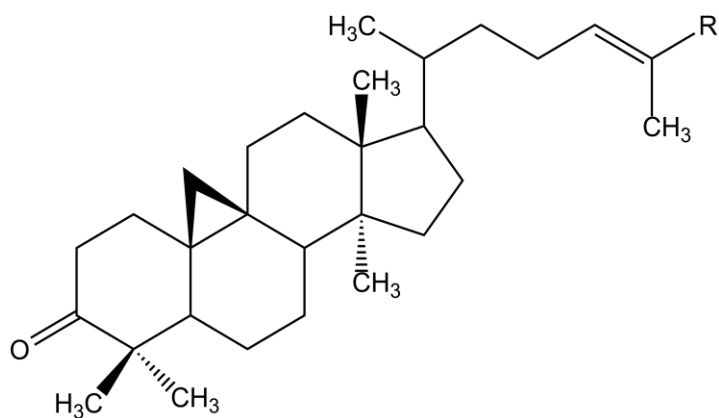
3 $\beta$ ,23-dihydroxy-cycloart-24*E*-en-26-oic acid (87)

OH	COOH
----	------

จุฬาลงกรณ์มหาวิทยาลัย  
CHULALONGKORN UNIVERSITY

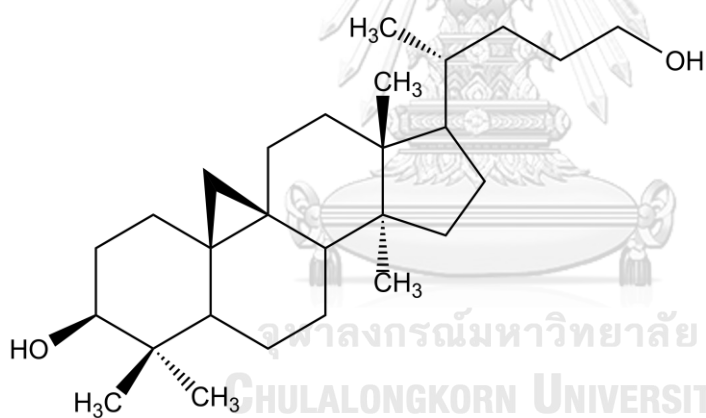
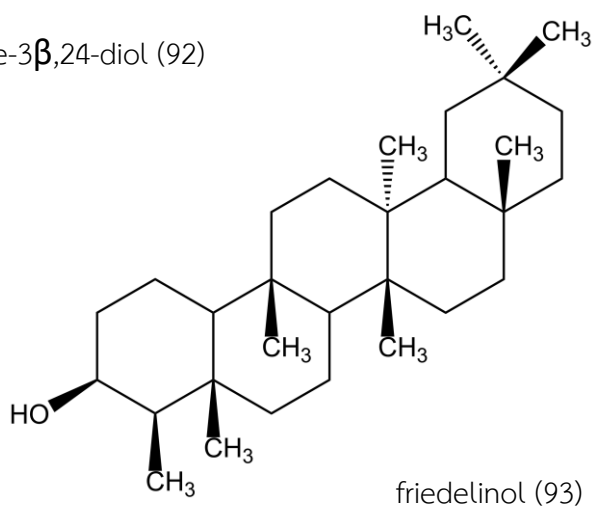


conocarpol (88)

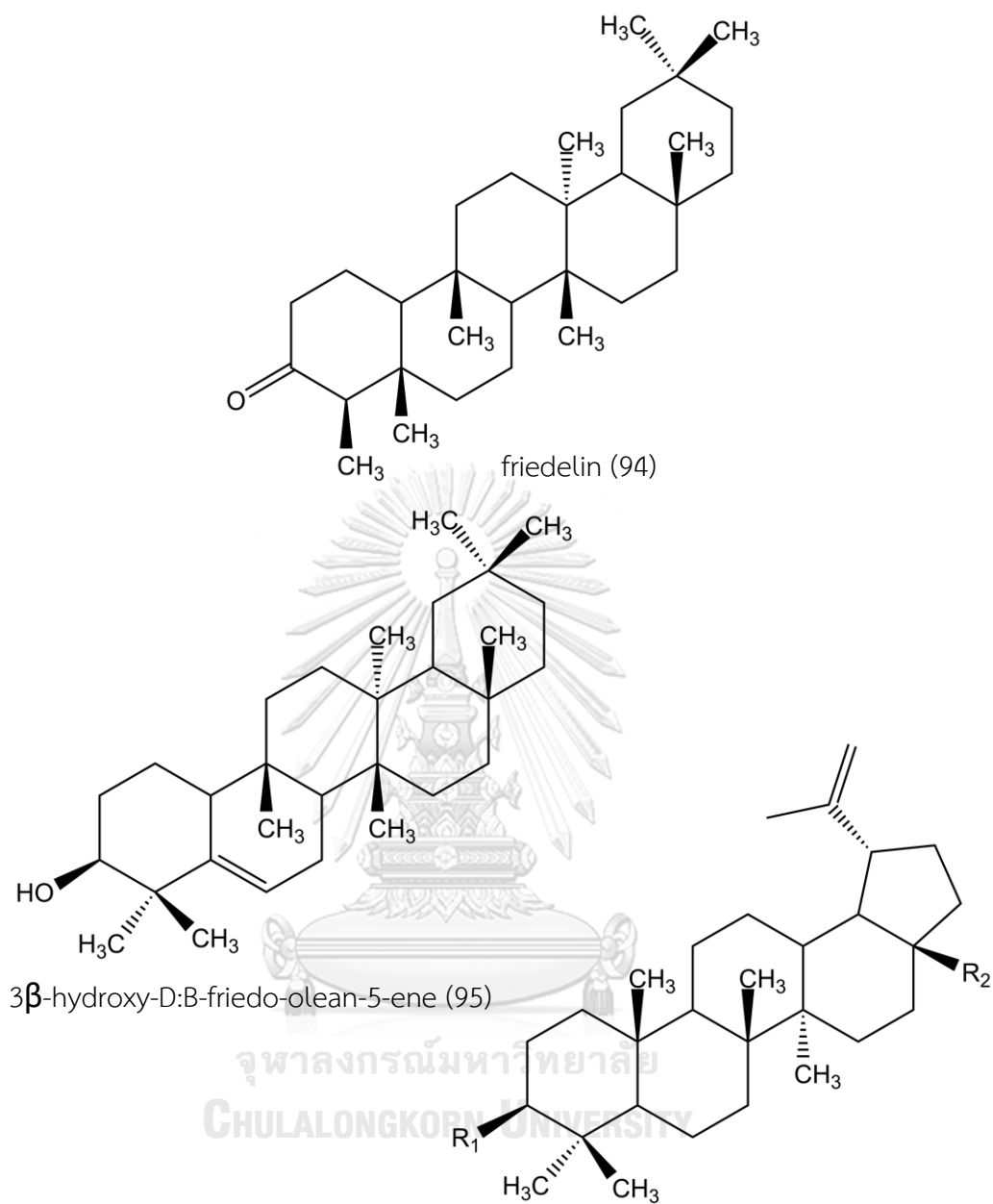


R

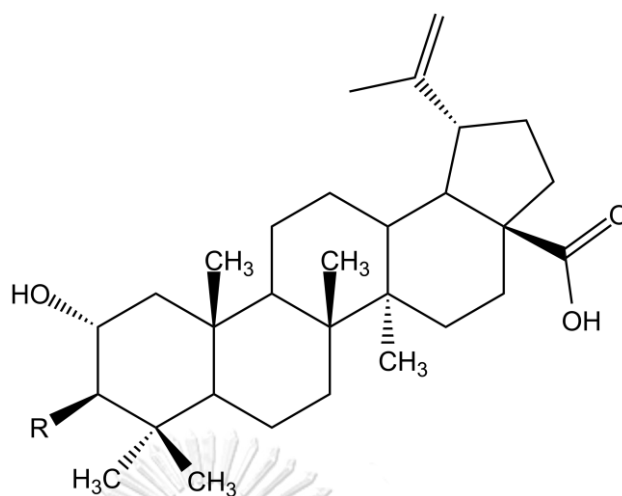
(24 <i>E</i> )-cycloart-24-en-26-ol-3-one (89)	CH <sub>2</sub> OH
(24 <i>E</i> )-3-oxocycloart-24-en-26-al (90)	CHO
mangiferonic acid (91)	COOH

4,4,14-trimethyl-9,19-cyclocholane-3 $\beta$ ,24-diol (92)

friedelinol (93)



	R <sub>1</sub>	R <sub>2</sub>
lupeol (96)	OH	CH <sub>3</sub>
lupeol acetate (97)	OAc	CH <sub>3</sub>
lupeol caffeate (98)	O- <i>trans</i> -caffeoyl	CH <sub>3</sub>
betulin (99)	OH	CH <sub>2</sub> OH
28-O-acetylbetulin (100)	OH	OAc
betunaldehyde (101)	OH	CHO
betulinic acid (102)	OH	COOH
3-O- <i>trans</i> -caffeoylbetulinic acid (103)	O- <i>trans</i> -caffeoyl	COOH



alphitolic acid (104)

3-*O*-*cis*-*p*-coumaroylalphitolic acid (105)

3-*O*-*trans*-*p*-coumaroylalphitolic acid (106)

eucalyptic acid (107)

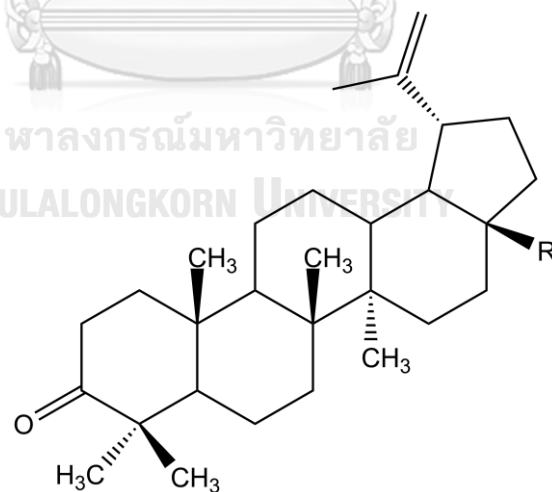
R

OH

*O*-*cis*-*p*-coumaroyl

*O*-*trans*-*p*-coumaroyl

*O*-*trans*-feruloyl



lupenone (108)

betulonaldehyde (109)

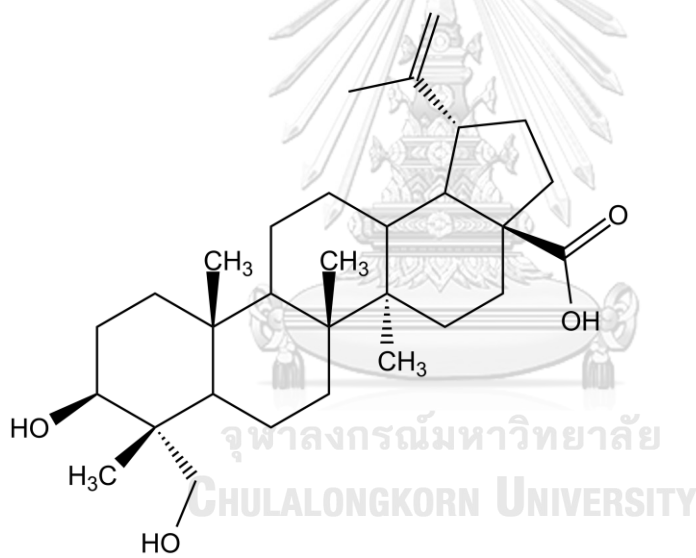
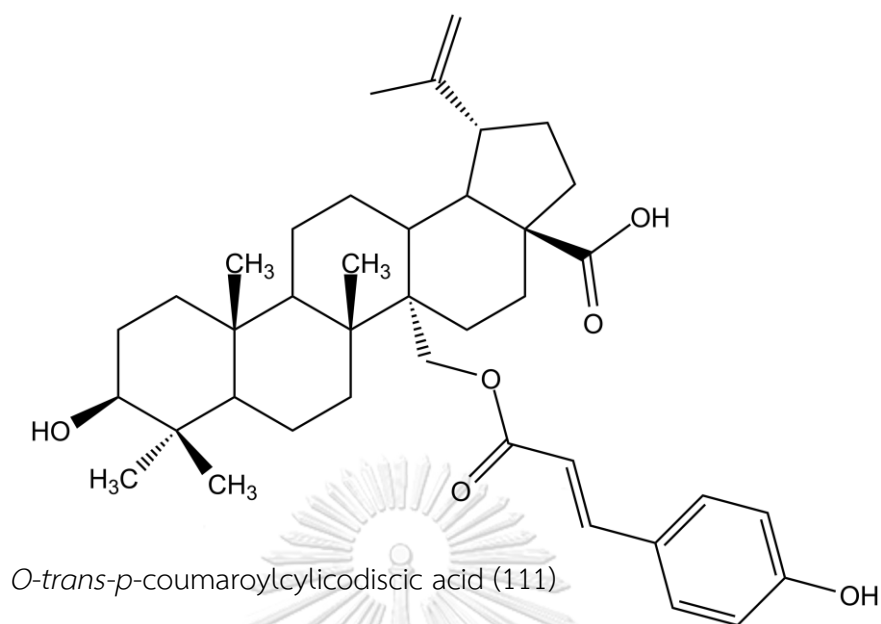
methyl lup-20(29)-en-3-on-28-oate (110)

R

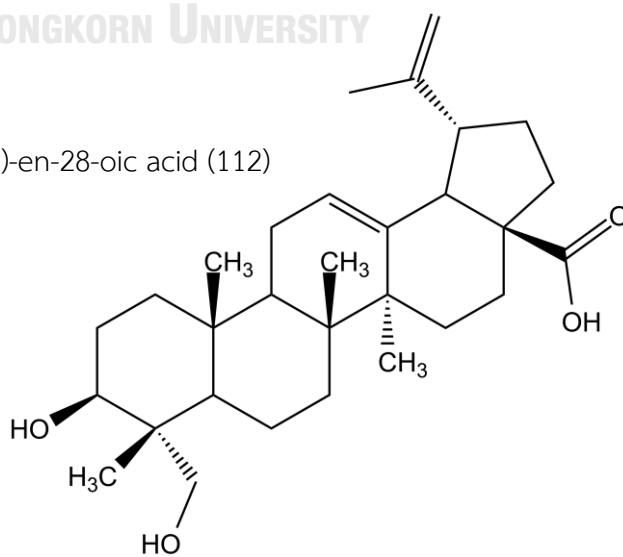
CH<sub>3</sub>

CHO

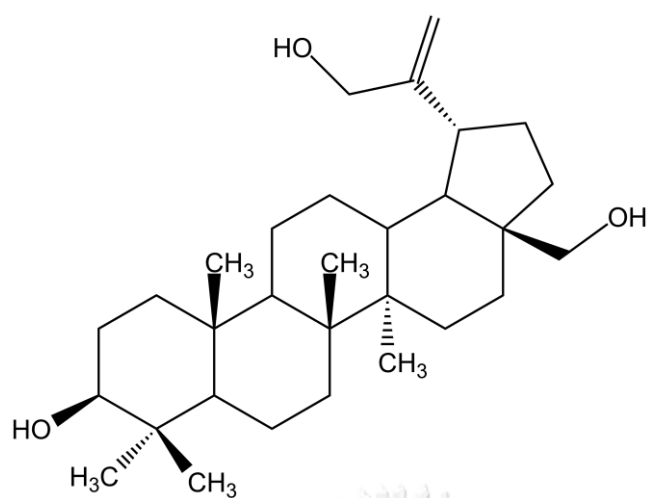
COOCH<sub>3</sub>



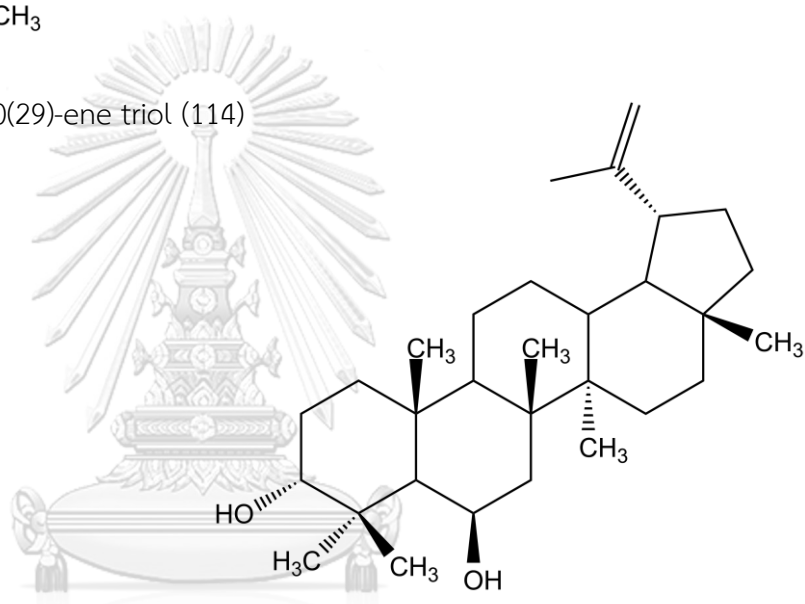
$(3\beta)$ -3,23-dihydroxylup-20(29)-en-28-oic acid (112)



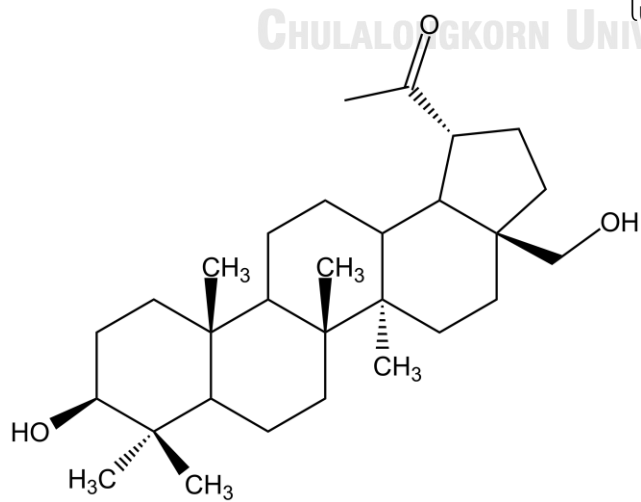
$(3\beta)$ -3,23-dihydroxylup-12,20(29)-dien-28-oic acid (113)



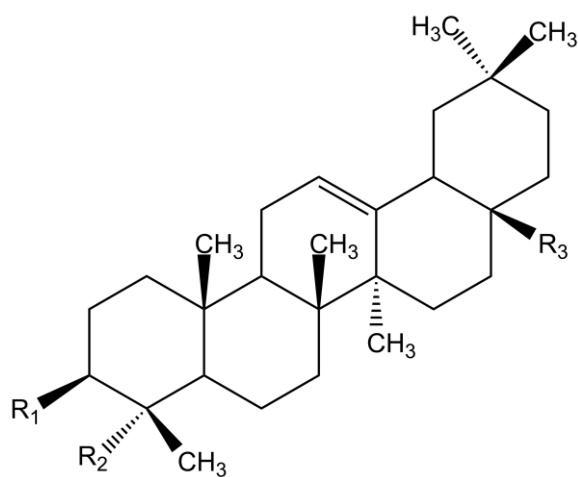
3 $\beta$ ,28,30-lup-20(29)-ene triol (114)



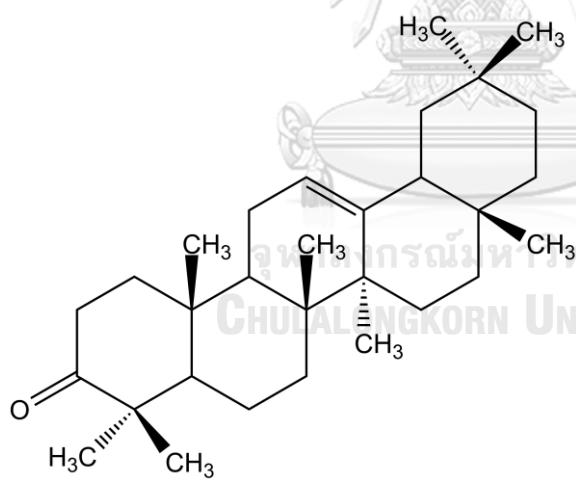
lup-20(29)-ene-3 $\alpha$ ,6 $\beta$ -diol (115)



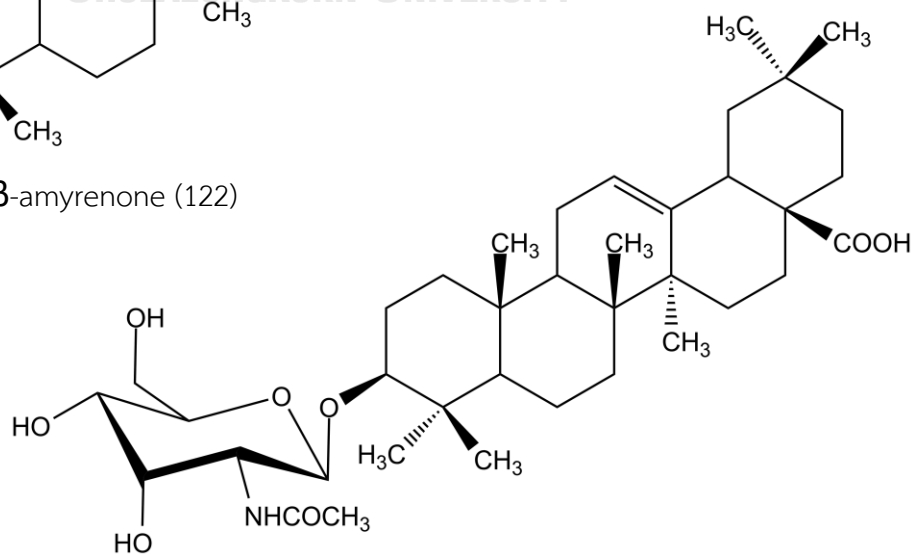
messagenin (116)



	R <sub>1</sub>	R <sub>2</sub>	R <sub>3</sub>
$\beta$ -amyrin (117)	OH	CH <sub>3</sub>	CH <sub>3</sub>
$\beta$ -amyrin acetate (118)	OAc	CH <sub>3</sub>	CH <sub>3</sub>
oleanolic acid (123)	OH	CH <sub>3</sub>	COOH
hederagenin (121)	OH	CH <sub>2</sub> OH	COOH

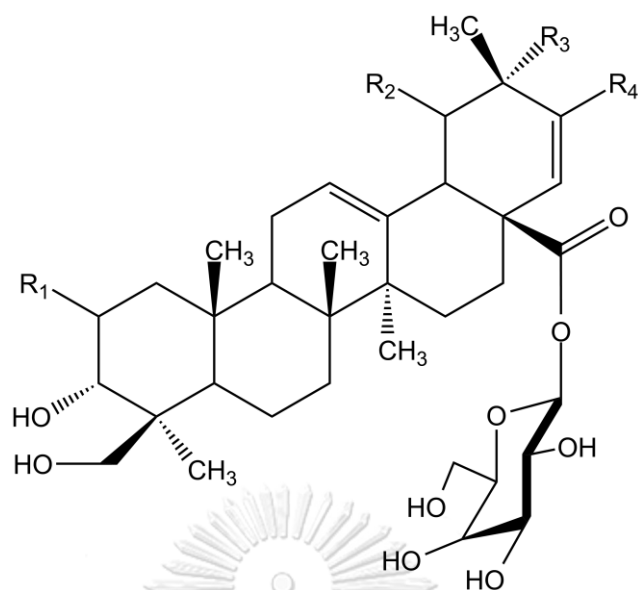


$\beta$ -amyrenone (122)



aridanin (123)





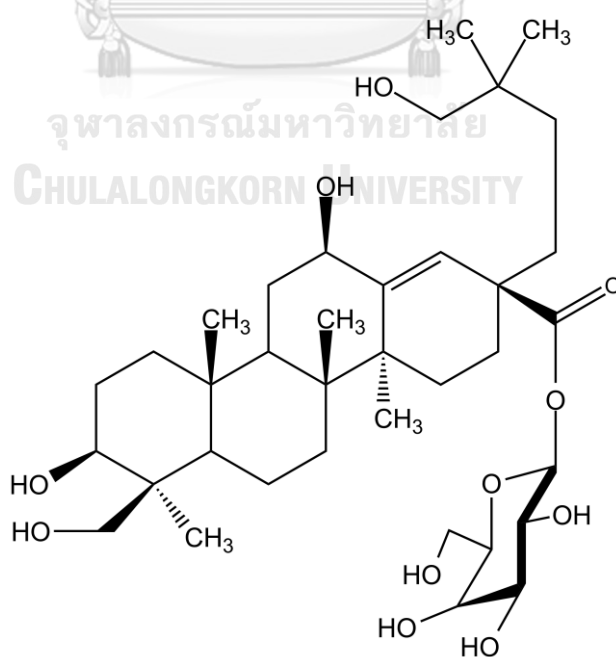
kakisaponin VII (123)

ryobunin C (124)

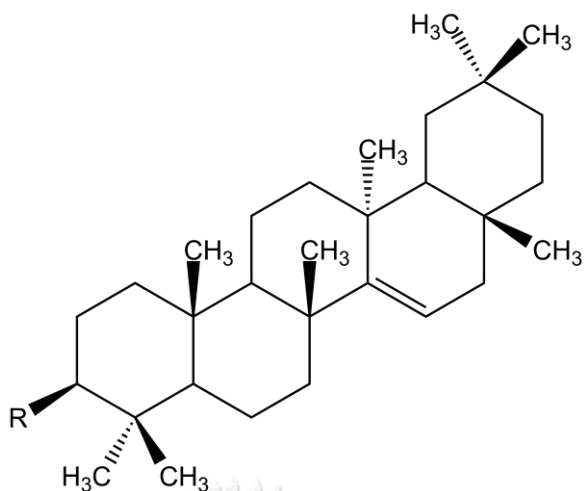
2 $\alpha$ , 3 $\alpha$ , 19 $\alpha$ , 24-tetrahydroxyolea-12-en-28-oic acid-

$\beta$ -D-glucopyranosyl ester (125)

R <sub>1</sub>	R <sub>2</sub>	R <sub>3</sub>	R <sub>4</sub>
H	H	CH <sub>2</sub> OH	H
H	$\alpha$ -OH	CH <sub>3</sub>	$\alpha$ -OH
$\alpha$ -OH	$\alpha$ -OH	CH <sub>3</sub>	H



kakisaponin IV (126)



$3\beta$ -taraxerol (127)

taraxeryl acetate (128)

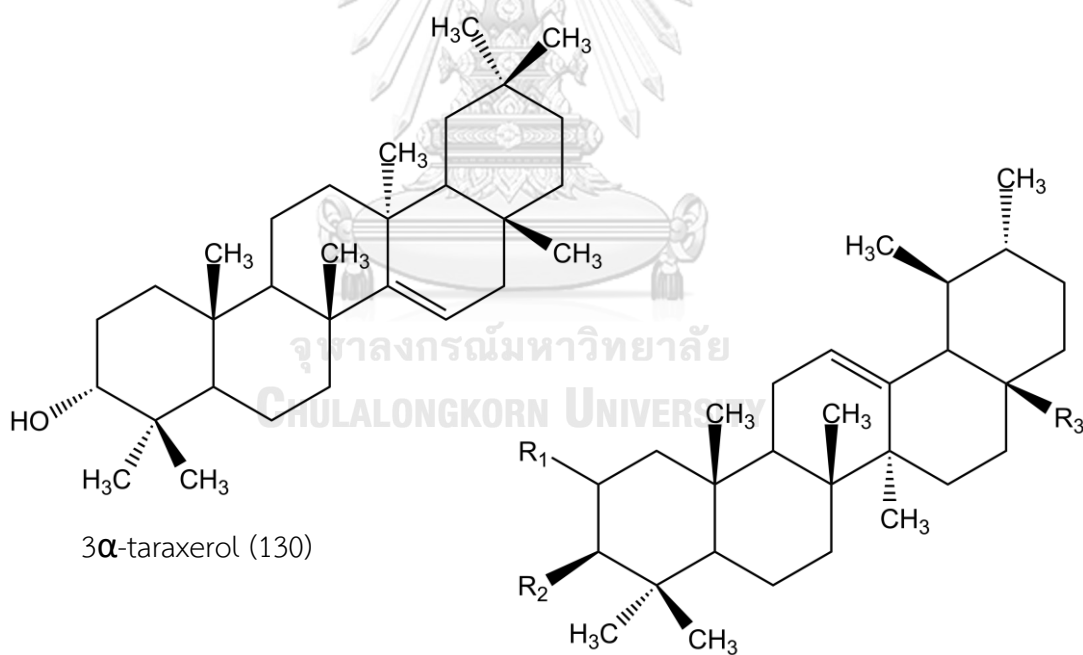
$3\beta$ -*E*-coumaroyltaraxerol (129)

R

OH

OAc

*O-trans-p*-coumaroyl



$3\alpha$ -taraxerol (130)

$\alpha$ -amyrin (131)

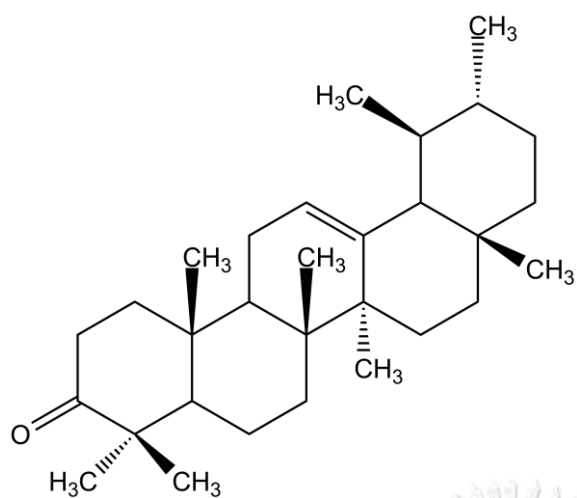
uvaol (132)

ursolic acid (133)

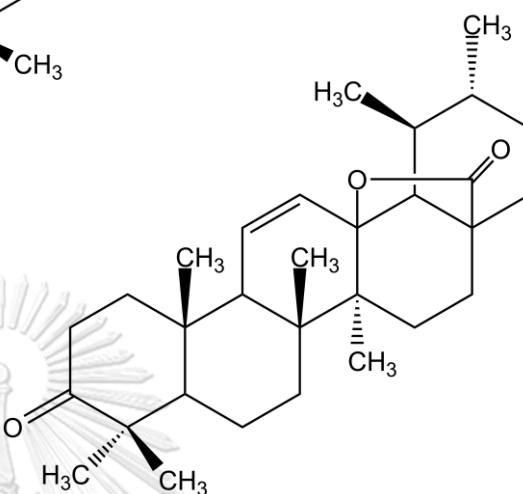
( $3\beta$ )-3-(acetyloxy)-urs-12-en-28-oic acid (134)

corosolic acid (135)

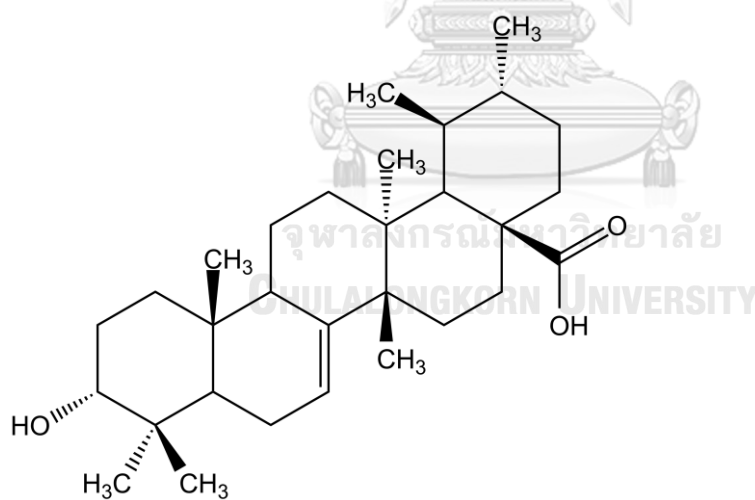
	R <sub>1</sub>	R <sub>2</sub>	R <sub>3</sub>
$\alpha$ -amyrin (131)	H	OH	CH <sub>3</sub>
uvaol (132)	H	OH	CH <sub>2</sub> OH
ursolic acid (133)	H	OH	COOH
( $3\beta$ )-3-(acetyloxy)-urs-12-en-28-oic acid (134)	H	OAc	COOH
corosolic acid (135)	$\alpha$ -OH	OH	COOH



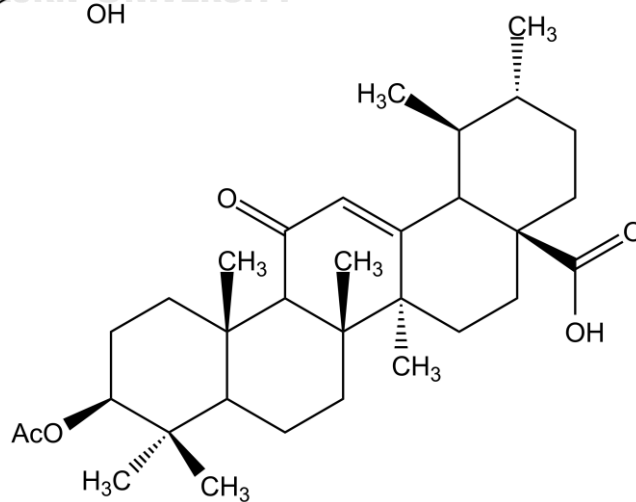
$\alpha$ -amyrenone (136)



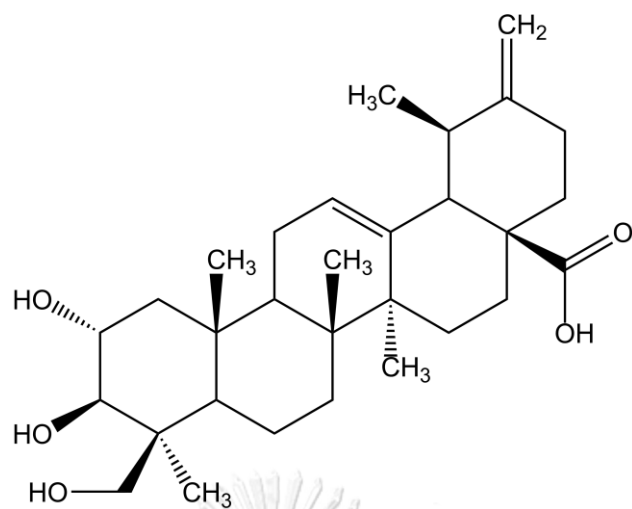
13,28-epoxyurs-11-ene-3,28-dione (137)



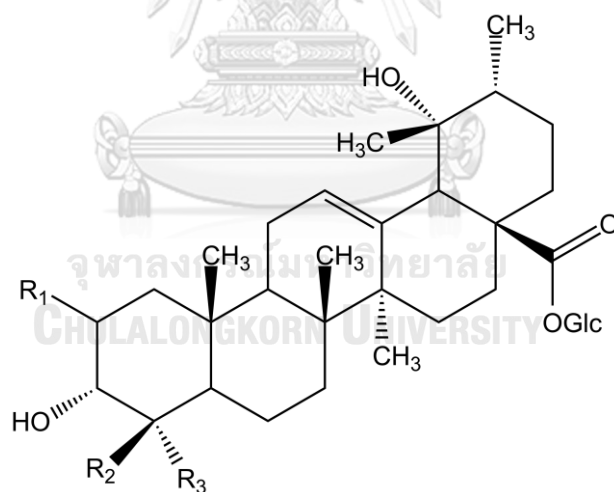
myrtifolic acid (138)



11-oxo-acetyl ursolic acid (139)



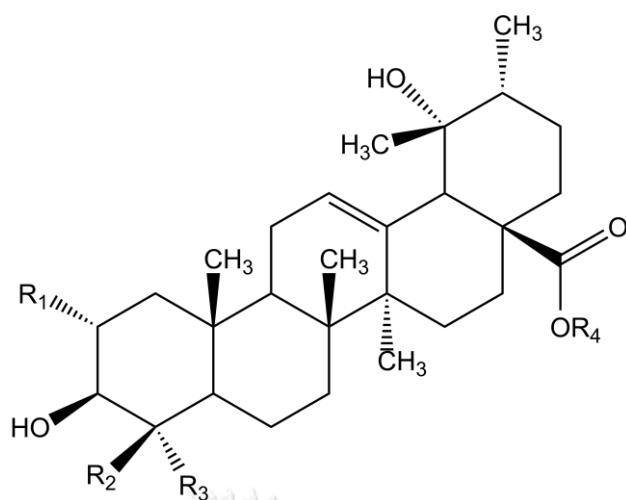
actinidic acid (140)



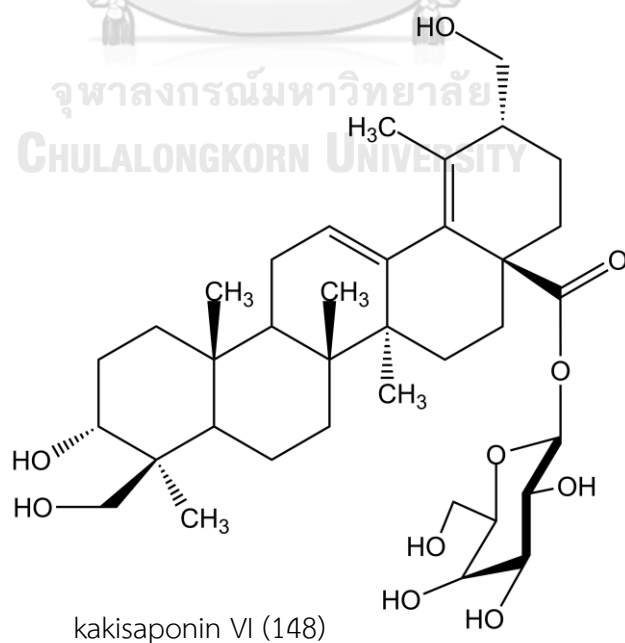
kakisaponin A (141)

 $2\alpha, 3\alpha, 19\alpha, 23$ - tetrahydroxyurs-12-en-28-oic acid- $O$ - $\beta$ -D-glucopyranosyl ester (142) $2\alpha, 3\alpha, 19\alpha, 24$ -tetrahydroxyurs-12- en-28-oic acid-28- $O$ - $\beta$ -D-glucopyranosyl ester (143)

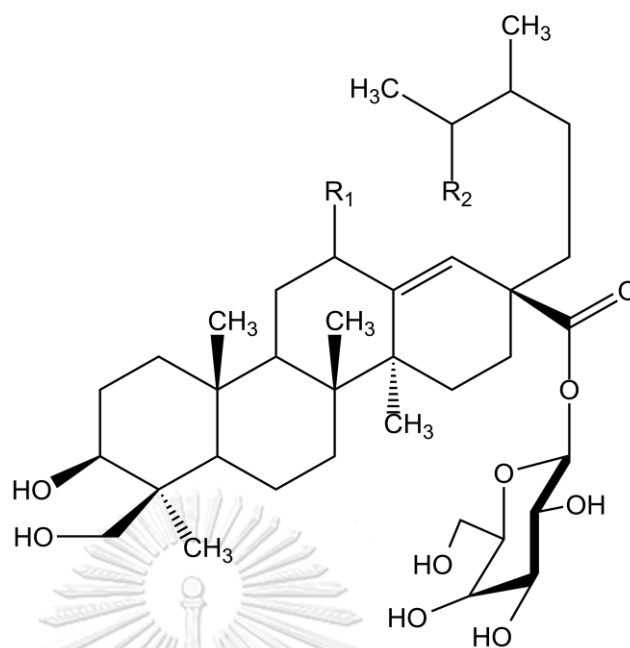
$R_1$	$R_2$	$R_3$
H	$CH_2OH$	$CH_3$
$\alpha$ -OH	$CH_3$	$CH_2OH$
$\alpha$ -OH	$CH_2OH$	$CH_3$



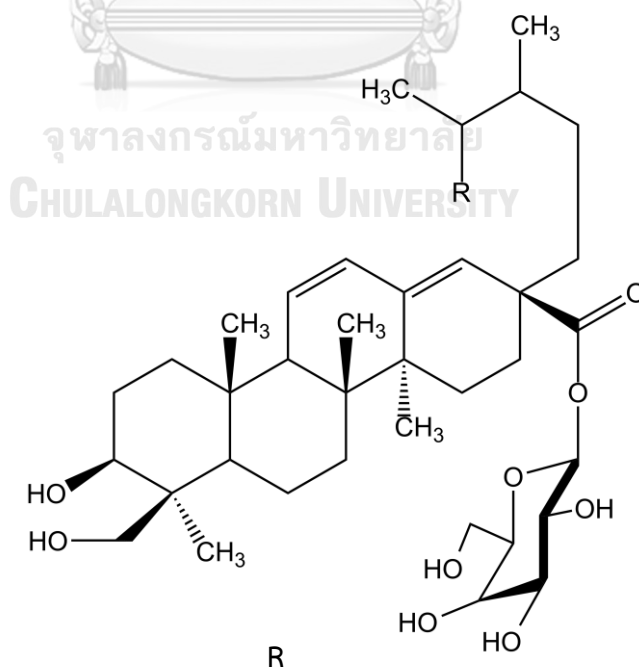
	R <sub>1</sub>	R <sub>2</sub>	R <sub>3</sub>	R <sub>4</sub>
rotungenic acid 28-O- $\alpha$ -L-rhamnopyranosyl-(1 $\rightarrow$ 2)- $\beta$ -D-glucopyranoside (144)	H	CH <sub>2</sub> OH	CH <sub>3</sub>	Glc-Rha
niga-ichigoside F <sub>1</sub> (145)	OH	CH <sub>3</sub>	CH <sub>2</sub> OH	Glc
28-O- $\alpha$ -L-rhamnopyranosyl(1 $\rightarrow$ 2)- $\beta$ -D-glucopyranoside tormentic acid ester (146)	OH	CH <sub>3</sub>	CH <sub>3</sub>	Glc-Rha
vismiaefolic acid (147)	OH	COOH	CH <sub>3</sub>	H



kakisaponin VI (148)



kakisaponin I (149)	$\beta$ -OH	OH
kakisaponin III (150)	$\beta$ -OH	=O
kakisaponin V (151)	$\alpha$ -OH	OH



kakisaponin B (152)	OH
kakisaponin II (153)	=O

## 2. Biological and Pharmacological Activities of *Diospyros* Plants

Plants belonging to the *Diospyros* genus have been widely utilized in folk medicine for the treatment of various diseases. Previous studies on the chemical compounds isolated from this genus have revealed their remarkable biological and pharmacological activities. The interest in the activities of *Diospyros* species continues unabated, with recent findings enriching the existing knowledge and providing promising avenues for future research (Fareed *et al.*, 2022; Ribeiro *et al.*, 2023). A summary on biological and pharmacological activities of *Diospyros* species, focusing on post-2012 research, is presented in **Table 3**.



**Table 3.** Biological and pharmacological activities of extracts from *Diospyros* species

Species	Part of plants	Activity	Reference
<i>D. bipindensis</i>	stem bark	anti-inflammatory	Cesari <i>et al.</i> , 2013
		anti-microbial	Cesari <i>et al.</i> , 2013
		antioxidant	Cesari <i>et al.</i> , 2013
<i>D. canaliculata</i>	stem bark	antiprotozoal	Lenta <i>et al.</i> , 2015
<i>D. carbonaria</i>	bark	antiviral	Peyrat <i>et al.</i> , 2017
<i>D. discolor</i>	leaves and stem bark	acetylcholinesterase	Somat <i>et al.</i> , 2020
		inhibitory	
<i>D. dumetorum</i>	leaves	xanthine oxidase	Deng <i>et al.</i> , 2017
		inhibitory	
<i>D. fleuryana</i>	leaves	cytotoxic	Ha <i>et al.</i> , 2020
<i>D. fragrans</i>	leaves	antibacterial	Tameye <i>et al.</i> , 2022
<i>D. gracilescens</i>	trunk	anti-leishmanial	Njanpa <i>et al.</i> , 2021
<i>D. gracilipes</i>	stems and leaves	antimicrobial	Rasamison <i>et al.</i> , 2016
<i>D. iturensis</i>	leaves	antioxidant	Feusso <i>et al.</i> , 2020
<i>D. longiflora</i>	stem bark	antioxidant	Dongmo <i>et al.</i> , 2018
<i>D. lotus</i>	roots	anti-nociceptive	Uddin <i>et al.</i> , 2014
		anti-inflammatory	Uddin <i>et al.</i> , 2014
		sedative	Uddin <i>et al.</i> , 2014
<i>D. shimbaensis</i>	stem and root bark	cytotoxic	Aronsson <i>et al.</i> , 2016
<i>D. villosa</i>	leaves and stem bark	antioxidant	Adu <i>et al.</i> , 2022
		antimicrobial	Adu <i>et al.</i> , 2022
<i>D. virginiana</i>	fruits	antibacterial	Rashed <i>et al.</i> , 2014
		antifungal	Rashed <i>et al.</i> , 2014
<i>D. zenkeri</i>	leaves and twigs	antioxidant	Feusso <i>et al.</i> , 2019
		antiproliferative	Feusso <i>et al.</i> , 2019
		lipoxigenase	Feusso <i>et al.</i> , 2019
		inhibitory	



## CHAPTER III

### EXPERIMENTAL

#### 1. Source of Plant Material

The stem of *Diospyros gracilis* H.R. Fletcher were collected from Suan Luang Rama IX Royal Botanical Garden, Bangkok, Thailand on May 30, 2019. The plant was identified by Asst. Prof. Thaya Jenjittikul, Department of Plant Science, Faculty of Science, Mahidol University, Bangkok, and the voucher specimen was prepared and deposited at the Museum of Natural Medicine, Faculty of Pharmaceutical Sciences, Chulalongkorn University for future reference and verification.

#### 2. General Techniques

##### 2.1 Chromatographic Technique

##### 2.1.1 Thin-Layer Chromatography (TLC)

Technique	One dimension, ascending
Adsorbent	Silica gel 60 F <sub>254</sub> (E. Merck) precoated plates
Layer thickness	0.2 mm
Distance	5 cm
Temperature	25-35 °C (laboratory temperature)
Detection	<ol style="list-style-type: none"> <li>1) Visual detection under daylight</li> <li>2) Ultraviolet light (254 and 365 nm)</li> <li>3) Spraying with 10% sulfuric acid in ethanol and heating at 110 °C for 5-10 minutes</li> <li>4) Spraying with Liebermann-Burchard reagent and heating at 100 °C for 5-10 minutes, then detected under UV 365 nm</li> </ol>

### 2.1.2 Column Chromatography (CC)

Column	Flat bottom glass column (assorted diameters)
Adsorbent	Silica gel 60 (No. 9385, E. Merck) with a particle size of 0.040-0.063 mm (230 - 400 mesh ASTM)
Packing method	Wet packing
Sample loading	1) dry packing The sample was dissolved in a minimal amount of organic solvent, mixed with a small quantity of adsorbent, triturated, dried and then deposited on the top of the column.
	2) Wet packing The sample was dissolved in a limited volume of the eluent, then placed at the top of the column.

## 2.2 Spectroscopy

### 2.2.1 Infrared (IR) Absorption Spectra

Infrared (IR) spectra were acquired on a Bruker Alpha FTIR spectrometer with Platinum-ATR module (Pharma Nueva, Bangkok, Thailand).

### 2.2.2 Mass Spectra

Direct analysis in real time (DART) - time of flight (TOF) mass spectra were acquired on a JEOL AccuTOF™ LC-plus JMS-T100LP (Faculty of Science, Chulalongkorn University).

### 2.2.3 Proton and Carbon-13 Nuclear Magnetic Resonance ( $^1\text{H}$ and $^{13}\text{C}$ NMR) Spectra

$^1\text{H}$  NMR and  $^{13}\text{C}$  NMR spectra were acquired on a Bruker Ascend 400 MHz NMR spectrometer (Faculty of Pharmaceutical Sciences, Chulalongkorn University).

The NMR solvent used in the experiment was  $\text{CDCl}_3$ . The chemical shifts were reported in ppm, using the chemical shift of the solvent as the reference signal.

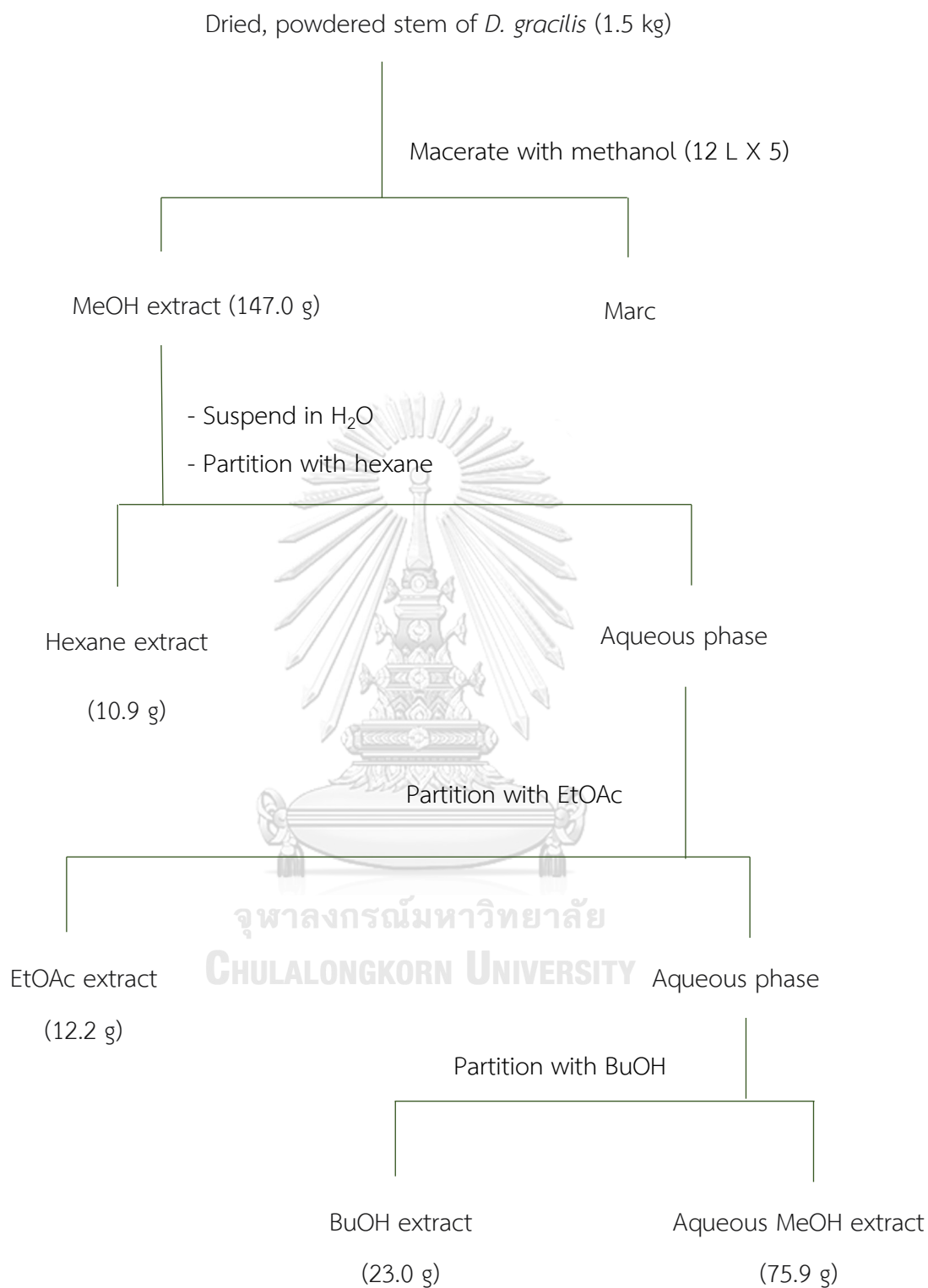
### 2.3 Solvent

All organic solvents used in this research work were of commercial grade and were redistilled prior to use.

## 3. Extraction and Isolation

### 3.1 Extraction

Dried and powdered stems of *Diospyros gracilis* (1.5 kg) were macerated with methanol (12 L x 5, 3 days each) at room temperature. The resulting extracts were combined and evaporated under reduced pressure to yield 147.0 g of dried crude methanol extract (9.8% of dry plant weight). The crude extract was suspended in water and then partitioned with hexane (300 mL x 15) to yield hexane extract (10.9 g, 0.7% of dry weight). The remaining aqueous layer was further partitioned with EtOAc (300 mL x 7) and then BuOH (4 mL x 4) to yield EtOAc extract (12.2 g, 0.8% of dry weight) and BuOH extract (23.0 g, 1.5% of dry weight), along with an aqueous methanol extract (75.9 g, 5.1% of dry weight).



**Scheme 1.** Extraction of *D. gracilis* stem

### 3.2 Isolation

A portion of the EtOAc extract (10.0 g) was fractionated on a silica gel column (400 g, 10 x 14 cm) which was eluted with a series of CH<sub>2</sub>Cl<sub>2</sub>-MeOH mixtures of increasing polarity, ranging from CH<sub>2</sub>Cl<sub>2</sub>-MeOH (1:0) to CH<sub>2</sub>Cl<sub>2</sub>-MeOH (13:7). A total of 80 fractions (50 mL each) were collected and combined into fourteen major fractions (E1-E14) based on their TLC patterns, as shown in **Table 4**. Afterward, the column was washed down with MeOH.

**Table 4.** Combined fractions from the EtOAc extract

Fraction	Number of eluates	Weight (g)
E1	1-2	0.02
E2	3-4	0.04
E3	5-6	0.05
E4	7-11	0.17
E5	12-13	0.08
E6	14-22	0.23
E7	23-28	0.15
E8	29-31	0.18
E9	32-34	0.47
E10	35-39	1.18
E11	40-49	2.78
E12	50-59	0.62
E13	60-74	1.15
E14	75-80	0.34
MeOH eluate		1.95

#### 1. Isolation of Compounds DG01 - DG04

Fraction E6 (0.23 g) was subjected to silica gel column chromatography. The column (60 g, 3 x 18 cm) was eluted with gradient mixtures of CH<sub>2</sub>Cl<sub>2</sub>-MeOH (1:0→4:1). Twenty-one fractions (50 ml each) were collected and then combined

based on their TLC patterns into five major fractions (E6A-E6E) as shown in **Table 5**. The column was then washed down with MeOH.

**Table 5.** Combined fractions from E6

Fraction	Number of eluates	Weight (mg)
E6A	1-2	115.9
E6B	3	6.6
E6C	4-6	75.7
E6D	7-9	18.9
E6E	10-21	14.0
MeOH eluate		12.3

Fraction E6A (115.9 mg) was subjected to silica gel column chromatography. The column (4 g, 1 x 11 cm) was eluted with hexane - EtOAc (19:1). A total of 26 fractions (2 ml each) were collected and then combined based on their TLC patterns into eight major fractions (E6A1-E6A8) as shown in **Table 6**. The column was then washed down with MeOH.

**Table 6.** Combined fractions from E6A

Fraction	Number of eluates	Weight (mg)
E6A1	1-5	5.3
E6A2	6-7	0.9
E6A3	8-9	1.3
E6A4	10	3.1
E6A5	11-12	3.6
E6A6	13-15	17.9
E6A7	16-22	68.4
E6A8	23-26	1.5
MeOH Eluate		12.7

Compound DG01 (5.3 mg) was obtained as colorless needles from fraction E6A1 after removal of the eluent. The compound gave a pale orange spot with 10% sulfuric acid in ethanol reagent and a blue fluorescent spot under UV 365 nm upon detection with Liebermann-Burchard reagent.

Compound DG02 (3.1 mg) was obtained as white amorphous powder from fraction E6A4 after removal of the eluent. The compound gave an orange spot with 10% sulfuric acid in ethanol reagent and a blue fluorescent spot under UV 365 nm upon detection with Liebermann-Burchard reagent.

Compound DG03 (68.4 mg) was obtained as colorless needles from fraction E6A7 after removal of the eluent. The compound gave a reddish orange spot with 10% sulfuric acid in ethanol reagent and a pink fluorescent spot under UV 365 nm upon detection with Liebermann-Burchard reagent.

After the eluent was removed from fraction E6D, compound DC04 (18.9 mg) was obtained as colorless needle crystals which gave a brownish purple spot with 10% sulfuric acid in ethanol reagent and a blue fluorescent spot when detected with Liebermann-Burchard reagent under UV 365 nm.

## 2. Isolation of Compound DG05

Fraction E11 (2.78 g) was separated on a silica gel column (150 g, 4.6 x 17 cm). Elution was carried out with progressively increasing polarity, ranging from a CH<sub>2</sub>Cl<sub>2</sub>-EtOAc-MeOH ratio of 1:0:0 to 0:1:4. A total of 104 fractions (50 ml each) were collected and then combined into six major fractions (E11A-E11F) based on their TLC patterns, as shown in **Table 7**. The column was then washed down with MeOH.

**Table 7.** Combined fractions from E11.

Fraction	Number of eluates	Weight (mg)
E11A	1-5	3.8
E11B	6-15	26.6
E11C	16-72	666.8
E11D	73-86	176.3
E11E	87-98	571.8
E11F	99-104	81.3
MeOH Eluate		32.3

Fraction E11C (666.8 mg) was purified by recrystallization in methanol to give compound DG05 (401.3 mg) as colorless needles. This compound gave a reddish purple color with 10% sulfuric acid in ethanol reagent and a light blue fluorescent spot under UV 365 nm upon detection with Liebermann-Burchard reagent.

### 3. Isolation of Compound DG06

Fraction E4 (0.17 g) was chromatographed on a silica gel column (50 g, 3 x 14 cm), eluted with mixtures of increasing polarity ranging from CH<sub>2</sub>Cl<sub>2</sub>-MeOH (1:0) to CH<sub>2</sub>Cl<sub>2</sub>-MeOH (9:1). A total of 14 fractions (50 ml each) were collected and then combined into four major fractions (E4A-E4D) based on their TLC patterns, as shown in **Table 8**. The column was then washed down with MeOH.

**Table 8.** Combined fractions from E4

Fraction	Number of eluates	Weight (mg)
E4A	1-3	26.2
E4B	4	38.7
E4C	5-9	no data*
E4D	10-14	7.4
MeOH Eluate		13.9

\* The weight measurement before combining with fraction E5B was omitted.



Fraction E5 (76.5 mg) was processed through column chromatography on a silica gel column (50 g, 3 x 15 cm). The column was eluted with mixtures of increasing polarity, ranging from CH<sub>2</sub>Cl<sub>2</sub>-MeOH (1:0) to CH<sub>2</sub>Cl<sub>2</sub>-MeOH (9:1). A total of 14 fractions (50 ml each) were collected and then combined into four major fractions (E5A-E5D) based on their TLC patterns, as shown in **Table 9**. The column was then washed down with MeOH.

**Table 9.** Combined fractions from E5

Fraction	Number of eluates	Weight (mg)
E5A	1	0.9
E5B	2-4	no data*
E5C	5-8	3.6
E5D	9-14	3.8
MeOH Eluate		10.9

\* The weight measurement before combining with fraction E4C was omitted.

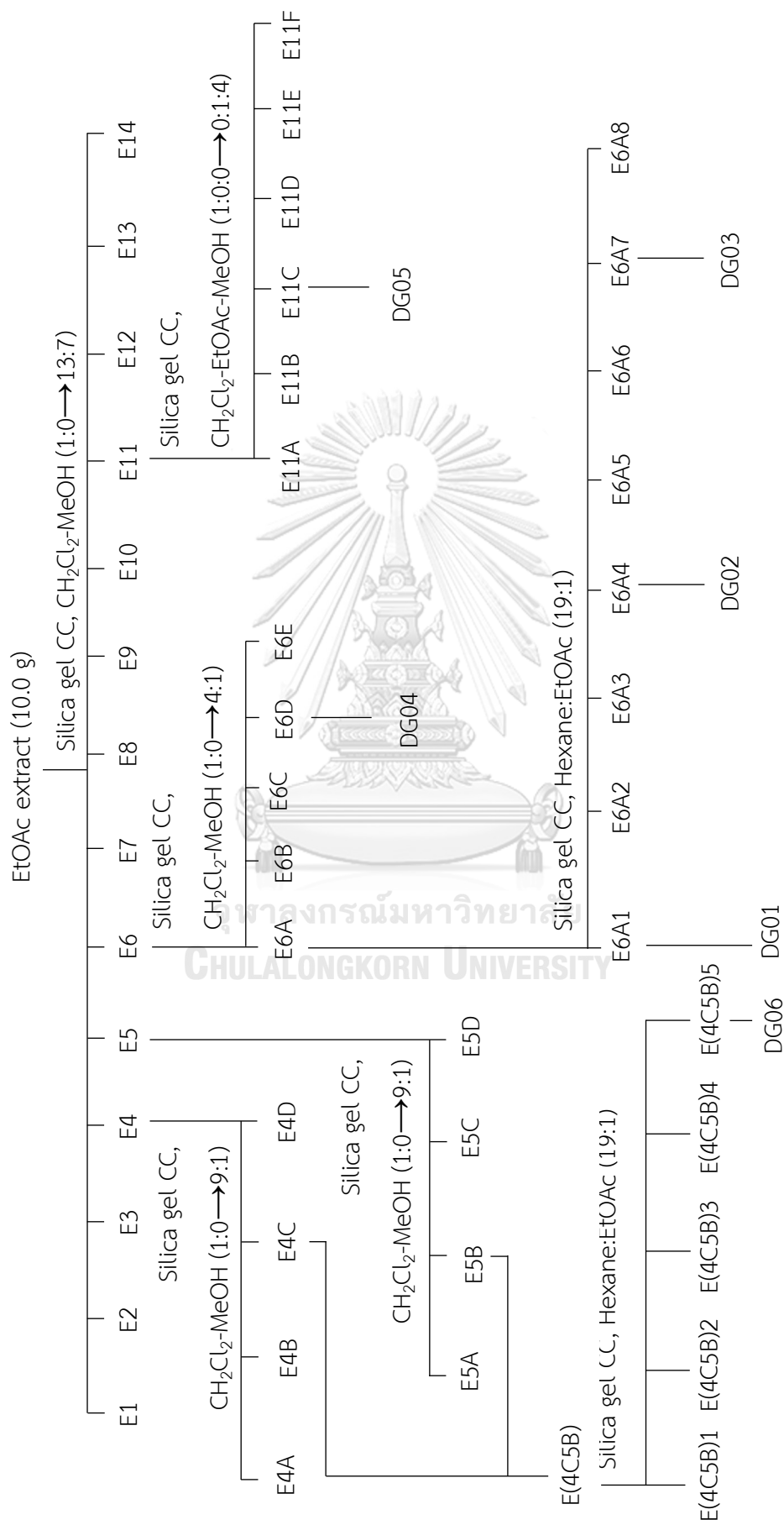
Fractions E4C and E5B which showed similar TLC patterns were combined (156.5 mg) and then separated on a silica gel column (4 g, 1 x 10.5 cm), eluted with hexane - EtOAc (95:5). A total of 15 fractions (2 ml each) were collected and then combined into five major fractions [E(4C5B)1-E(4C5B)5], as shown in **Table 10**. The column was then washed down with MeOH.

**Table 10.** Combined fractions from E(4C5B)

Fraction	Number of eluates	Weight (mg)
E(4C5B)1	1-3	2.7
E(4C5B)2	4-5	5.1
E(4C5B)3	6-9	113.6
E(4C5B)4	10-12	18.3
E(4C5B)5	13-15	3.2
MeOH Eluate		6.1

Compound DG06 (3.2 mg) was obtained from fraction E(4C5B)5 as a white amorphous powder after removal of the eluent. The compound gave a purple color with 10% sulfuric acid in ethanol reagent and a blue fluorescent spot under UV 365 nm upon detection with Liebermann-Burchard reagent.





**Scheme 2.** Isolation of the EtOAc extract

#### 4. Physical and Spectral Data of Isolated Compounds

##### 4.1 Compound DG01

Appearance	: colorless needles
Solubility	: soluble in hexane
IR $\nu_{\max}$ $\text{cm}^{-1}$	: 2924, 2856, 1715, 1459, 1389 ( <b>Figure 2</b> ).
$^1\text{H}$ NMR ( $\delta$ ppm, 400 MHz, $\text{CDCl}_3$ )	: 0.74 (s), 0.89 (s), 0.90 (d, $J = 6.4$ Hz), 0.97 (s), 1.02 (s), 1.03 (s), 1.07 (s), 1.20 (s), 1.71, 1.99 (m), 2.27, 2.33, 2.41 (ddd, $J = 11.6, 5.2, 2.0$ Hz) ( <b>Table 11</b> and <b>Figures 3a-3b</b> ).
$^{13}\text{C}$ NMR ( $\delta$ ppm, 100 MHz, $\text{CDCl}_3$ )	: 6.8, 14.7, 17.9, 18.2, 18.7, 20.3, 22.3, 28.2, 30.0, 30.5, 31.8, 32.1, 32.4, 32.8, 35.0, 35.3, 35.6, 36.0, 37.4, 38.3, 39.3, 39.7, 41.3, 41.5, 42.2, 42.8, 53.1, 58.2, 59.5, 213.3 ( <b>Table 11</b> and <b>Figures 4a-4b</b> ).
DART-TOF MS $m/z$	: 427.3926 $[\text{M}+\text{H}]^+$ ( <b>Figure 5</b> )

##### 4.2 Compound DG02

Appearance	: white amorphous powder
Solubility	: soluble in dichloromethane
IR $\nu_{\max}$ $\text{cm}^{-1}$	: 3400, 2924, 2851, 1449, 1386 ( <b>Figure 6</b> ).
$^1\text{H}$ NMR ( $\delta$ ppm, 400 MHz, $\text{CDCl}_3$ )	: 0.88 (s), 0.96 (d, $J = 6.8$ Hz), 0.97 (s), 0.99 (s), 1.01 (s), 1.02 (s), 1.03 (s), 1.19 (s), 3.76 ( $q$ -like, $J =$ 2.4 Hz) ( <b>Table 12</b> and <b>Figures 7a-7b</b> )
$^{13}\text{C}$ NMR ( $\delta$ ppm, 100 MHz, $\text{CDCl}_3$ )	: 11.6, 15.8, 16.4, 17.6, 18.3, 18.7, 20.1, 28.2, 30.0, 30.6, 31.8, 32.1, 32.3, 32.8, 35.0, 35.2, 35.3, 35.6, 36.1, 37.1, 37.8, 38.4, 39.3, 39.7, 41.7, 42.8, 49.2, 53.2, 61.3, 72.8 ( <b>Table 12</b> and <b>Figures 8a-8b</b> )
DART-TOF MS $m/z$	: 429.4007 $[\text{M}+\text{H}]^+$ ( <b>Figure 9</b> )

## 4.3 Compound DG03

Appearance : colorless needles

Solubility : soluble in dichloromethane

IR  $\nu_{\max}$   $\text{cm}^{-1}$  : 3369, 2940, 1454, 1386 (**Figure 10**).

$^1\text{H}$  NMR ( $\delta$  ppm, 400 MHz,  $\text{CDCl}_3$ ) : 0.70 (*br d*), 0.78 (*s*), 0.81(*s*), 0.85 (*s*), 0.96 (*s*), 0.98 (*s*), 1.05 (*s*), 1.34, 1.70 (*s*), 1.94 (*m*) 2.39 (*ddd*,  $J = 10.8, 10.8, 5.6$  Hz), 3.20 (*dd*,  $J = 11.2, 5.2$  Hz), 4.58 (*dd*,  $J = 4.2, 1.2$  Hz), 4.70 (*d*,  $J = 2.4$  Hz) (**Table 13** and **Figures 11a-11b**)

$^{13}\text{C}$  NMR ( $\delta$  ppm, 100 MHz,  $\text{CDCl}_3$ ) : 14.5, 15.3, 15.9, 16.1, 18, 18.3, 19.3, 20.9, 25.1, 27.4, 27.4, 28, 29.7, 34.2, 35.6, 37.1, 38.0, 38.7, 38.8, 40.0, 40.8, 42.8, 43.0, 48.0, 48.3, 50.4, 55.3, 79.0, 109.3, 151.0 (**Table 13** and **Figures 12a-12b**)

DART-TOF MS  $m/z$  : 427.3885  $[\text{M}+\text{H}]^+$  (**Figure 13**)

## 4.4 Compound DG04

Appearance : colorless needles

Solubility : soluble in dichloromethane, methanol

IR  $\nu_{\max}$   $\text{cm}^{-1}$  : 3295, 2924, 2863, 1636, 1456, 1374 (**Figure 14**).

$^1\text{H}$  NMR ( $\delta$  ppm, 400 MHz,  $\text{CDCl}_3$ ) : 0.70 (*br d*), 0.78 (*s*), 0.84 (*s*), 0.99 (*s*), 1.00 (*s*), 1.04 (*s*), 1.70 (*s*), 2.40 (*ddd*,  $J = 10.8, 10.8, 6.0$  Hz), 3.20 (*dd*,  $J = 11.2, 4.8$  Hz), 3.35 (*d*,  $J = 10.8$  Hz), 3.82 (*dd*,  $J = 10.8, 1.6$  Hz), 4.60 (*dd*,  $J = 2.0, 1.2$  Hz), 4.70 (*d*,  $J = 2.0$  Hz) (**Table 14** and **Figures 15a-15b**)

$^{13}\text{C}$  NMR ( $\delta$  ppm, 100 MHz,  $\text{CDCl}_3$ ) : 14.7, 15.3, 16.0, 16.1, 18.3, 19.1, 20.8, 25.2, 27.0, 27.4, 28.0, 29.2, 29.7, 34.0, 34.2, 37.1, 37.3, 38.7, 38.8, 40.9, 42.7, 47.8, 47.8, 48.7, 50.4, 55.3, 60.5,

79.0, 109.7, 150.5 (Table 14 and Figures 16a-16b)

DART-TOF MS  $m/z$  : 443.3913 [M+H]<sup>+</sup> (Figure 17)

#### 4.5 Compound DG05

Appearance : colorless needles

Solubility : soluble in ethanol

IR  $\nu_{\max}$   $\text{cm}^{-1}$  : 3424, 2926, 2868, 1686, 1461 (Figure 19).

<sup>1</sup>H NMR ( $\delta$  ppm, 400 MHz, CDCl<sub>3</sub>) : 0.70 (*br d*), 0.77 (*s*), 0.84 (*s*), 0.95 (*s*), 0.98 (*s*), 0.99 (*s*), 1.71 (*s*), 3.02 (*ddd*,  $J = 10.8, 10.8, 4.8$  Hz), 3.21 (*dd*,  $J = 11.2, 5.2$  Hz), 4.63 (*br s*), 4.76 (*br s*) (Table 15 and Figures 20a-20b)

<sup>13</sup>C NMR ( $\delta$  ppm, 100 MHz, CDCl<sub>3</sub>) : 14.8, 15.4, 16.1, 16.2, 18.4, 19.5, 20.9, 25.6, 27.5, 28.1, 29.8, 30.6, 32.2, 34.4, 37.1, 37.3, 38.5, 38.8, 39.0, 40.8, 42.5, 47.0, 49.4, 50.6, 55.4, 56.4, 79.1, 109.8, 150.5, 180.3 (Table 15 and Figures 22a-22b)

DART-TOF MS  $m/z$  : 457.3672 [M+H]<sup>+</sup> (Figure 25)

#### 4.6 Compound DG06

Appearance : white amorphous powder

Solubility : soluble in dichloromethane

IR  $\nu_{\max}$   $\text{cm}^{-1}$  : 3401, 2931, 2868, 1711, 1453 (Figure 26)

<sup>1</sup>H NMR ( $\delta$  ppm, 400 MHz, CDCl<sub>3</sub>) : 0.68 (*br d*), 0.76 (*s*), 0.84 (*s*), 0.92 (*s*), 0.97 (*s*), 1.26 (*s*), 1.70 (*s*), 2.87 (*ddd*,  $J = 11.2, 11.2, 5.6$  Hz), 3.19 (*dd*,  $J = 11.2, 4.8$  Hz), 4.64 (*br s*), 4.76 (*br s*), 9.69 (*s*) (Table 16 and Figures 27a-27b)

<sup>13</sup>C NMR ( $\delta$  ppm, 400 MHz, CDCl<sub>3</sub>) : 14.3, 15.4, 15.9, 16.2, 18.3, 19.0, 20.8, 25.5, 27.3, 28.0, 28.8, 29.3, 29.9, 33.2, 34.3, 37.2, 38.7, 38.7,

38.9, 40.8, 42.6, 47.6, 48.1, 50.5, 55.3, 59.4, 79.0, 110.2, 149.8, 206.8 (Table 16 and Figures 28a-28b)

## 5. Determination of Biological Activities

### 5.1 Cell Culture and Treatments

Human glioblastoma U87 cells (ATCC) were cultured in Eagle's Minimum Essential Medium (EMEM). Human breast cancer MDA-MB231 cells (ATCC) and human endothelial EA.hy926 cells (ATCC) were cultured in Dulbecco's Modified Eagle Medium (DMEM), and human T lymphoblastoid Jurkat E6-1 cells (ATCC) were cultured in RPMI1640 medium. All culture media were supplemented with 10% heat-inactivated fetal bovine serum (FBS). The cells were maintained at humidified atmosphere of 5% CO<sub>2</sub> at 37°C and routinely subcultured every three days. All tested compounds were dissolved in DMSO and diluted in culture medium, maintaining final DMSO concentration at 0.5%.

### 5.2 Determination of Cytotoxicity by MTT Assay.

Human glioblastoma U87 cells, human breast cancer MDA-MB231 cells, and human endothelial EA.hy926 cells were seeded into 96-well plates at a density of  $4 \times 10^4$  cells/well and subjected to an overnight incubation at 37 °C under 5% CO<sub>2</sub> atmosphere. The cells were treated with a range of concentrations (0.01 – 100 µM) of each tested compound. After 24-hour incubation, the medium containing samples was replaced with 100 µL of a 0.5 mg/mL MTT [3-(4,5-dimethylthiazol-2-yl)-2,5-diphenyltetrazolium bromide] solution and the cells were further incubated for 4 hours. After removal of the cell supernatant, 100 µL of DMSO were added into each well to dissolve the resultant formazan crystals. Absorbance was measured at a wavelength of 570 nm. The percentages of cell viability were calculated from the equation shown below.

$$\% \text{ Cell viability} = A_s/A_c \times 100$$

$A_s$  = Absorbance of the samples

$A_c$  = Absorbance of the control

IC<sub>50</sub> values of the tested compounds were derived from the dose response curve using GraphPad software.

### 5.3 Determination of Inhibitory Activity on T Cell Activation

Jurkat T cells were seeded into 96-well plate at a density of  $10 \times 10^4$  cells/well and pre-treated with various concentrations of the tested compounds for 24 hours. Subsequently, the cells were stimulated with 10 ng/mL of anti-CD3 antibody (BioLegend, USA) and 10 ng/mL of anti-CD28 antibody (BioLegend, USA), and further incubated for 72 hours. After incubation, the cell supernatants were collected from each well and analyzed for the level of Interleukin-2 (IL-2) by using ELISA MAX™ Deluxe Set Human IL-2 (BioLegend, USA).

The determination on cytotoxic activity and inhibitory activity on T cell activation of isolated compounds was performed by Dr. Nonthaneth Nalinratana at the Department of Pharmacology and Physiology, Faculty of Pharmaceutical Sciences, Chulalongkorn University.



## CHAPTER IV

### RESULTS AND DISCUSSION

The phytochemical investigation conducted on the EtOAc extract of the dried stem of *Diospyros gracilis* led to the isolation of six chemical constituents. The identification of these compounds was based on spectroscopic analysis and confirmed by comparison with the values reported in the literature. Certain isolated compounds were investigated for their biological activities, including cytotoxic activity and inhibitory activity on T cell activation.

#### 1. Identification of Isolated Compounds

##### 1.1 Compound DG01 (friedelin)

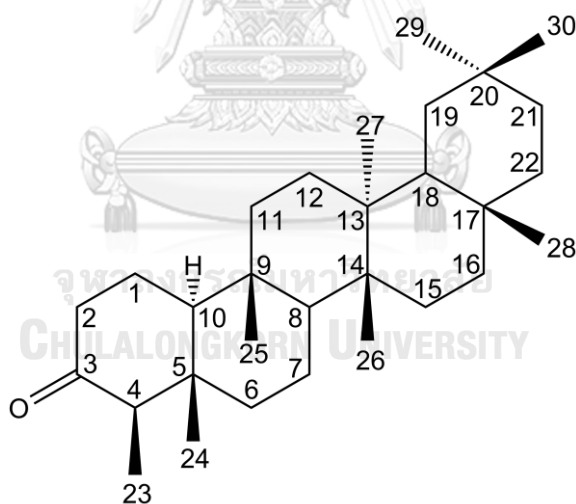
Compound DG01 was obtained as colorless needles. Its IR spectrum (**Figure 2**) showed a peak at  $1715\text{ cm}^{-1}$ , which suggested the presence of a carbonyl group in the molecule.

The  $^1\text{H}$  NMR spectrum of DG01 (**Figures 3a-3b**) exhibited eight methyl signals representing one secondary and seven tertiary methyl groups, which were characteristic of the friedelane triterpenoid skeleton. These signals comprised a doublet corresponding to one secondary methyl at  $\delta$  0.90 ( $J = 6.4\text{ Hz}$ , Me-23) and singlets corresponding to seven tertiary methyls at  $\delta$  0.74 (Me-24), 0.89 (Me-25), 0.97 (Me-29), 1.02 (Me-30), 1.03 (Me-26), 1.07 (Me-27), and 1.20 (Me-28).

The  $^{13}\text{C}$  NMR spectrum (**Figures 4a-4b**) showed 30 carbon signals. The most downfield signal at  $\delta$  213.3 ppm was indicative of the 3-keto group. Comparison of  $^{13}\text{C}$  NMR data of the compound with those of friedelin revealed complete concordance (Akihisa *et al.*, 1992). Based on the comparison, the 30 carbon signals of DG01 could be divided into eight methyl signals at  $\delta$  6.8 (C-23), 14.7 (C-24), 17.9 (C-25), 18.7 (C-27), 20.3 (C-26), 31.8 (C-30), 32.1 (C-28), and 35.0 (C-29) ppm; eleven methylene signals at  $\delta$  18.2 (C-7), 22.3 (C-1), 30.5 (C-12), 32.4 (C-15), 32.8 (C-21), 35.3

(C-19), 35.6 (C-11), 36.0 (C-16), 39.3 (C-22), 41.3 (C-6), and 41.5 (C-2) ppm; four methine signals at  $\delta$  42.8 (C-18), 53.1 (C-8), 58.2 (C-4), and 59.5 (C-10) ppm; and seven quaternary signals at  $\delta$  28.2 (C-20), 30.0 (C-17), 37.4 (C-9), 38.3 (C-14), 39.7 (C-13), 42.2 (C-5), and 213.3 (C-3) ppm. The most downfield signals at 213.3 ppm represented the keto carbonyl group.

All the information obtained from the IR and NMR spectra suggested the structure of friedelin, a friedelane-type triterpenoid with the 3-keto substituent. The DART-TOF mass spectrum of DG01 (**Figure 5**) displayed a pseudomolecular peak  $[M+H]^+$  at  $m/z$  427.3926, corresponding to the molecular formula of  $C_{30}H_{50}O$ . This information confirmed that DG01 was friedelin.  $^1H$  and  $^{13}C$  NMR assignments of DG01, in comparison with those of friedelin, are shown in **Table 11**. The structure of the compound is shown below.



Friedelin

**Table 11.**  $^1\text{H}$  (400 MHz) and  $^{13}\text{C}$  (100 MHz) NMR assignments of compound DG01 and friedelin (in  $\text{CDCl}_3$ )

Position	Compound DG01		Friedelin*	
	$\delta_{\text{H}}$ (ppm), (mult., $J$ in Hz)	$\delta_{\text{C}}$ (ppm)	$\delta_{\text{H}}$ (ppm), (mult., $J$ in Hz)	$\delta_{\text{C}}$ (ppm)
1	1.71**, 1.99 ( <i>m</i> )	22.3	1.69 ( <i>m</i> ), 1.97 ( <i>m</i> )	22.3
2	2.33**, 2.41 ( <i>ddd</i> , 11.6, 5.2, 2.0)	41.5	2.31 ( <i>m</i> ), 2.39 ( <i>m</i> )	41.5
3		213.3		213.2
4	2.27**	58.2	2.25 ( <i>m</i> )	58.2
5		42.2		42.1
6		41.3		41.3
7		18.2		18.2
8		53.1		53.1
9		37.4		37.4
10		59.5		59.4
11		35.6		35.6
12		30.5		30.5
13		39.7		39.7
14		38.3		38.3
15		32.4		32.4
16		36.0		36.0
17		30.0		30.0
18		42.8		42.8
19		35.3		35.3
20		28.2		28.1
21		32.8		32.7
22		39.3		39.2
23	0.90 ( <i>d</i> , 6.4)	6.8	0.88 ( <i>d</i> , 7)	6.8
24	0.74 ( <i>s</i> )	14.7	0.73 ( <i>s</i> )	14.6
25	0.89 ( <i>s</i> )	17.9	0.87 ( <i>s</i> )	17.9

**Table 11.**  $^1\text{H}$  (400 MHz) and  $^{13}\text{C}$  (100 MHz) NMR assignments of compound DG01 and friedelin (in  $\text{CDCl}_3$ ) (continued)

Position	Compound DG01		Friedelin*	
	$\delta_{\text{H}}$ (ppm), (mult., $J$ in Hz)	$\delta_{\text{C}}$ (ppm)	$\delta_{\text{H}}$ (ppm), (mult., $J$ in Hz)	$\delta_{\text{C}}$ (ppm)
26	1.03 (s)	20.3	1.01 (s)	20.2
27	1.07 (s)	18.7	1.05 (s)	18.6
28	1.20 (s)	32.1	1.18 (s)	32.1
29	0.97 (s)	35.0	0.95 (s)	35.0
30	1.02 (s)	31.8	1.00 (s)	31.8

\*  $^1\text{H}$  (400 MHz) and  $^{13}\text{C}$  (100 MHz) NMR; Akihisa *et al.*, 1992.

\*\* Overlapped signal

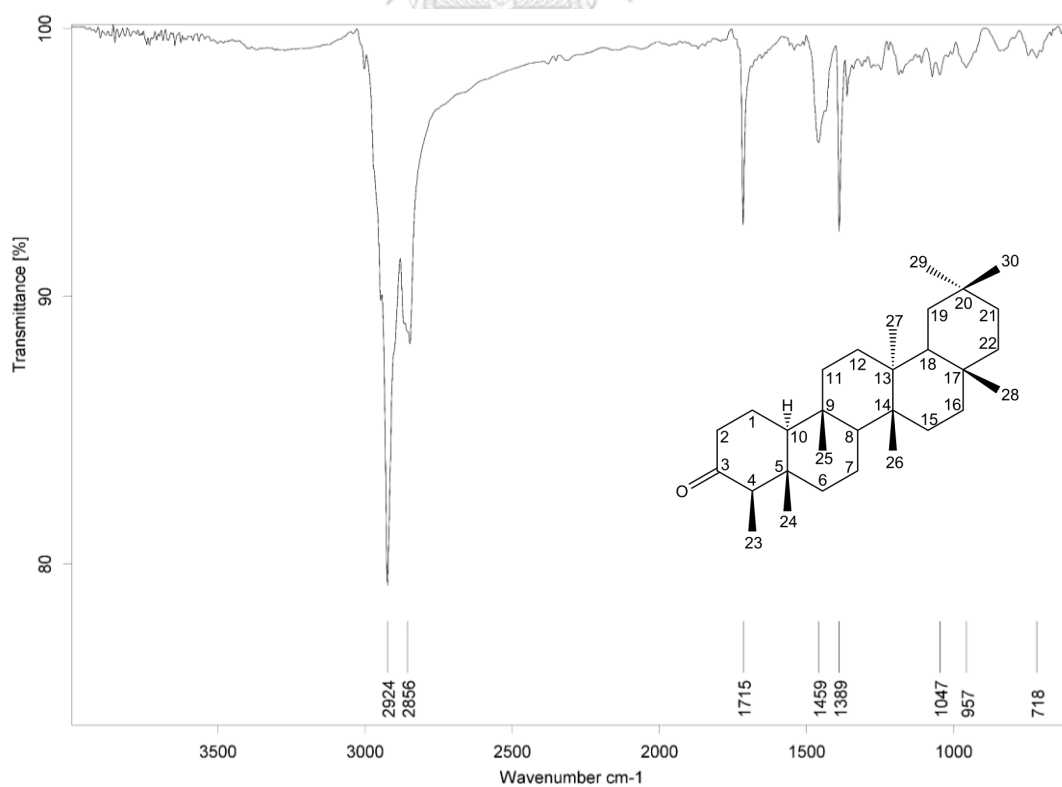


**Figure 2.** IR spectrum of compound DG01



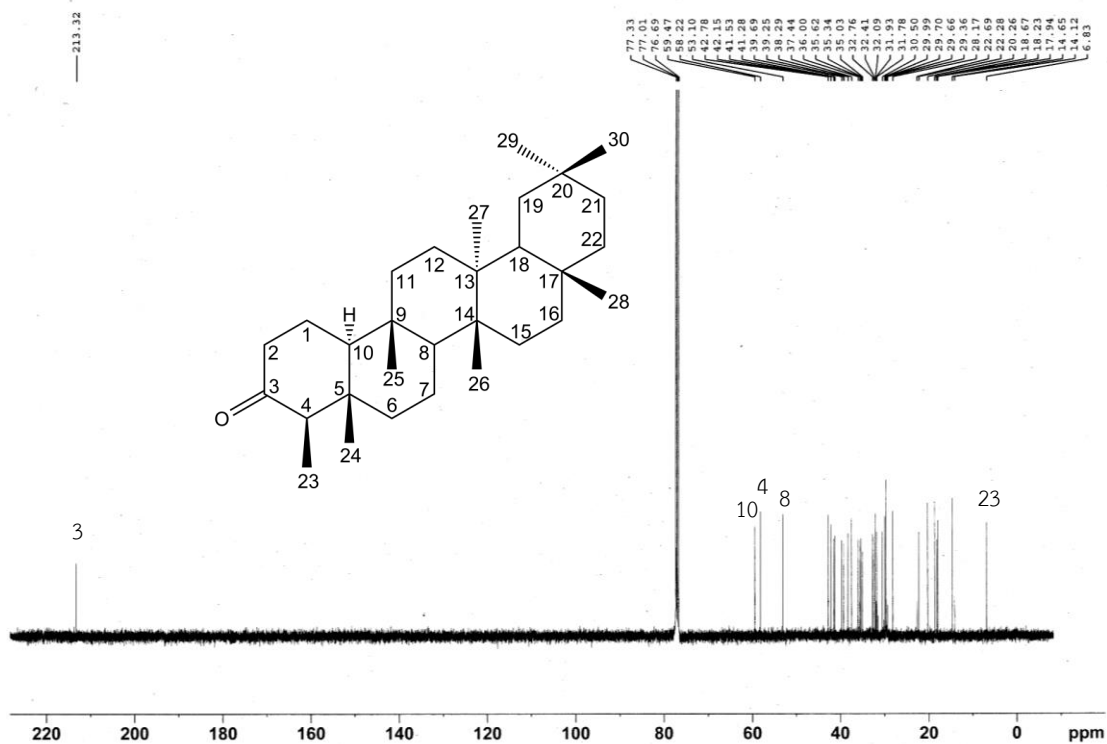


Figure 4a.  $^{13}\text{C}$  NMR (100 MHz) spectrum of compound DG01 (in  $\text{CDCl}_3$ )

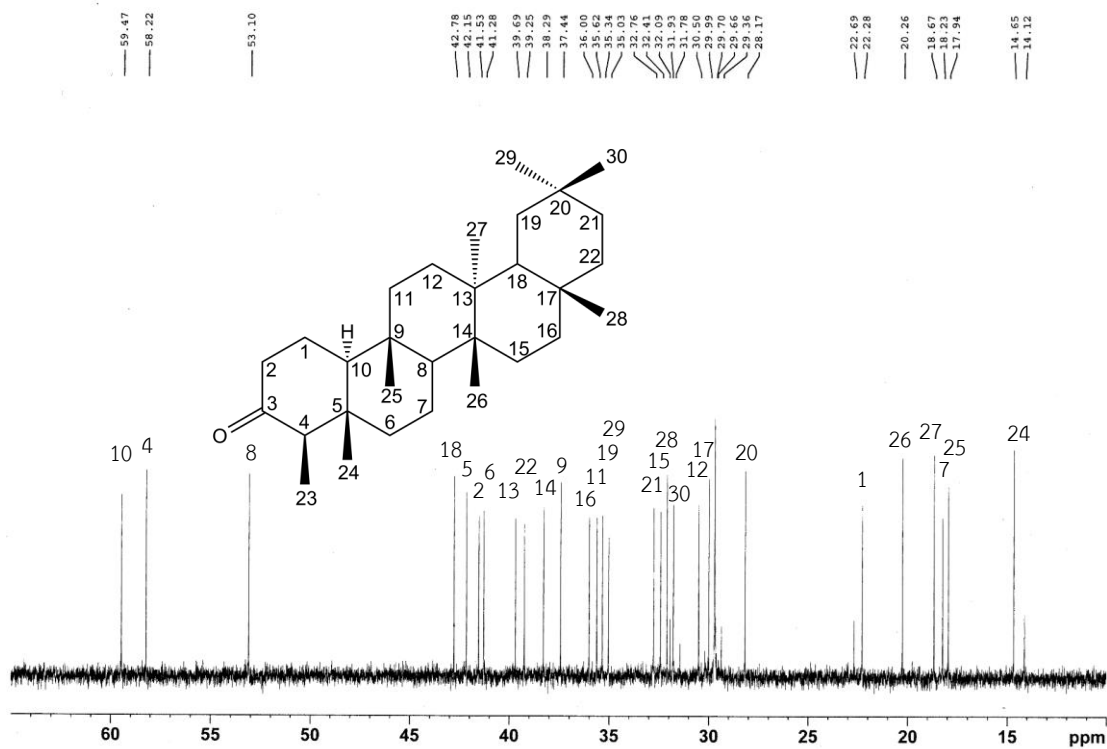
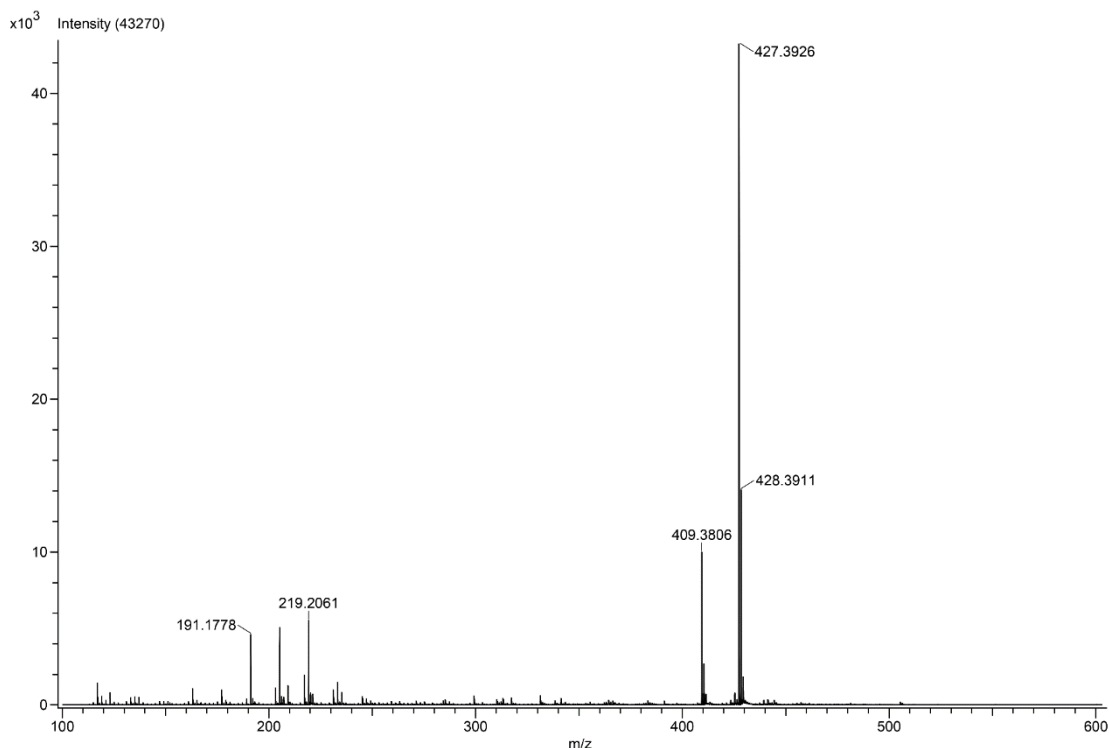


Figure 4b.  $^{13}\text{C}$  NMR (100 MHz) spectrum of compound DG01 (in  $\text{CDCl}_3$ ) (expanded)



**Figure 5.** DART-TOF Mass spectrum of compound DG01

Friedelin is widely distributed in nature. The cork of various plants is the source of friedelin. Friedelin has been isolated from some *Diospyros* species such as *D. collinsae*, *D. glandulosa* and *D. ferrea* (Thanakijcharoenpath and Theanphong, 2007; Bumroong and Thanakijcharoenpath, 2016; Radi *et al.*, 2023). In addition, friedelin can be obtained from other natural sources such as lichens, green algae, and fungi. Friedelin has been reported to exhibit various pharmacological activities, including antibacterial, antiviral, cytotoxic, and anti-inflammatory (Radi *et al.*, 2023).

## 1.2 Compound DG02 (epifriedelanol)

DG02 was obtained as a white amorphous powder. Its IR spectrum (**Figure 6**) displayed a broad absorption band at  $3400\text{ cm}^{-1}$ , indicating the presence of a hydroxy group in the molecule.

The  $^1\text{H}$  and  $^{13}\text{C}$  NMR spectra of DG02 were similar to those of DG01, implying their related chemical structures. The  $^1\text{H}$  NMR spectrum (**Figure 7a-7b**) showed the

presence of eight methyl signals corresponding to one secondary ( $\delta$  0.96 ppm,  $d$ ,  $J$  = 6.8 Hz, Me-23) and seven tertiary methyl groups ( $\delta$  0.88, Me-25,  $\delta$  0.97, Me-29,  $\delta$  0.99 Me-26,  $\delta$  1.01, Me-27,  $\delta$  1.02, Me-30,  $\delta$  1.03, Me-24, and  $\delta$  1.19, Me-28). The  $^1\text{H}$  NMR spectrum of DG02 was different from that of DG01 in showing an additional quartet-like at  $\delta$  3.76 ppm ( $J$  = 2.4 Hz), which represented a hydroxymethine proton (H-3). The  $^{13}\text{C}$  NMR spectrum (**Figure 8a-8b**) showed 30 carbon signals; the most downfield signal was observed at  $\delta$  72.8 instead of the keto carbonyl at  $\delta$  213.3 ppm in the  $^{13}\text{C}$  NMR spectrum of DG01. This information from the NMR spectra suggested that DG02 was a friedelane derivative with the 3-hydroxy group. When compared with the  $^{13}\text{C}$  NMR data of epifriedelanol (Salazar *et al.*, 2000), they were in full agreement.

The DART-TOF MS of DG02 (**Figure 9**) displayed a pseudomolecular peak  $[\text{M}+\text{H}]^+$  at  $m/z$  429.4007, which was consistent with the molecular formula of  $\text{C}_{30}\text{H}_{52}\text{O}$ , thereby confirming the identity of DG02 as epifriedelanol ( $3\beta$ -friedelinol), the structure of which is shown below. Comparison of  $^1\text{H}$  and  $^{13}\text{C}$  NMR assignments of DG02 and epifriedelanol is shown in **Table 12**.

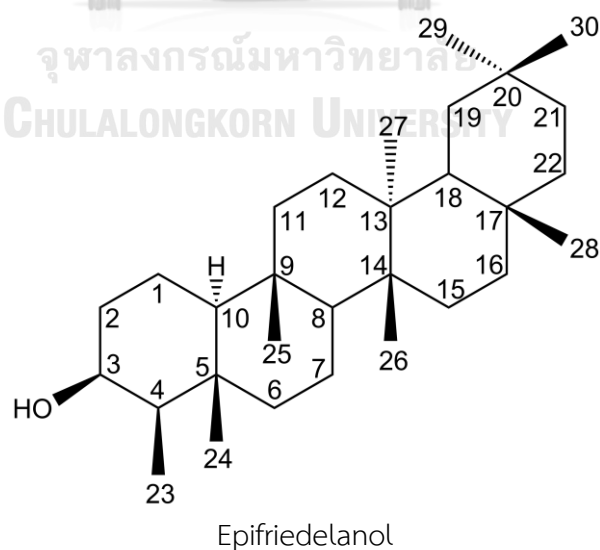




**Table 12.**  $^1\text{H}$  (400 MHz) and  $^{13}\text{C}$  (100 MHz) NMR assignments of compound DG02 and epifriedelanol (in  $\text{CDCl}_3$ )

Position	Compound DG02		Epifriedelanol*	
	$\delta_{\text{H}}$ (ppm), (mult., $J$ in Hz)	$\delta_{\text{C}}$ (ppm)	$\delta_{\text{H}}$ (ppm), (mult., $J$ in Hz)	$\delta_{\text{C}}$ (ppm)
1		15.8		16.2
2		36.1		36.1
3	3.76 ( <i>q</i> -like, 2.4)	72.8	3.81 ( <i>q</i> -like, 2.0)	71.6
4		49.2		49.6
5		37.8		38.1
6		41.7		42.0
7		17.6		17.7
8		53.2		53.3
9		37.1		37.2
10		61.3		61.7
11		35.3		35.7
12		30.6		30.7
13		38.4		38.4
14		39.7		39.7
15		32.3		32.3
16		35.6		35.9
17		30.0		30.0
18		42.8		42.9
19		35.2		35.4
20		28.2		28.2
21		32.8		32.9
22		39.3		39.3
23	0.96 ( <i>d</i> , 6.8)	11.6	1.02 ( <i>d</i> , 7.0)	12.1
24	1.03 ( <i>s</i> )	16.4	1.10 ( <i>s</i> )	16.6
25	0.88 ( <i>s</i> )	18.3	0.89 ( <i>s</i> )	18.4
26	0.99 ( <i>s</i> )	20.1	0.99 ( <i>s</i> )	20.1

**Table 12.**  $^1\text{H}$  (400 MHz) and  $^{13}\text{C}$  (100 MHz) NMR assignments of compound DG02 and epifriedelanol (in  $\text{CDCl}_3$ ) (continued)

Position	Compound DG02		Epifriedelanol*	
	$\delta_{\text{H}}$ (ppm), (mult., $J$ in Hz)	$\delta_{\text{C}}$ (ppm)	$\delta_{\text{H}}$ (ppm), (mult., $J$ in Hz)	$\delta_{\text{C}}$ (ppm)
27	1.01 (s)	18.7	1.02 (s)	18.7
28	1.19 (s)	32.1	1.18 (s)	32.1
29	0.97 (s)	35.0	0.97 (s)	35.0
30	1.02 (s)	31.8	1.02 (s)	31.9

\*  $^1\text{H}$  (400 MHz) and  $^{13}\text{C}$  (100 MHz); Salazar *et al.*, 2000.

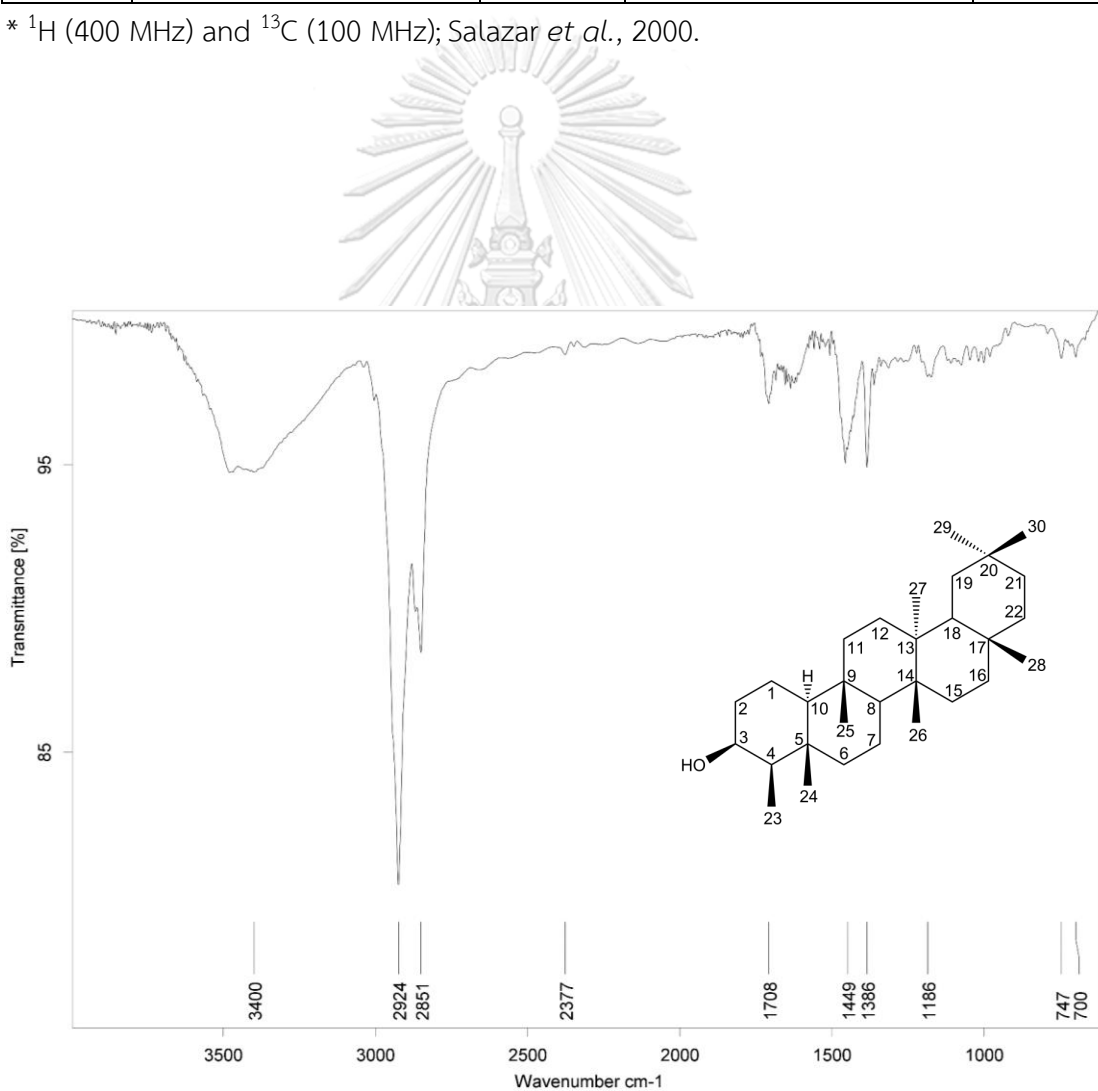


**Figure 6.** IR spectrum of compound DG02

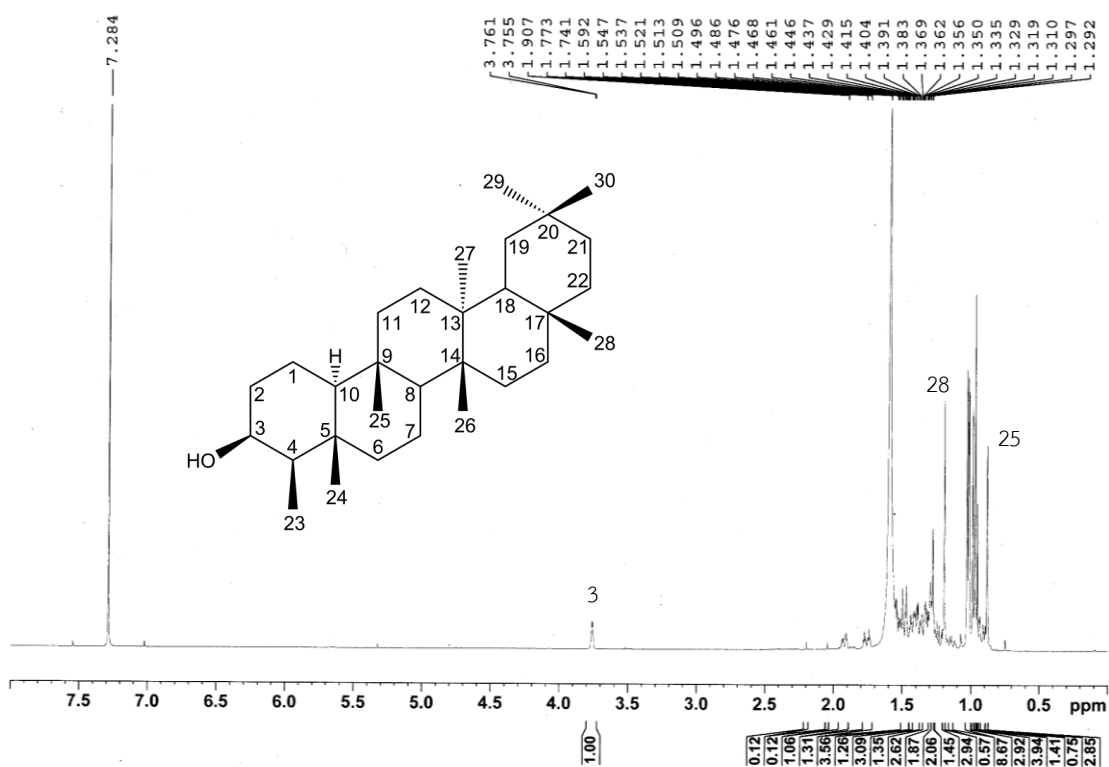


Figure 7a.  $^1\text{H}$  NMR (400 MHz) spectrum of compound DG02 (in  $\text{CDCl}_3$ )

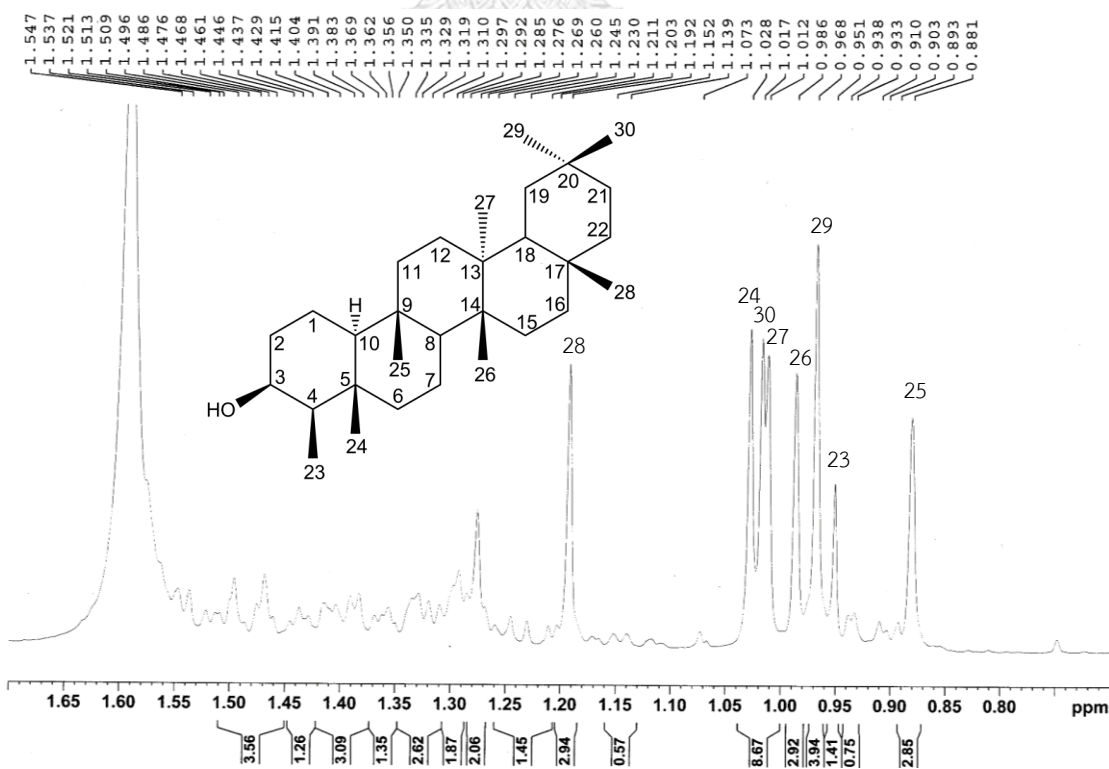


Figure 7b.  $^1\text{H}$  NMR (400 MHz) spectrum of compound DG02 (in  $\text{CDCl}_3$ ) (expanded)

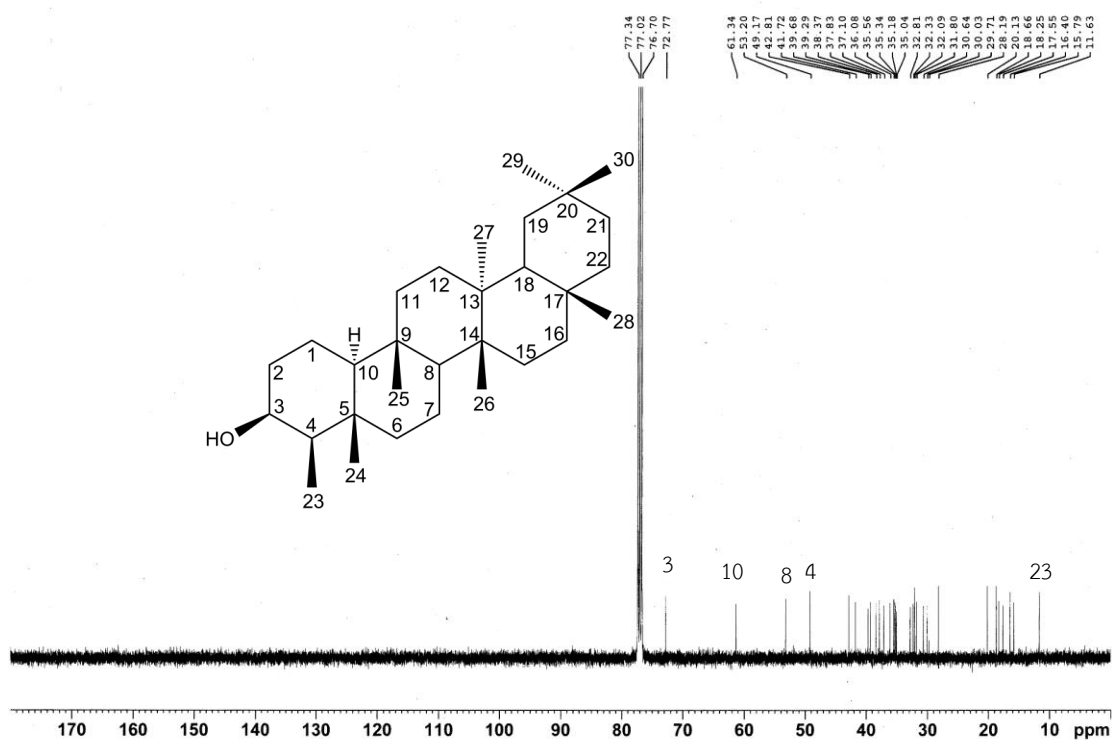


Figure 8a.  $^{13}\text{C}$  NMR (100 MHz) spectrum of compound DG02 (in  $\text{CDCl}_3$ )

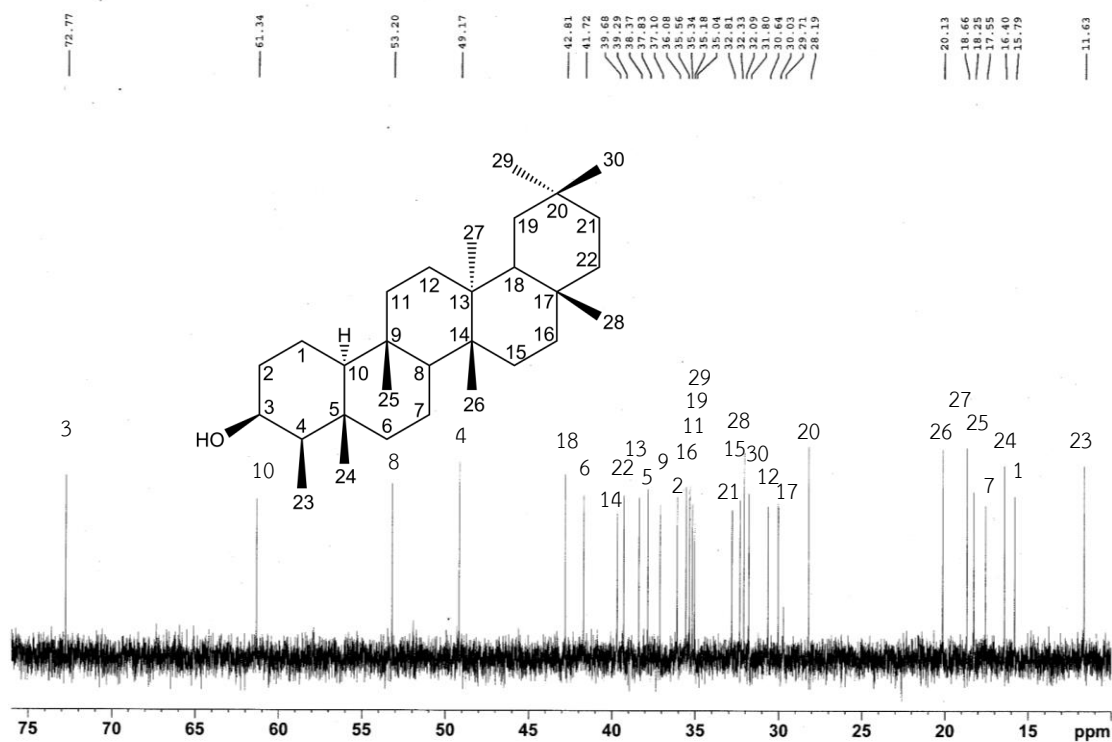
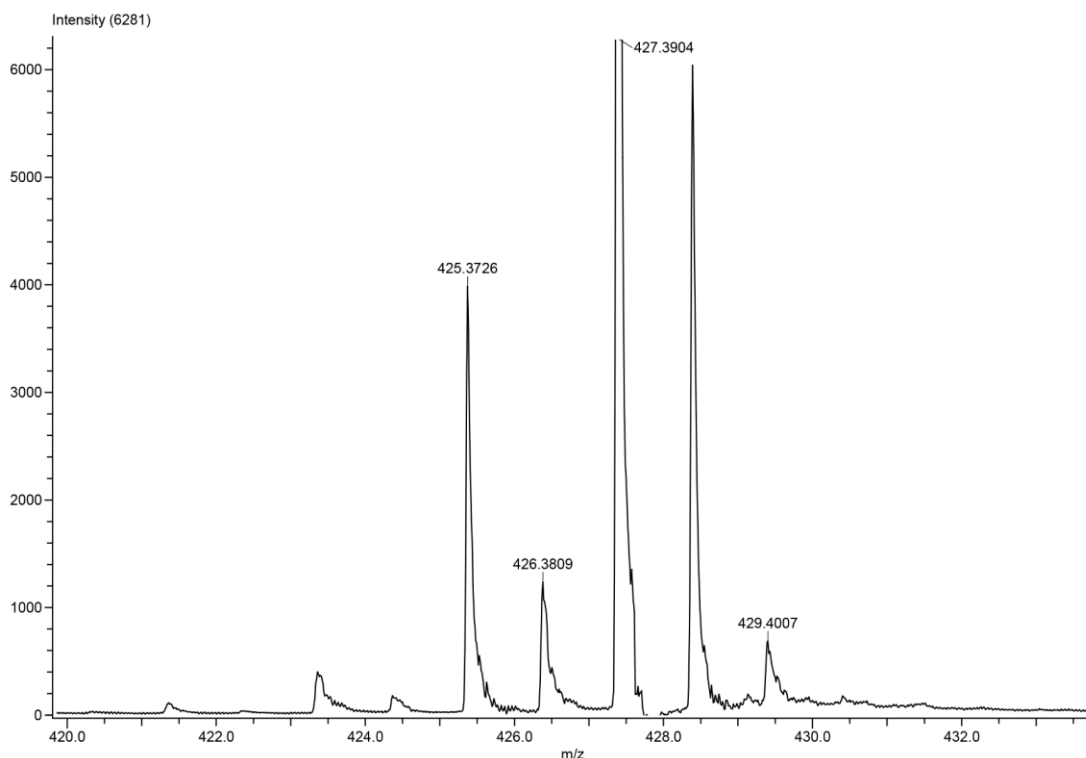


Figure 8b.  $^{13}\text{C}$  NMR (100 MHz) spectrum of compound DG02 (in  $\text{CDCl}_3$ ) (expanded)



**Figure 9.** DART-TOF Mass spectrum of compound DG02

Epifriedelanol, similar to friedelin, can be found in various plant families including Asteraceae, Euphorbiaceae, Phyllanthaceae, etc. Epifriedelanol has been reported to exhibit several pharmacological activities such as cytotoxic, and antihyperglycemic (Radi *et al.*, 2023).

### 1.3 Compound DG03 (lupeol)

DG03 was obtained as colorless needles. Its IR spectrum (**Figure 10**) showed a broad absorption band at  $3369\text{ cm}^{-1}$ , suggesting the presence of the hydroxy group in the molecule.

The  $^1\text{H}$  NMR spectrum of DG03 (**Figures 11a-11b**) displayed seven methyl singlets at  $\delta$  0.78 (Me-24), 0.81 (Me-28), 0.85 (Me-25), 0.96 (Me-27), 0.98 (Me-23), 1.05 (Me-26), 1.70 (Me-30) ppm, and a pair of singlet-like signals at  $\delta$  4.58 (*dd*,  $J = 2.4, 1.2$  Hz, H-29<sub>a</sub>), and  $\delta$  4.70 (*d*,  $J = 2.4$  Hz, H-29<sub>b</sub>) ppm. These signals were indicative of the methyl groups and the isopropenyl group of a lupane-type triterpenoid. In addition, a

doublet of doublets at  $\delta$  3.20 ( $J = 11.2, 5.2$  Hz) ppm, representative of the hydroxymethine proton (H-3), was observed. The  $^{13}\text{C}$  NMR spectrum (Figures 12a-12b) showed 30 carbon signals which supported the triterpenoid nature. Seven methyl groups were represented by seven signals at  $\delta$  14.5 (C-27), 15.3 (C-24), 15.9 (C-26), 16.1 (C-25), 18.0 (C-28), 19.3 (C-30), 28.0 (C-23) ppm while the isopropenyl group by two signals at  $\delta$  109.3 (C-29) and 151.0 (C-20) ppm. The presence of the hydroxy group was confirmed by the signal at  $\delta$  79.0 (C-3) ppm.

This information suggested that DG03 was lupeol, a lupane derivative with the 3-hydroxy group. When compared with the  $^{13}\text{C}$  NMR data of lupeol (Reynolds *et al.*, 1986), the data of DG03 were found to be in full agreement. The identity of the compound was further confirmed by the DART-TOF MS (Figure 13) which displayed a pseudomolecular peak  $[\text{M}+\text{H}]^+$  at  $m/z$  427.3880, consistent with the molecular formula of  $\text{C}_{30}\text{H}_{50}\text{O}$ . Therefore, DG03 was identified to be lupeol, the structure of which is shown below.  $^1\text{H}$  and  $^{13}\text{C}$  NMR assignments of DG03, in comparison with those of lupeol, are shown in Table 13.

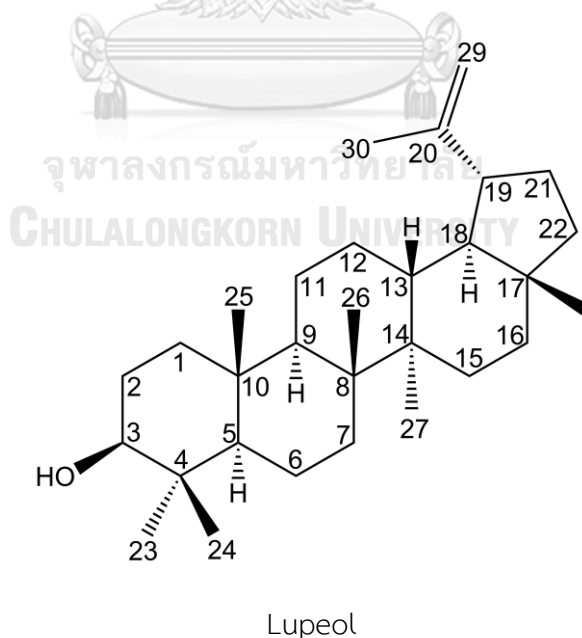


**Table 13.**  $^1\text{H}$  (400 MHz) and  $^{13}\text{C}$  (100 MHz) NMR assignments of compound DG03 and lupeol (in  $\text{CDCl}_3$ )

Position	Compound DG03		Lupeol*	
	$\delta_{\text{H}}$ (ppm), (mult., $J$ in Hz)	$\delta_{\text{C}}$ (ppm)	$\delta_{\text{H}}$ (ppm), (mult., $J$ in Hz)	$\delta_{\text{C}}$ (ppm)
1		38.7		38.7
2		27.4		27.4
3	3.20 ( <i>dd</i> , 11.2, 5.2)	79.0	3.18 ( <i>dd</i> )	78.9
4		38.8		38.8
5	0.70 ( <i>br d</i> )	55.3	0.69 ( <i>d</i> )	55.3
6		18.3		18.3
7		34.2		34.2
8		40.8		40.8
9		50.4		50.4
10		37.1		37.1
11		20.9		20.9
12		25.1		25.1
13		38.0		38.0
14		42.8		42.8
15		27.4		27.4
16		35.6		35.5
17		43.0		43.0
18		48.3		48.2
19	2.39 ( <i>ddd</i> , 10.8, 10.8, 5.6)	48.0	2.30 ( <i>m</i> )	47.9
20		151.0		150.9
21	1.34**, 1.94 ( <i>m</i> )	29.7	1.33 ( <i>m</i> ), 1.93 ( <i>m</i> )	29.8
22		40.0		40.0
23	0.98 ( <i>s</i> )	28.0	0.98 ( <i>s</i> )	28.0
24	0.78 ( <i>s</i> )	15.3	0.77 ( <i>s</i> )	15.4
25	0.85 ( <i>s</i> )	16.1	0.84 ( <i>s</i> )	16.1

**Table 13.**  $^1\text{H}$  (400 MHz) and  $^{13}\text{C}$  (100 MHz) NMR assignments of compound DG03 and lupeol (in  $\text{CDCl}_3$ ) (continued)

Position	Compound DG03		Lupeol*	
	$\delta_{\text{H}}$ (ppm), (mult., $J$ in Hz)	$\delta_{\text{C}}$ (ppm)	$\delta_{\text{H}}$ (ppm), (mult., $J$ in Hz)	$\delta_{\text{C}}$ (ppm)
26	1.05 (s)	15.9	1.04 (s)	15.9
27	0.96 (s)	14.5	0.97 (s)	14.5
28	0.81 (s)	18.0	0.79 (s)	18.0
29	4.58 (dd, 2.4, 1.2), 4.70 (d, 2.4)	109.3	4.56 (m), 4.69 (m)	109.3
30	1.70 (s)	19.3	1.69 (s)	19.3

\*  $^1\text{H}$  (400 MHz) and  $^{13}\text{C}$  (100 MHz); Reynolds *et al.*, 1986.

\*\* Overlapped signal

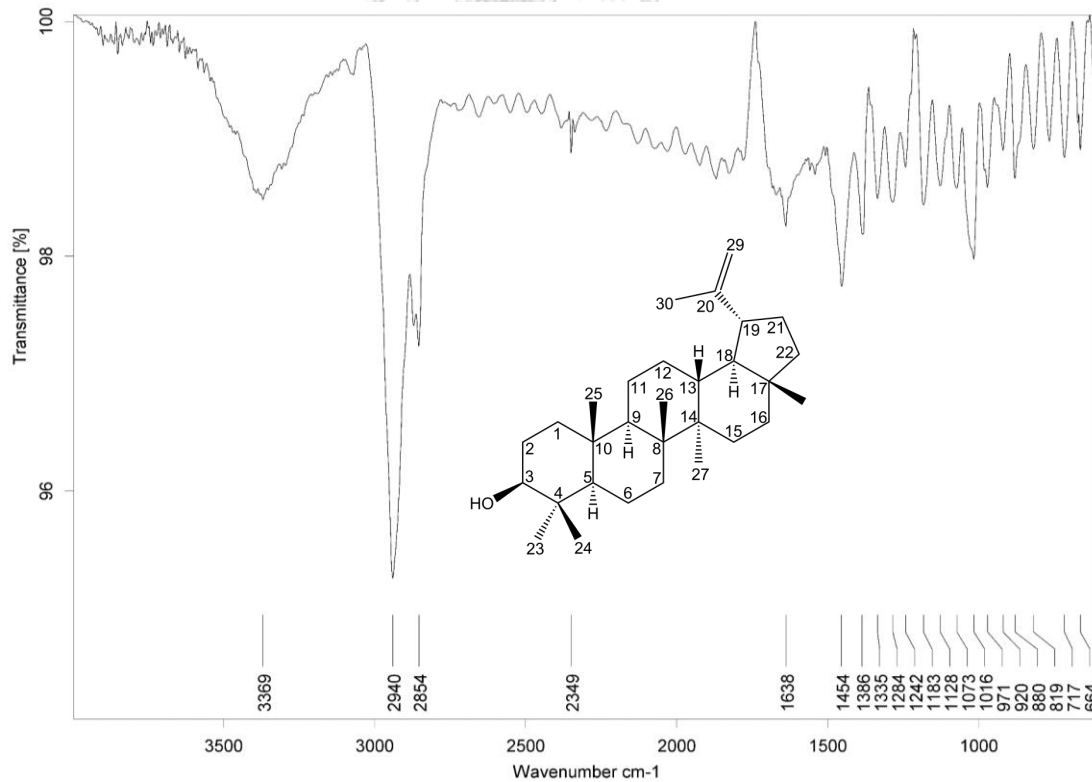


**Figure 10.** IR spectrum of compound DG03



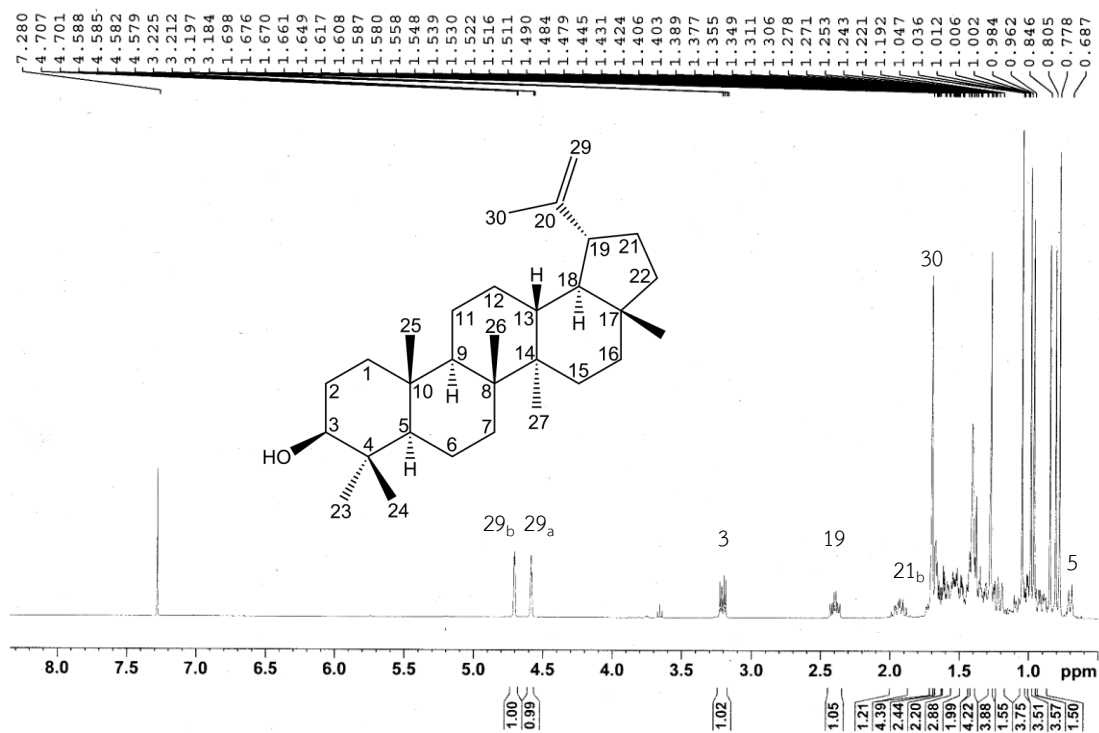


Figure 11a.  $^1\text{H}$  NMR (400 MHz) spectrum of compound DG03 (in  $\text{CDCl}_3$ )

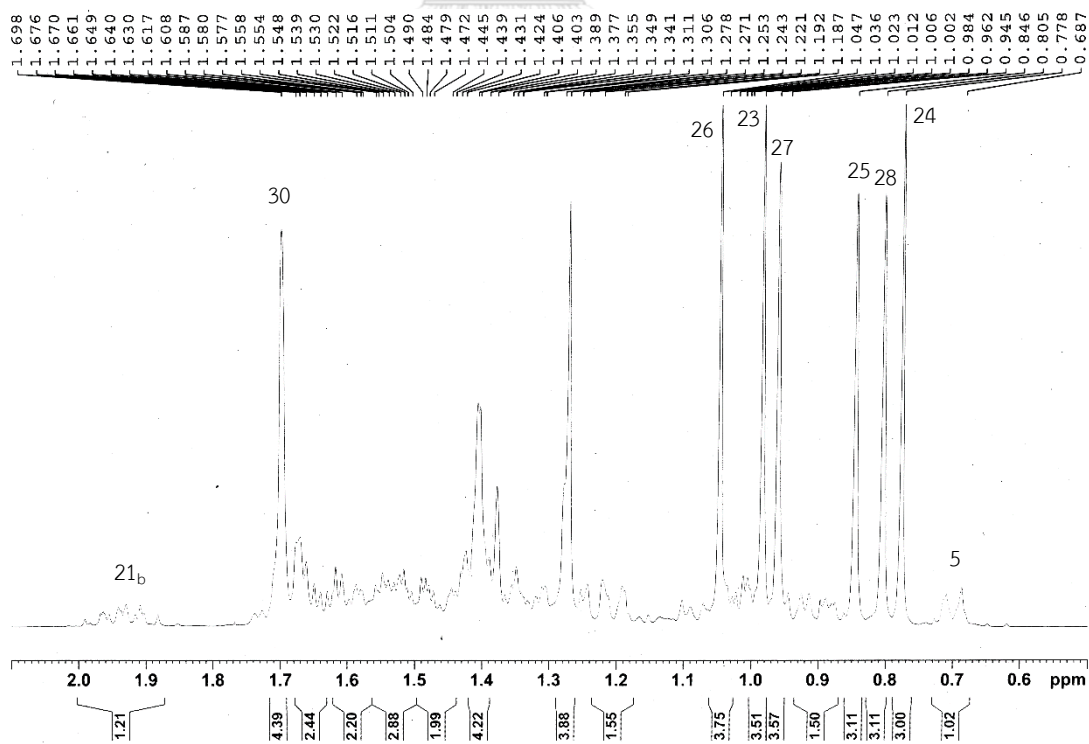


Figure 11b.  $^1\text{H}$  NMR (400 MHz) spectrum of compound DG03 (in  $\text{CDCl}_3$ ) (expanded)

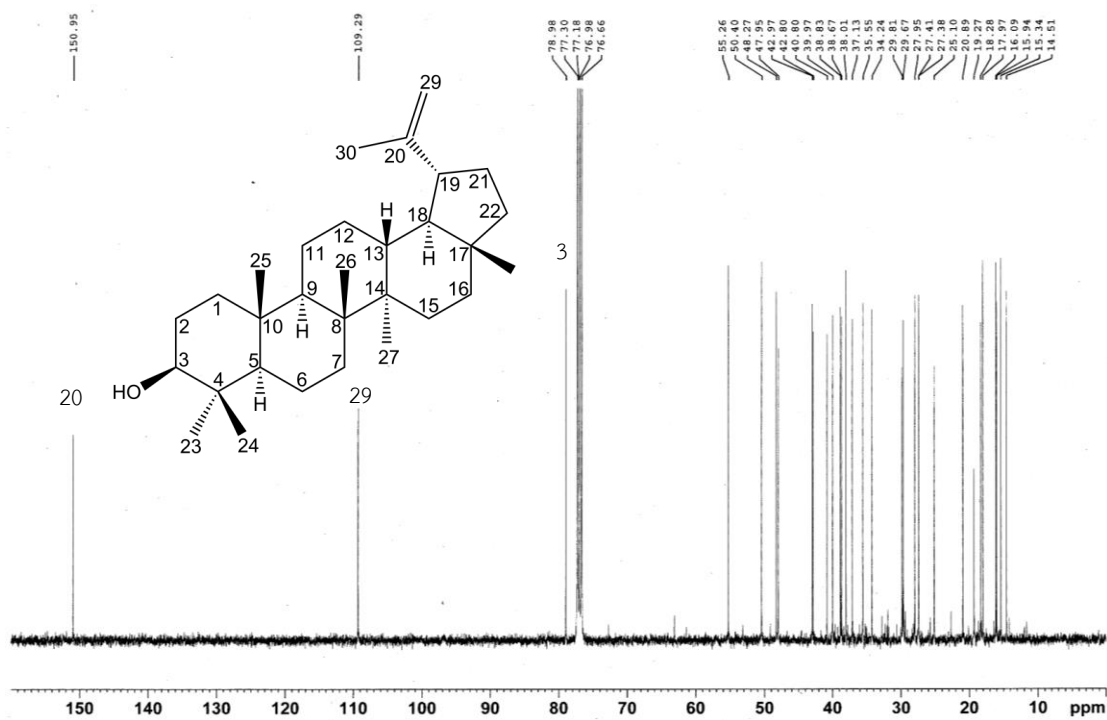


Figure 12a.  $^{13}\text{C}$  NMR (100 MHz) spectrum of compound DG03 (in  $\text{CDCl}_3$ )

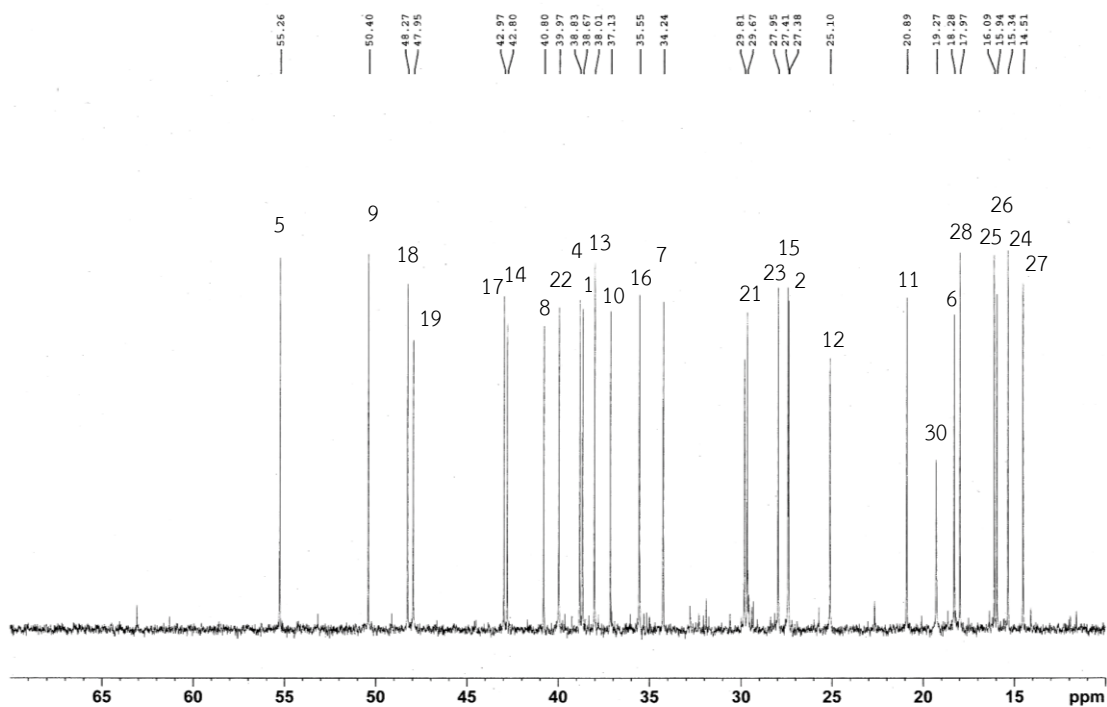
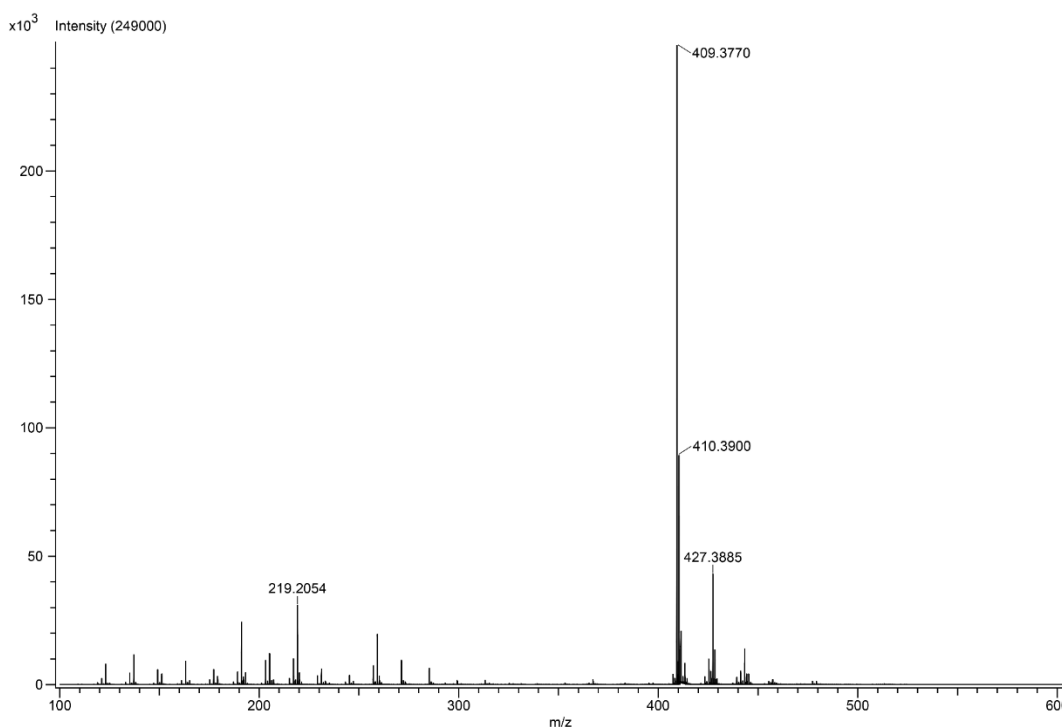


Figure 12b.  $^{13}\text{C}$  NMR (100 MHz) spectrum of compound DG03 (in  $\text{CDCl}_3$ ) (expanded)



**Figure 13.** DART-TOF Mass spectrum of compound DG03

Lupeol can be found in several *Diospyros* plants such as *D. anisandra*, *D. mespiliformis*, *D. virginiana* (Fareed *et al.*, 2022). Besides Ebenaceae, the compound can be found in Euphorbiaceae, Fabaceae, Apocynaceae, Capparidaceae, and many others. It was rarely found in fungi and animals. Various biological activities of lupeol have been reported e.g., anti-inflammatory, anticancer, antimalarial, hepatoprotective activities (Gallo and Sarachine, 2009).

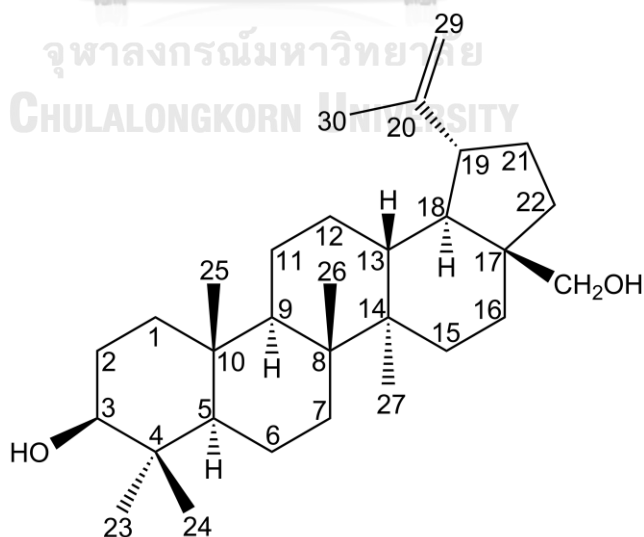
#### 1.4 Compound DG04 (betulin)

DG04 was obtained as colorless needles. Its IR spectrum (**Figure 14**) displayed a broad absorption band at 3295 cm<sup>-1</sup>, indicating the hydroxy group in the molecule.

The <sup>1</sup>H NMR spectrum of DG04 (**Figures 15a-15b**) suggested that the compound was a lupane-type triterpenoid by showing six methyl singlets at  $\delta$  0.78 (Me-24), 0.84 (Me-25), 0.99 (Me-23), 1.00 (Me-27), 1.04 (Me-26), 1.70 (Me-30) ppm and a pair of singlet-like signals at  $\delta$  4.60 (*dd*, *J*= 2.0, 1.2 Hz, H-29<sub>a</sub>), 4.70 (*d*, *J*= 2.0 Hz, H-

29<sub>b</sub>) ppm. The doublet at  $\delta$  3.20 (*dd*,  $J = 11.2, 4.8$  Hz, H-3) ppm, implying the presence of the 3-hydroxy group, was also observed. When compared with the  $^1\text{H}$  NMR spectrum of DG03, the spectrum of DG04 revealed the absence of one methyl singlet and the addition of a pair of signals at  $\delta$  3.35 (*d*,  $J = 10.8$  Hz) and 3.82 (*dd*,  $J = 10.8, 1.6$  Hz) ppm, suggesting that one methyl group of DG03 was replaced by a primary alcoholic group. The  $^{13}\text{C}$  NMR spectrum (**Figures 16a-16b**) exhibited 30 carbon signals, corresponding to the structure of a triterpenoid. The two signals at  $\delta$  109.7 (C-29) and 150.5 (C-20) ppm represented the isopropenyl group, and those at  $\delta$  79.0 and 60.5 ppm corresponded to hydroxymethine (C-3) and hydroxymethylene (C-28) carbons, respectively. Based on these data, DG04 was proposed to be betulin, a derivative of lupeol with the 28-hydroxy group.

The DART-TOF mass spectrum (**Figure 17**) of DG04 displayed a pseudomolecular peak  $[\text{M}+\text{H}]^+$  at  $m/z$  443.3913, corresponding to the molecular formula of betulin ( $\text{C}_{30}\text{H}_{50}\text{O}_2$ ). Comparison of  $^1\text{H}$  and  $^{13}\text{C}$  NMR assignments of DG04 with those of betulin is shown in **Table 14**. The structure of DG04 is shown below.



Betulin

**Table 14.**  $^1\text{H}$  (400 MHz) and  $^{13}\text{C}$  (100 MHz) NMR assignments of compound DG04 and betulin (in  $\text{CDCl}_3$ )

Position	Compound DG04		Betulin*	
	$\delta_{\text{H}}$ (ppm), (mult., $J$ in Hz)	$\delta_{\text{C}}$ (ppm)	$\delta_{\text{H}}$ (ppm), (mult., $J$ in Hz)	$\delta_{\text{C}}$ (ppm)
1		38.7		38.9
2		27.4		27.6
3	3.20 ( <i>dd</i> , 11.2, 4.8)	79.0	3.19 ( <i>dd</i> , 11.2, 4.9)	79.1
4		38.8		39.0
5	0.70 ( <i>br d</i> )	55.3	0.67 ( <i>m</i> )	55.4
6		18.3		18.5
7		34.2		34.4
8		40.9		41.1
9		50.4		50.6
10		37.1		37.3
11		20.8		21.0
12		25.2		25.4
13		37.3		37.5
14		42.7		42.9
15		27.0		27.2
16		29.2		29.3
17		47.8		48.0
18		48.7		48.9
19	2.40 ( <i>ddd</i> , 10.8, 10.8, 6.0)	47.8	2.38 ( <i>m</i> )	48.0
20		150.5		150.6
21		29.7		29.9
22		34.0		34.1
23	0.99 ( <i>s</i> )	28.0	0.96 ( <i>s</i> )	28.1
24	0.78 ( <i>s</i> )	15.3	0.76 ( <i>s</i> )	15.5
25	0.84 ( <i>s</i> )	16.1	0.82 ( <i>s</i> )	16.3

**Table 14.**  $^1\text{H}$  (400 MHz) and  $^{13}\text{C}$  (100 MHz) NMR assignments of compound DG04 and betulin (in  $\text{CDCl}_3$ ) (continued)

Position	Compound DG04		Betulin*	
	$\delta_{\text{H}}$ (ppm), (mult., $J$ in Hz)	$\delta_{\text{C}}$ (ppm)	$\delta_{\text{H}}$ (ppm), (mult., $J$ in Hz)	$\delta_{\text{C}}$ (ppm)
26	1.04 (s)	16.0	1.02 (s)	16.1
27	1.00 (s)	14.7	0.98 (s)	14.9
28	3.35 (d, 10.8), 3.82 (dd, 10.8, 1.6)	60.5	3.33 (d, 10.6), 3.80 (d, 10.8)	60.7
29	4.60 (dd, 2.0, 1.2), 4.70 (d, 2.0)	109.7	4.58 (m), 4.68 (d, 2.2)	109.8
30	1.70 (s)	19.1	1.68 (s)	19.2

\*  $^1\text{H}$  (400 MHz) and  $^{13}\text{C}$  (100 MHz); Li *et al.*, 2015.

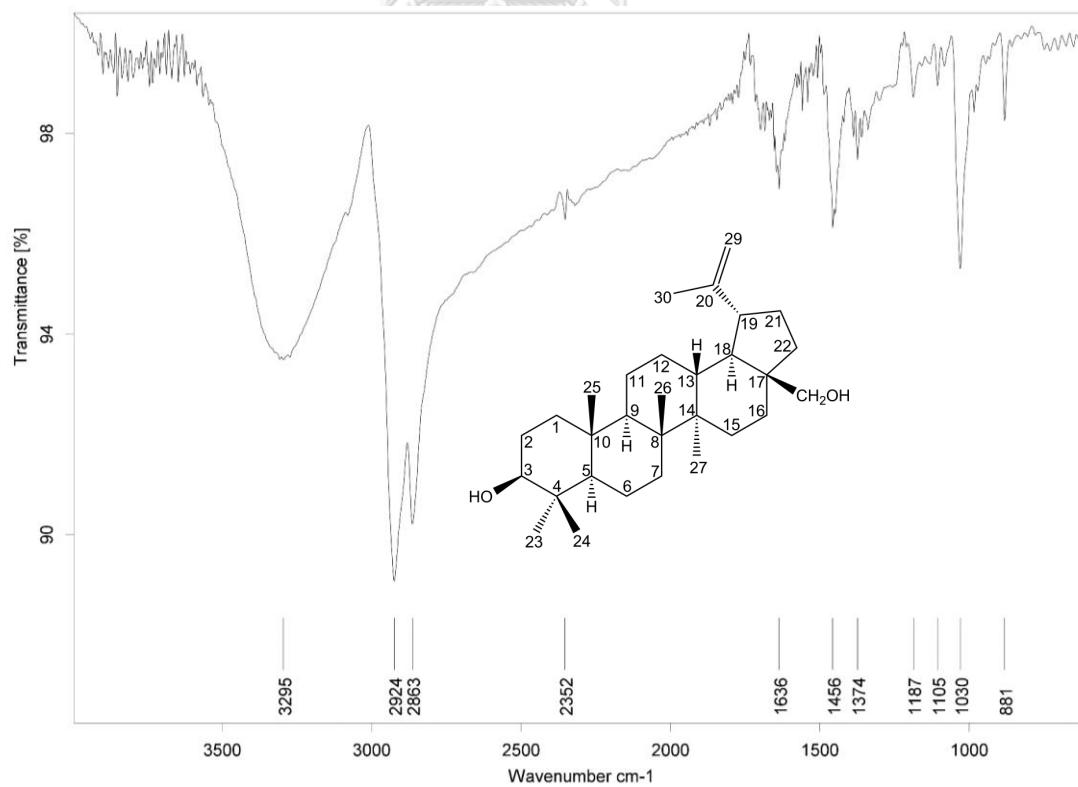


**Figure 14.** IR spectrum of compound DG04

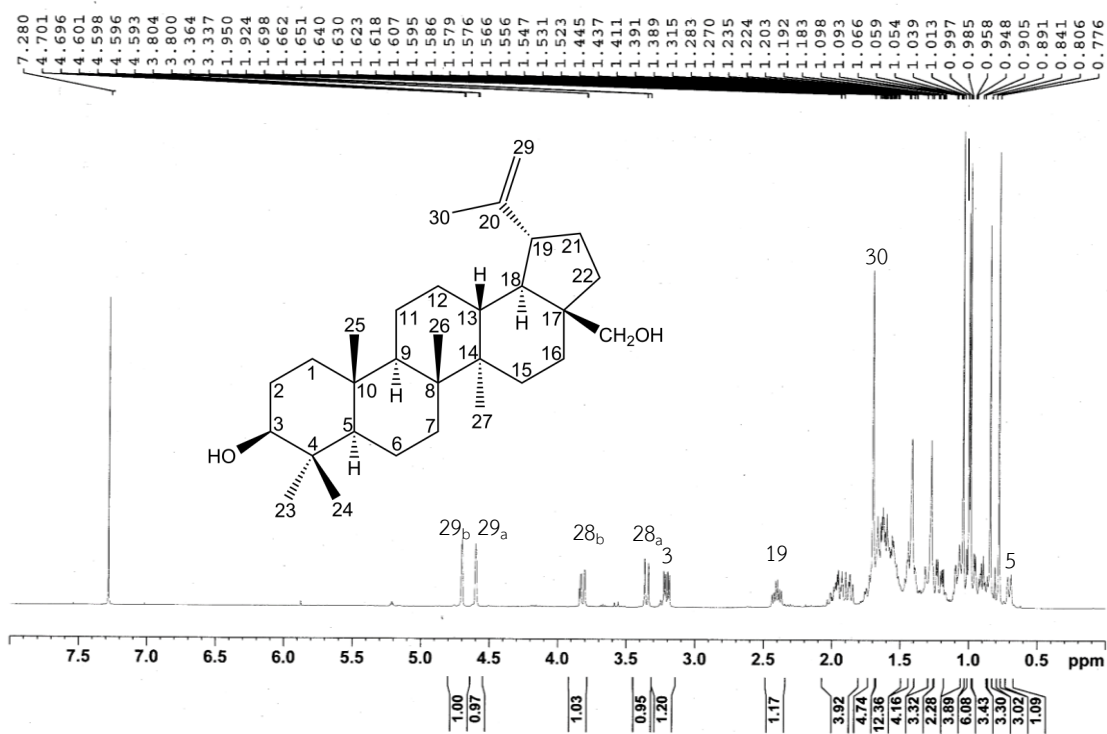


Figure 15a.  $^1\text{H}$  NMR (400 MHz) spectrum of compound DG04 (in  $\text{CDCl}_3$ )

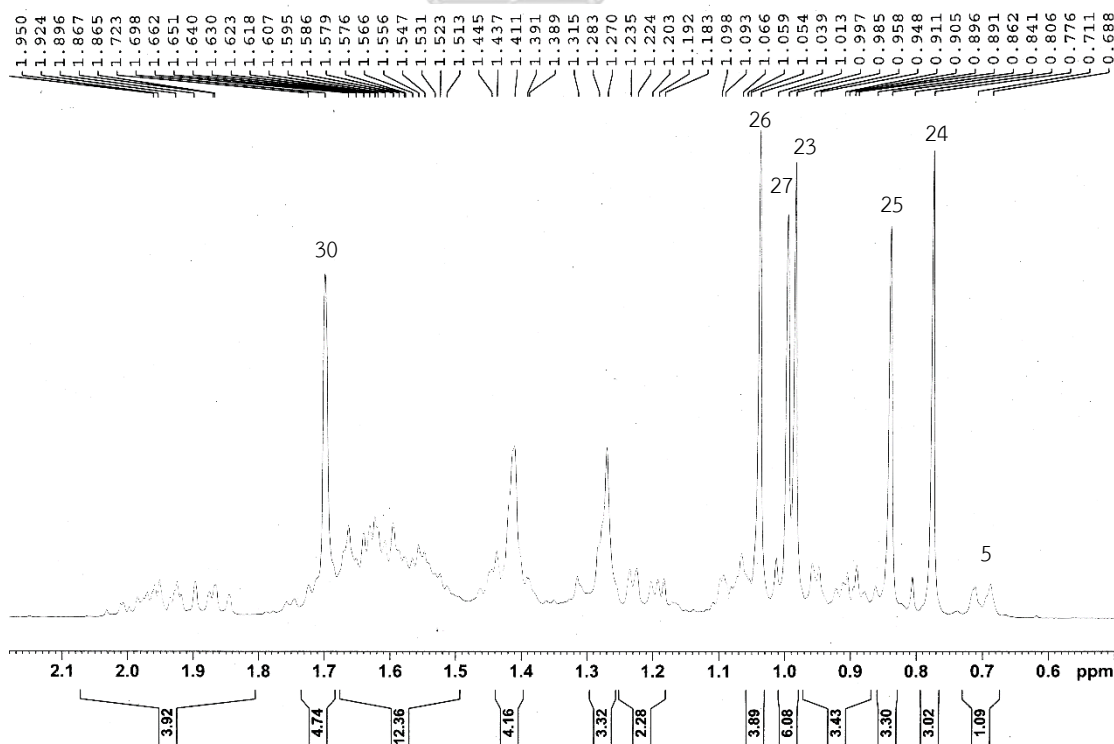


Figure 15b.  $^1\text{H}$  NMR (400 MHz) spectrum of compound DG04 (in  $\text{CDCl}_3$ ) (expanded)

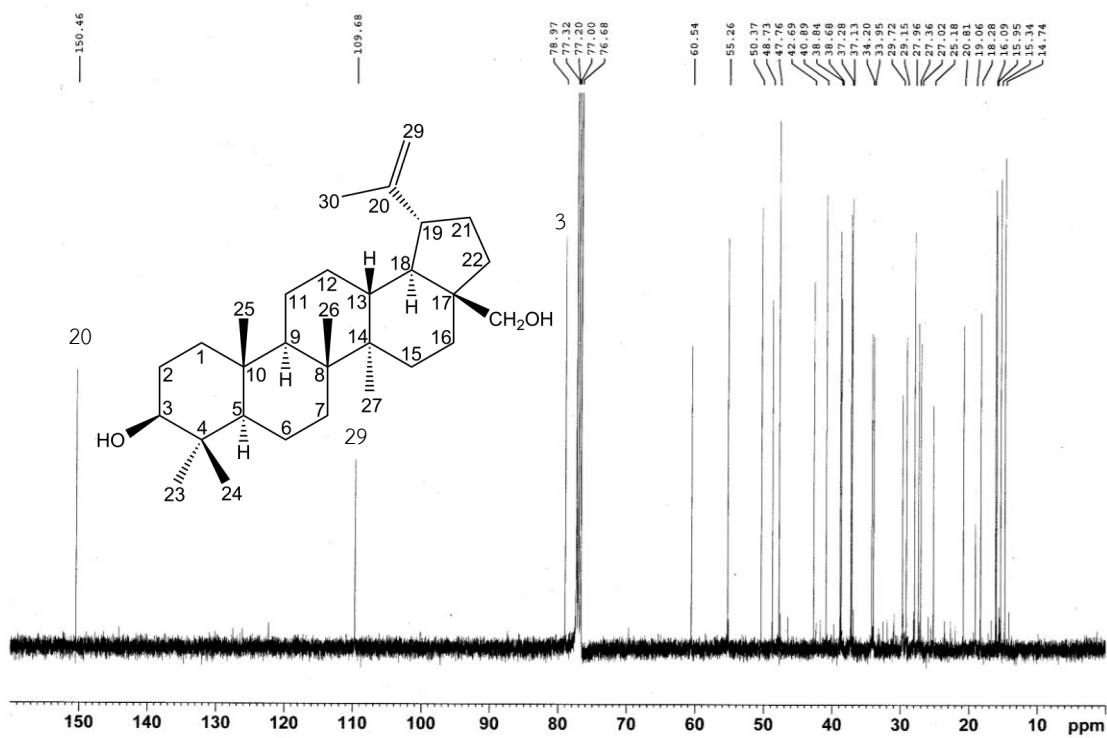


Figure 16a.  $^{13}\text{C}$  NMR (100 MHz) spectrum of compound DG04 (in  $\text{CDCl}_3$ )

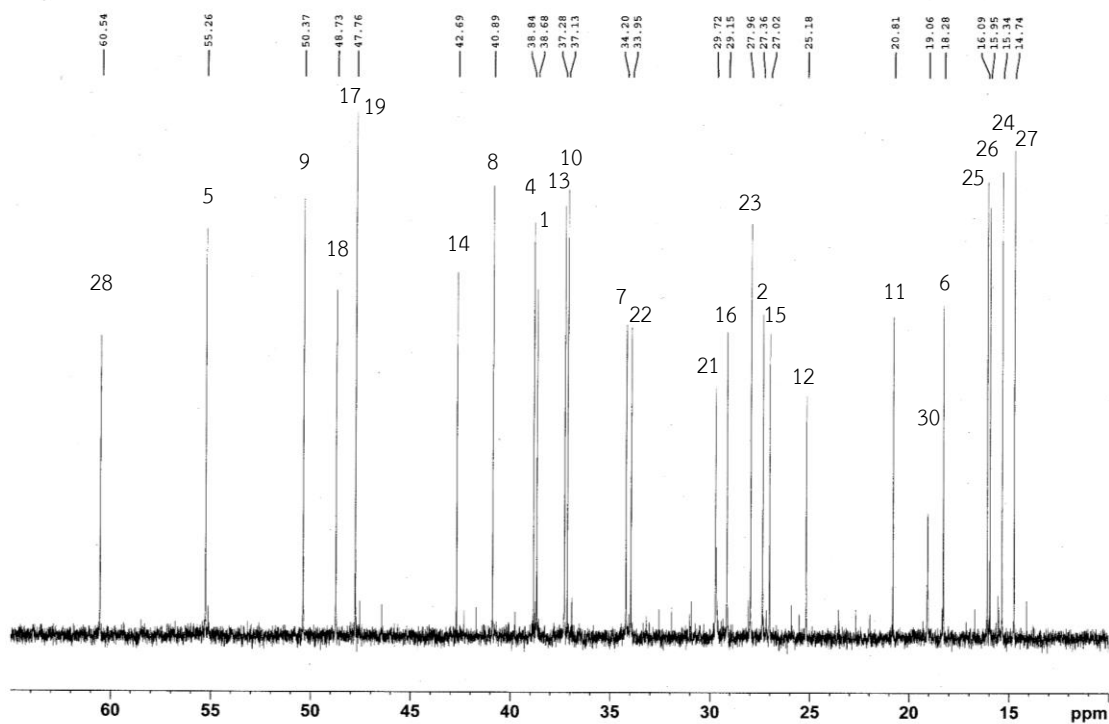
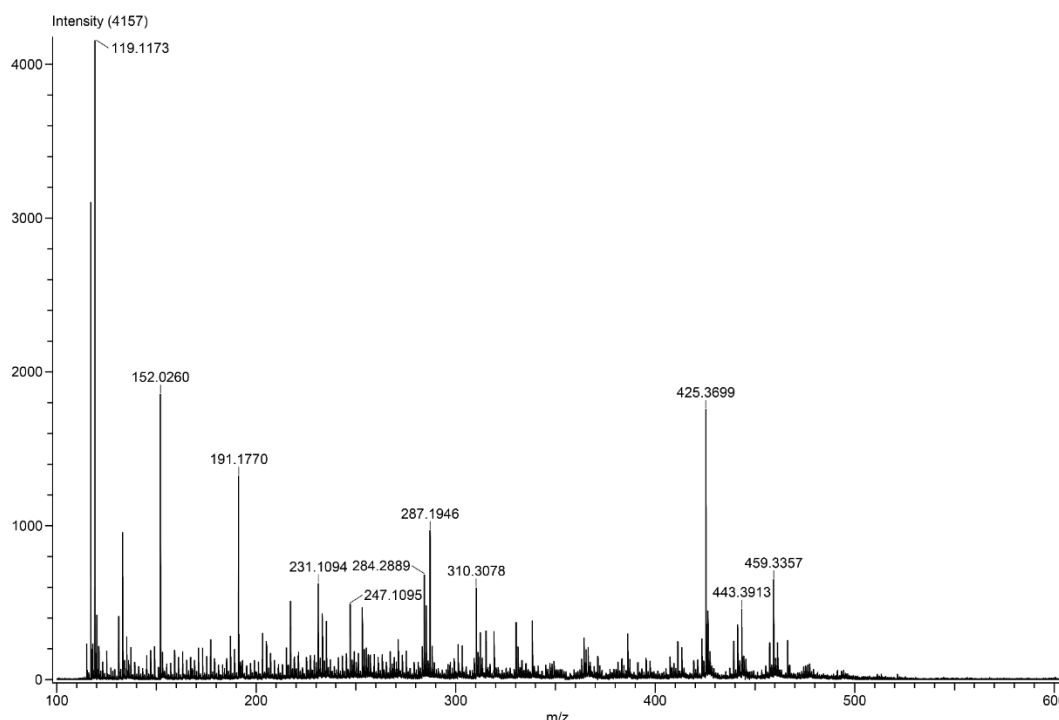


Figure 16b.  $^{13}\text{C}$  NMR (100 MHz) spectrum of compound DG04 (in  $\text{CDCl}_3$ ) (expanded)





**Figure 17.** DART-TOF Mass spectrum of compound DG04

Betulin can be found in several members *Diospyros* such as *D. anisandra*, *D. carbonaria*, *D. virginiana* (Fareed *et al.*, 2022). It can be found in more than two hundred plant species. The richest source is Betulaceae family. Betulin has been reported to display activities e.g., anti-tumor, anti-proliferative, anti-viral, and anti-inflammatory (Hordyjewska *et al.*, 2019).

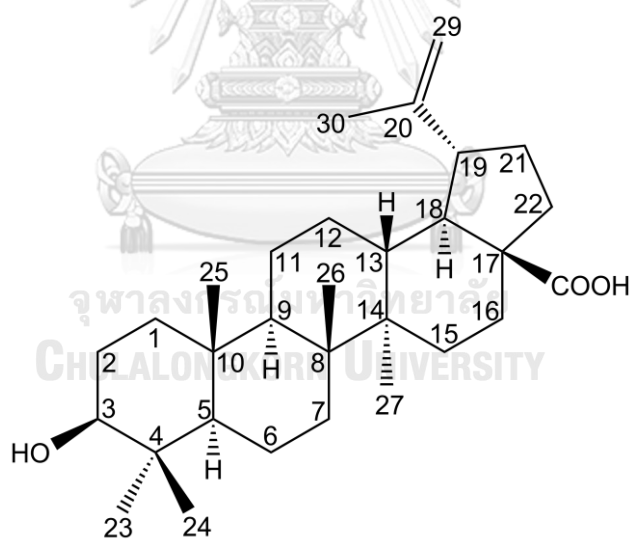
### 1.5 Compound DG05 (betulinic acid)

DG05 was obtained as colorless needles. Its IR spectrum (**Figure 19**) displayed absorption bands at 1686, and 3424  $\text{cm}^{-1}$ , indicating the presence of the carboxyl and the hydroxy groups, respectively.

The  $^1\text{H}$  NMR spectrum of DG05 (**Figures 20a-20b**), similar to that of DG03, exhibited a pair of broad singlets at  $\delta$  4.63 (H-29<sub>a</sub>), 4.76 (H-29<sub>b</sub>) ppm, representing the isopropenyl group, and a doublet of doublets at  $\delta$  3.21 ( $J = 11.2, 5.2$  Hz) ppm, corresponding to a hydroxymethine proton (H-3). The significant difference between the two spectra was the number of methyl singlets observed for DG03 and DG05,

which was seven and six, respectively. In the  $^{13}\text{C}$  NMR spectrum (Figures 22a-22b), 30 carbon signals were observed. The two signals at  $\delta$  110.2 and 149.8 ppm were indicative of the isopropenyl group while that at  $\delta$  79.1 ppm represented the hydroxy substituted C-3. The most downfield signal at  $\delta$  180.3 ppm suggested the presence of a carboxylic group.

All the above information indicated that DG05 was betulinic acid. This deduction was supported by the DART-TOF mass spectrum (Figure 25), which displayed a pseudomolecular peak  $[\text{M}+\text{H}]^+$  at  $m/z$  457.3672, corresponded to the molecular formula of  $\text{C}_{30}\text{H}_{48}\text{O}_3$ , confirming the identity of DG05 as betulinic acid. The structure of the compound is shown below.  $^1\text{H}$  and  $^{13}\text{C}$  NMR assignments of DG05 and those previously reported for betulinic acid are presented in Table 15.



Betulinic acid

**Table 15.**  $^1\text{H}$  (400 MHz) and  $^{13}\text{C}$  (100 MHz) NMR assignments of compound DG05 and betulinic acid (in  $\text{CDCl}_3$ )

Position	Compound DG05		Betulinic acid*	
	$\delta_{\text{H}}$ (ppm), (mult., $J$ in Hz)	$\delta_{\text{C}}$ (ppm)	$\delta_{\text{H}}$ (ppm), (mult., $J$ in Hz)	$\delta_{\text{C}}$ (ppm)
1		38.8		38.7
2		27.5		27.4
3	3.21 ( <i>dd</i> , 11.2, 5.2)	79.1	3.19 ( <i>dd</i> , 10.0, 4.7)	78.9
4		39.0		38.8
5	0.70 ( <i>br d</i> )	55.4		55.3
6		18.4		18.3
7		34.4		34.3
8		40.8		40.7
9		50.6		50.5
10		37.3		37.2
11		20.9		20.8
12		25.6		25.5
13		38.5		38.4
14		42.5		42.4
15		29.8		30.5
16		32.2		32.1
17		56.4		56.3
18		49.4		46.8
19	3.02 ( <i>ddd</i> , 10.8, 10.8, 4.8)	47.0	2.99 ( <i>ddd</i> , 11.0, 11.0, 5.5)	49.2
20		150.5		150.3
21		30.6		29.7
22		37.1		37.0
23	0.98 ( <i>s</i> )	28.1	0.93 ( <i>s</i> )	27.9
24	0.77 ( <i>s</i> )	15.4	0.75 ( <i>s</i> )	15.3
25	0.84 ( <i>s</i> )	16.1	0.82 ( <i>s</i> )	16.0

**Table 15.**  $^1\text{H}$  (400 MHz) and  $^{13}\text{C}$  (100 MHz) NMR assignments of compound DG05 and betulinic acid (in  $\text{CDCl}_3$ ) (continued)

Position	Compound DG05		Betulinic acid*	
	$\delta_{\text{H}}$ (ppm), (mult., $J$ in Hz)	$\delta_{\text{C}}$ (ppm)	$\delta_{\text{H}}$ (ppm), (mult., $J$ in Hz)	$\delta_{\text{C}}$ (ppm)
26	0.95 (s)	16.2	0.96 (s)	16.1
27	0.99 (s)	14.8	0.97 (s)	14.7
28		180.3		180.5
29	4.63 (br s), 4.76 (br s)	109.8	4.60 (d, 1.5), 4.73 (d, 1.5)	109.6
30	1.71 (s)	19.5	1.68 (s)	19.4

\*  $^1\text{H}$  (400 MHz) and  $^{13}\text{C}$  (100 MHz); Siddiqui *et al.*, 1988.

$^1\text{H}$  and  $^{13}\text{C}$  NMR assignments of DG05 were done with the assistance of 2D NMR experiments including NOESY (Figure 21), HSQC (Figure 23) and HMBC (Figure 24a-24c). The signal assignments for proton and carbon of DG05 as shown in Table 15 are almost in full agreement with the previously reported ones except for the reversed assignments for the two methylene carbons at positions 15 and 21 (DG05:  $\delta$  29.8 and 30.6 ppm; reported values:  $\delta$  30.5 and 29.7 ppm), as well as the two methine carbons at positions 18 and 19 (DG05:  $\delta$  49.4 and 47.0 ppm; reported values:  $\delta$  46.8 and 49.2 ppm). The signal assignments for these carbons were evidenced by three-bond correlations observed in the HMBC spectrum. The differentiation of signals for C-15 and C-21 could be deduced from the correlation between the proton signal at  $\delta$  0.99 (Me-27) ppm and the carbon signal at  $\delta$  29.8 (C-15) ppm, while that for C-18 and C-19 from the correlation between the proton signal at  $\delta$  1.71 (Me-30) ppm and the carbon signal at  $\delta$  47.0 (C-19) ppm. Important correlations observed in the HMBC and NOESY spectra of DG05 are shown in Figure 18.

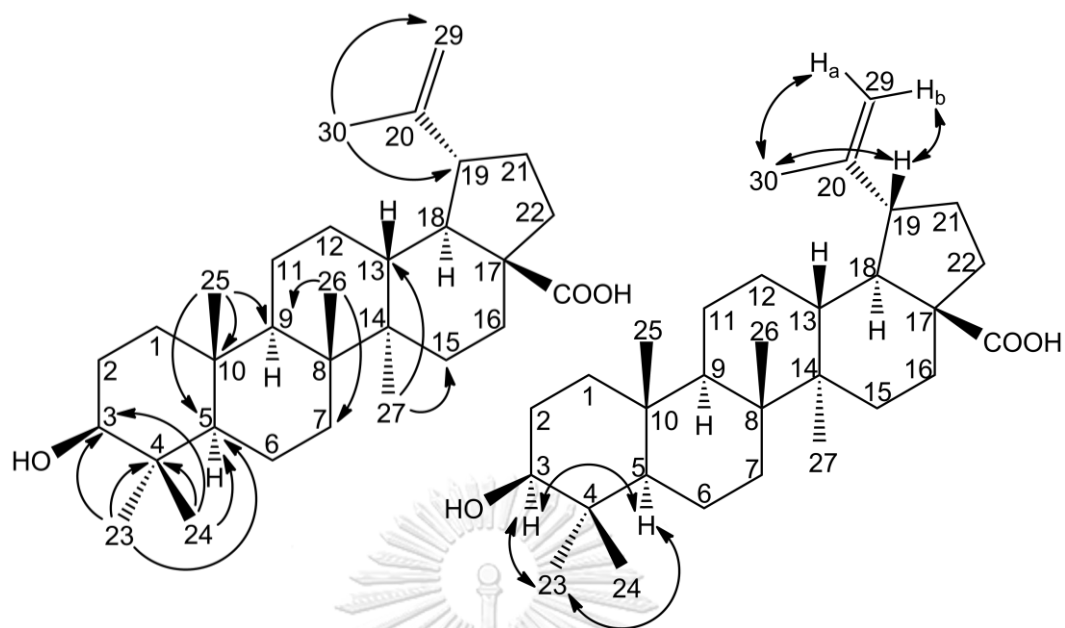


**Figure 18.** HMBC and NOESY Correlations of DG05

→ HMBC correlations of DG05

↔ NOESY correlations of DG05

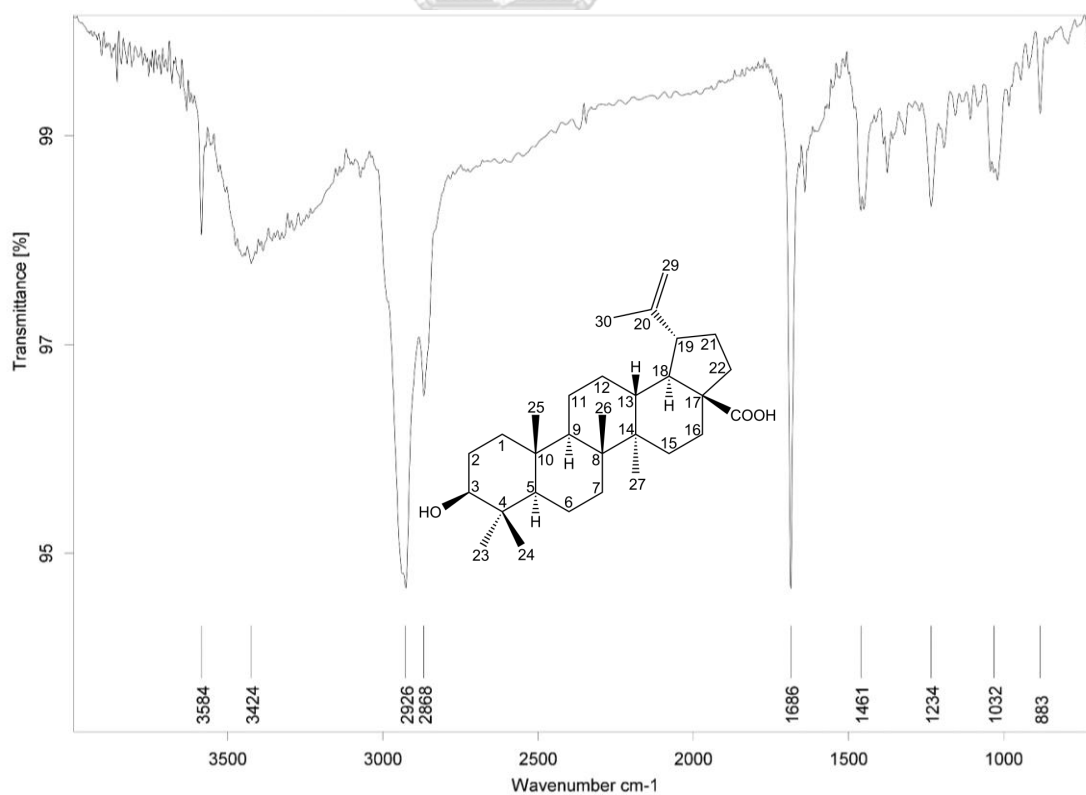


**Figure 19.** IR spectrum of compound DG05

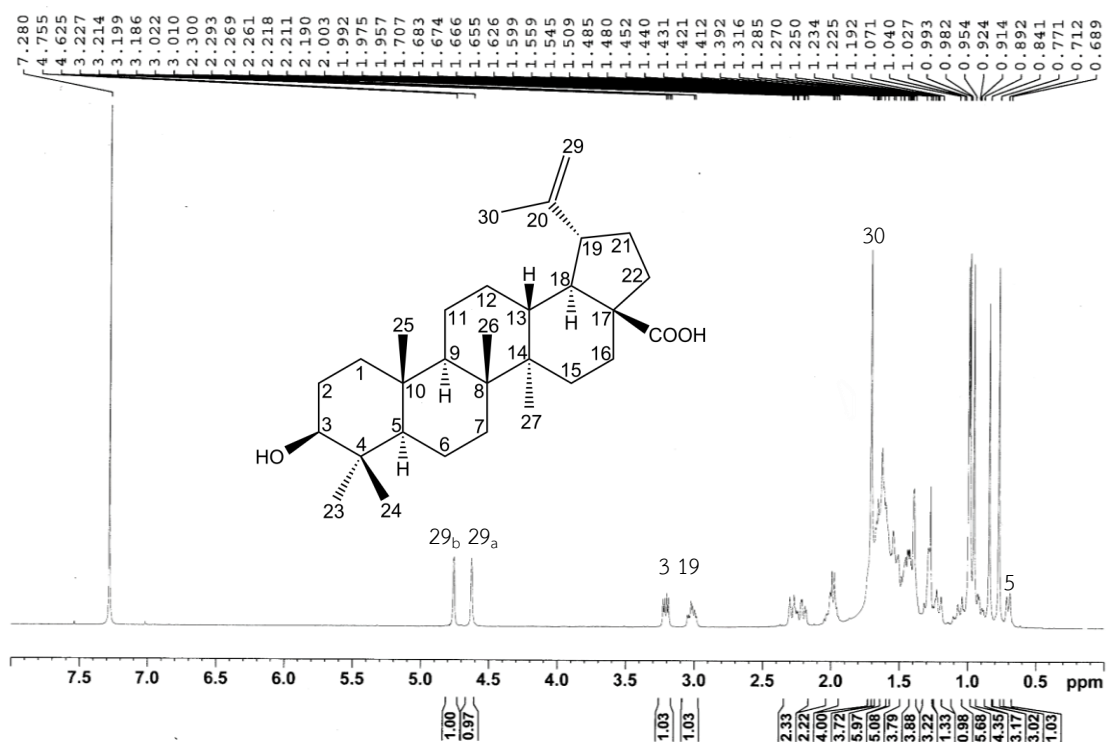


Figure 20a.  $^1\text{H}$  NMR (400 MHz) spectrum of compound DG05 (in  $\text{CDCl}_3$ )

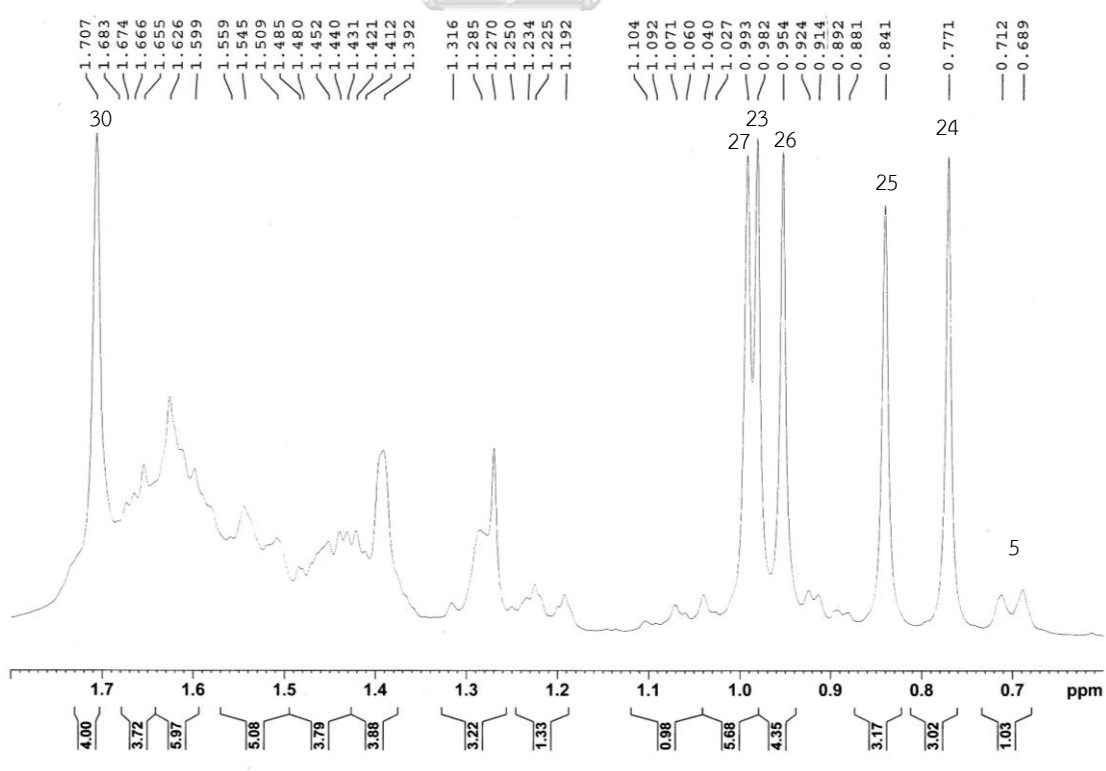
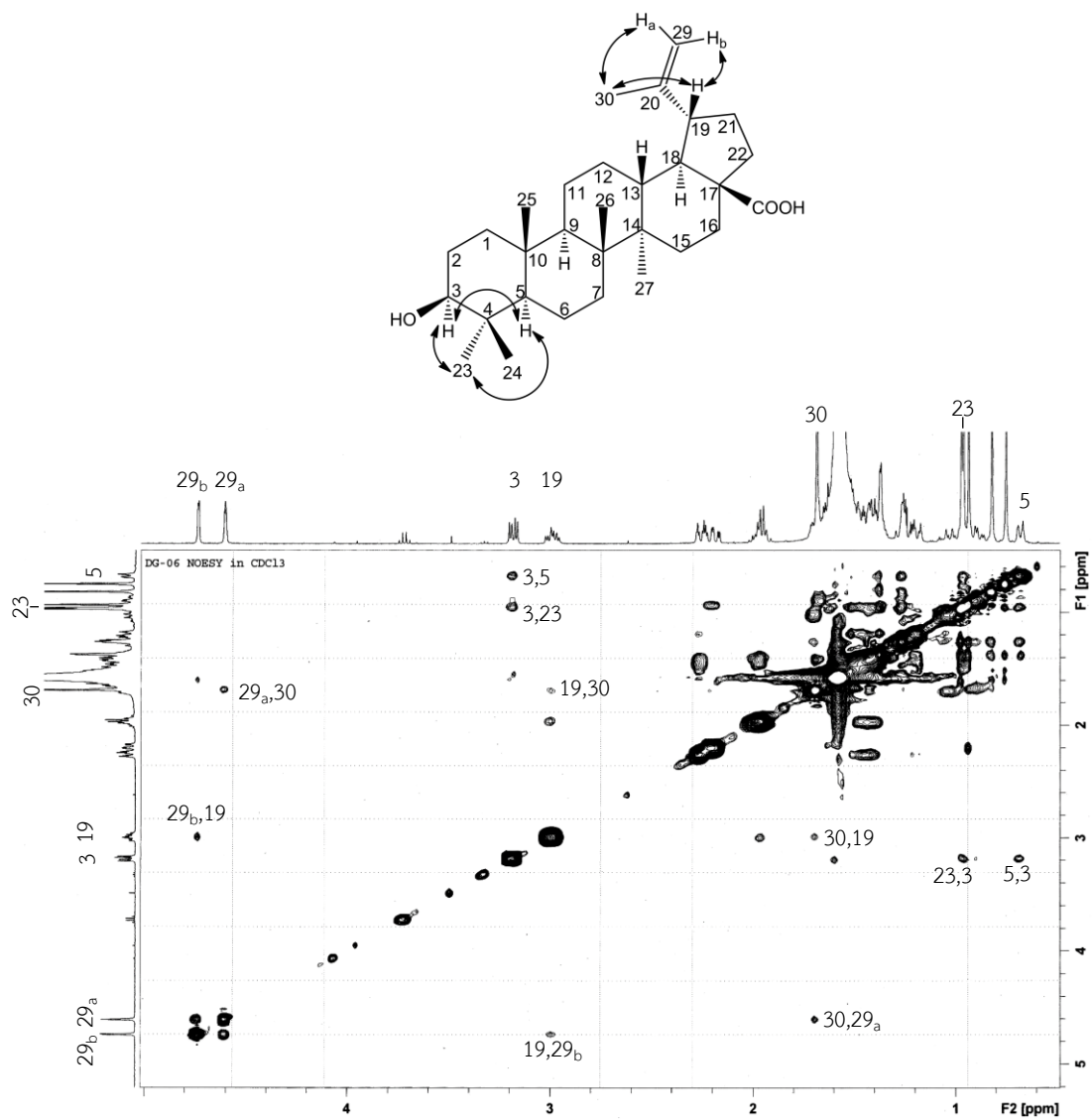


Figure 20b.  $^1\text{H}$  NMR (400 MHz) spectrum of compound DG05 (in  $\text{CDCl}_3$ ) (expanded)



CHULALONGKORN UNIVERSITY  
 Figure 21.  $^1\text{H}$ - $^1\text{H}$  NOESY spectrum of compound DG05

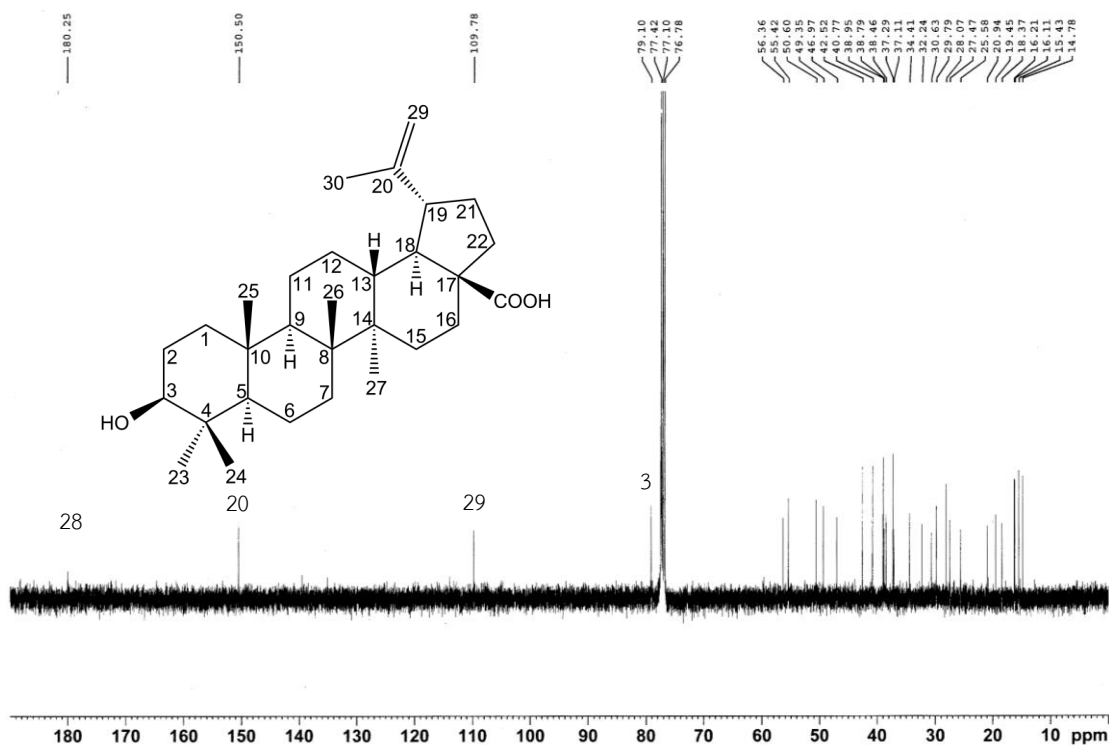


Figure 22a.  $^{13}\text{C}$  NMR (100 MHz) spectrum of compound DG05 (in  $\text{CDCl}_3$ )

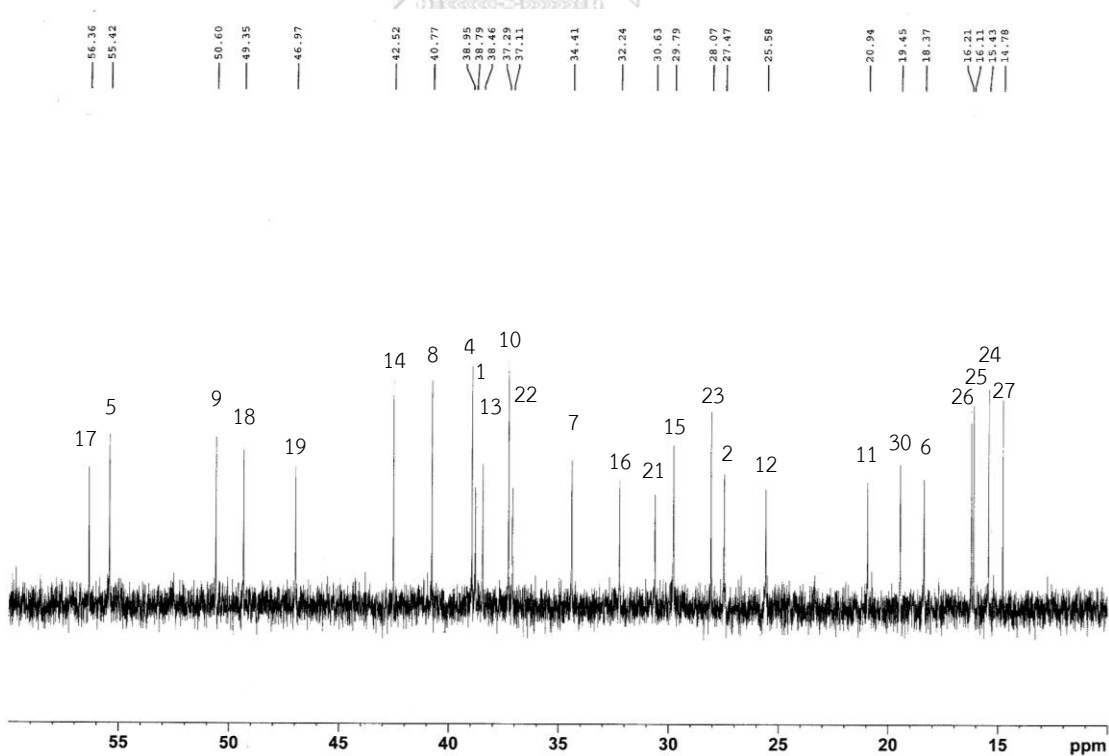


Figure 22b.  $^{13}\text{C}$  NMR (100 MHz) spectrum of compound DG05 (in  $\text{CDCl}_3$ ) (expanded)



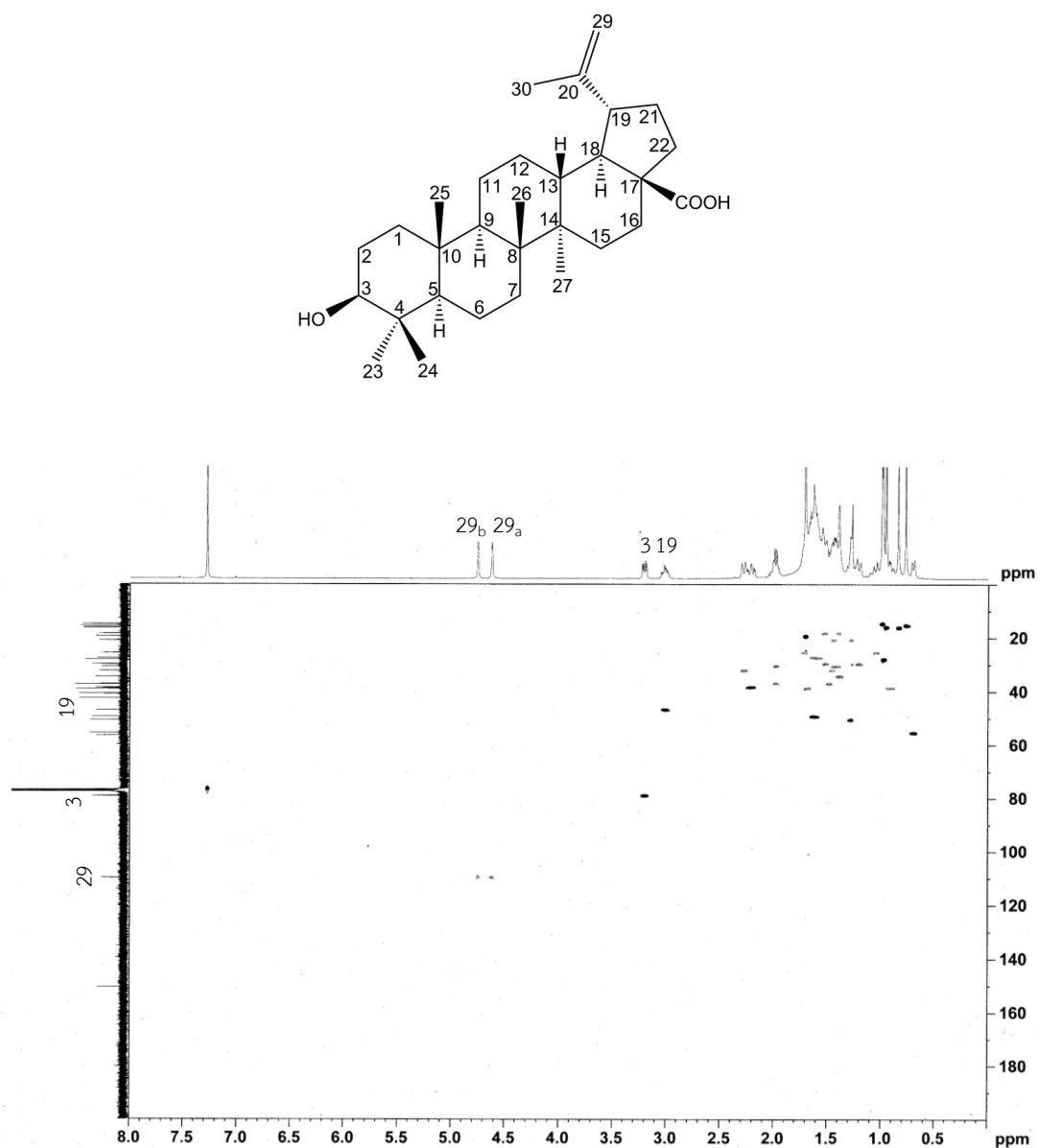


Figure 23. HSQC spectrum of compound DG05

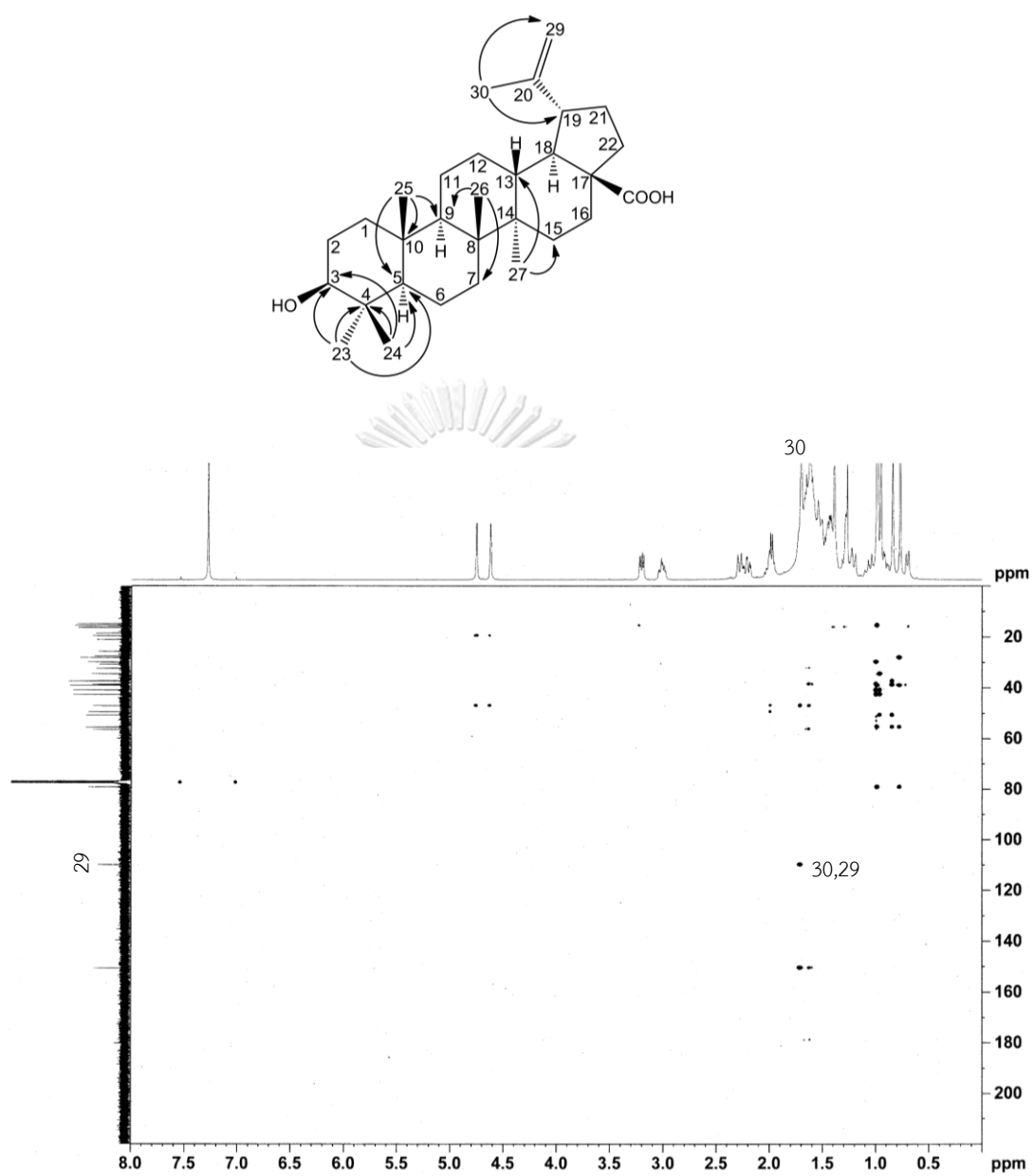


Figure 24a. HMBC spectrum of compound DG05

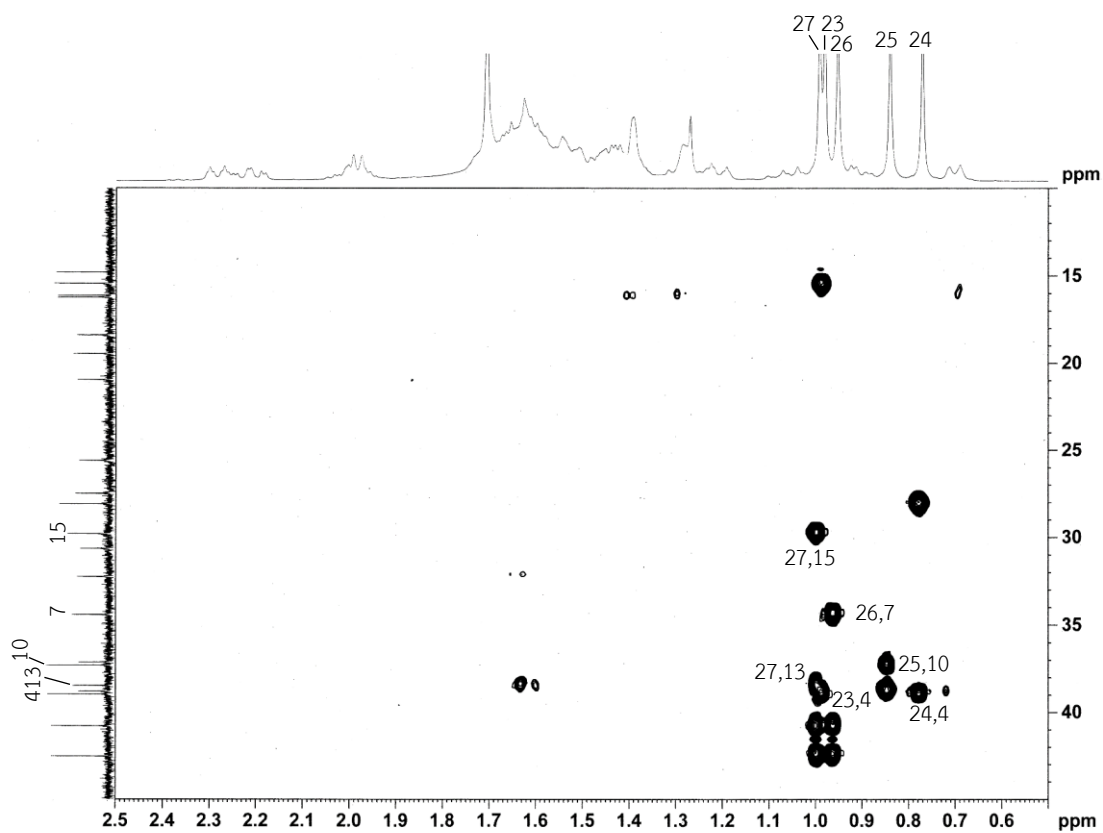


Figure 24b. HMBC spectrum of compound DG05 (expanded)

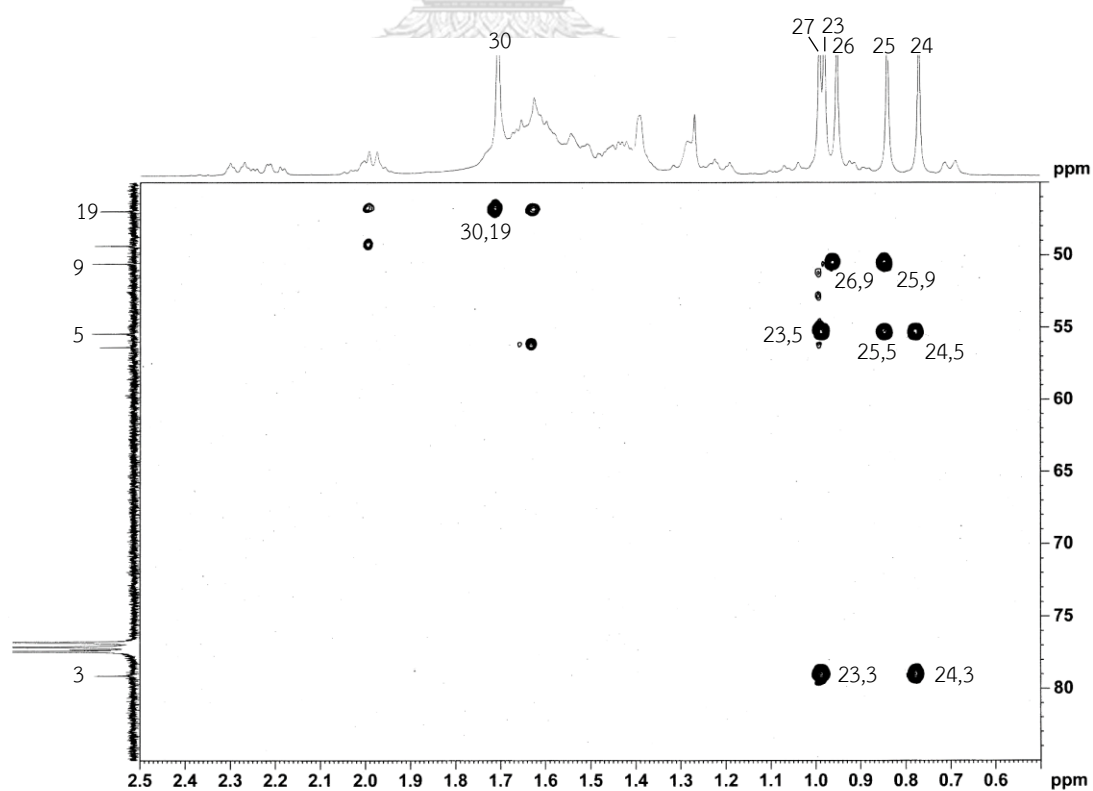
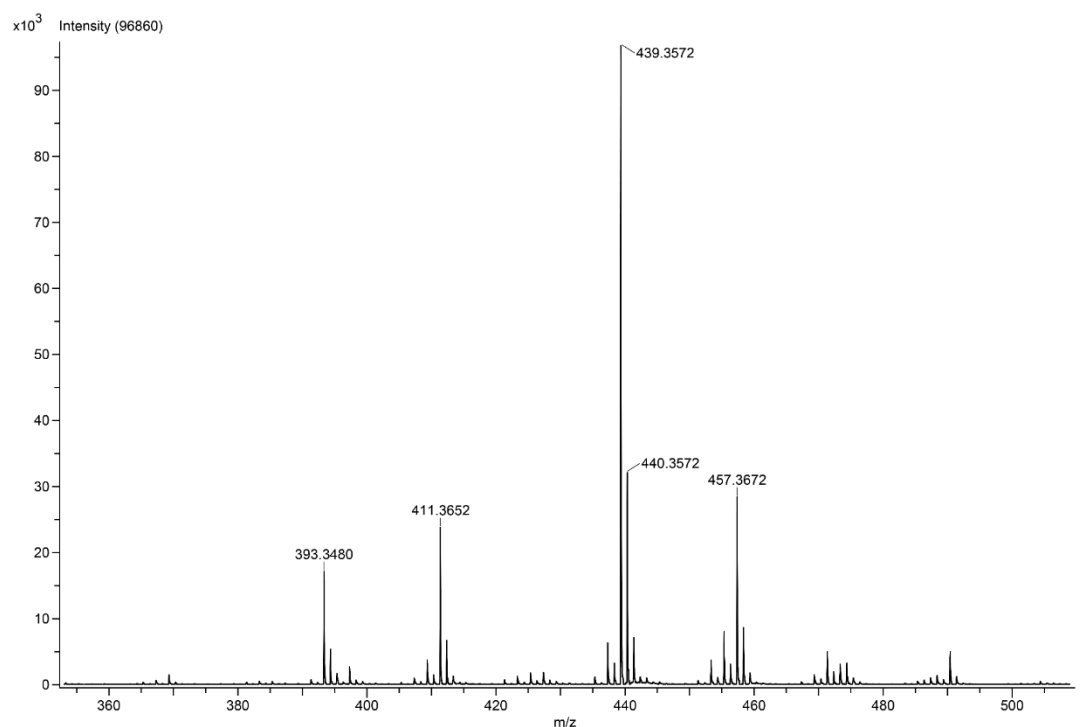


Figure 24c. HMBC spectrum of compound DG05 (expanded)



**Figure 25.** DART-TOF Mass spectrum of compound DG05

Many *Diospyros* species are sources of betulinic acid, for example, *D. anisandra*, *D. carbonaria*, *D. crassiflora*, *D. glans*, *D. kaki*, *D. mespiliformis*, and *D. virginiana* (Fareed *et al.*, 2022). It has a high potential in killing cancer cells. Other bioactivities of betulinic acid are antiviral, antibacterial, anthelmintic, and anti-inflammatory effects (Mullauer *et al.*, 2010).

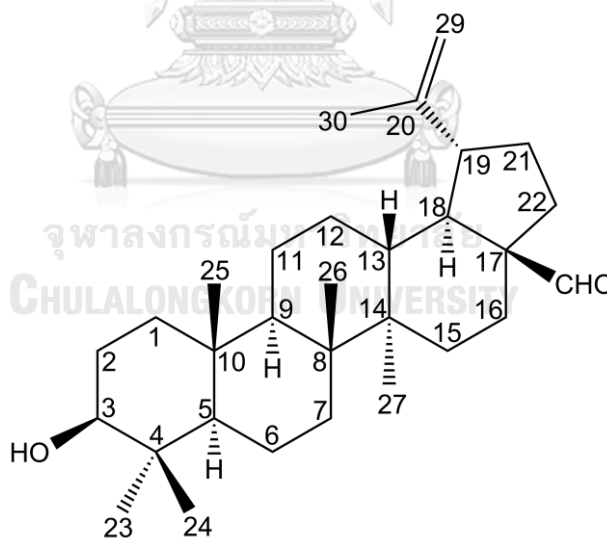
### 1.6 Compound DG06 (betulinaldehyde)

DG06 was obtained as white amorphous powder. The IR spectrum of DG06 (**Figure 26**) showed absorption bands at 1711 and 3401  $\text{cm}^{-1}$ , indicating the presence of the aldehyde and hydroxy groups in the molecule, respectively.

The  $^1\text{H}$  and  $^{13}\text{C}$  NMR spectra of DG06 were similar to those of DG05, suggesting that the two compounds were structurally related. The  $^1\text{H}$  NMR spectrum of DG06 (**Figures 27a-27b**) showed six methyl singlets at  $\delta$  0.76 (Me-24), 0.84 (Me-25), 0.92 (Me-23), 0.97 (Me-26), 1.26 (Me-27), 1.70 (Me-30) ppm, a pair of broad singlets at  $\delta$

4.64 (H-29<sub>a</sub>), 4.76 (H-29<sub>b</sub>) ppm, and a doublet of doublets at  $\delta$  3.19 ( $J = 11.2, 4.8$ , H-3) ppm. The most downfield signal at  $\delta$  9.69 ppm, which was absent in the spectrum of DG05, indicated the presence of the formyl group. Its  $^{13}\text{C}$  NMR spectrum (**Figures 28a-28b**) exhibited 30 carbon signals. In terms of chemical shift values, almost all of these signals corresponded to those in the spectrum of DG05, except for the most downfield one at  $\delta$  206.8 ppm which was significantly different from that observed for DG05 ( $\delta$  180.3 ppm). This signal represented the aldehyde carbon, instead of the carboxyl carbon of DG05. Therefore, DG06 was proposed to be betulinaldehyde, a derivative of betulinic acid which contained an aldehyde group instead of a carboxyl group.

The NMR spectral data of DG06 were found to be in consistence with those of betulinaldehyde (Theerachayanan *et al.*, 2007), the structure of which is shown below. The IR data also supported this structure. Comparison of their  $^1\text{H}$  and  $^{13}\text{C}$  NMR assignments is presented in **Table 16**.



Betulinaldehyde

**Table 16.**  $^1\text{H}$  (400 MHz) and  $^{13}\text{C}$  (100 MHz) NMR assignments of compound DG06 and betulinaldehyde (in  $\text{CDCl}_3$ )

Position	Compound DG06		Betulinaldehyde*	
	$\delta_{\text{H}}$ (ppm), (mult., $J$ in Hz)	$\delta_{\text{C}}$ (ppm)	$\delta_{\text{H}}$ (ppm), (mult., $J$ in Hz)	$\delta_{\text{C}}$ (ppm)
1		38.7		38.6
2		27.3		27.3
3	3.19 ( <i>dd</i> , 11.2, 4.8)	79.0	3.20 ( <i>q</i> )	78.9
4		38.9		38.8
5	0.68 ( <i>br d</i> )	55.3		55.2
6		18.3		18.2
7		34.3		34.3
8		40.8		40.8
9		50.5		50.4
10		37.2		37.1
11		20.8		20.7
12		25.5		25.5
13		38.7		38.7
14		42.6		42.5
15		29.3		29.2
16		28.8		28.8
17		59.4		59.3
18		48.1		48.0
19	2.87 ( <i>ddd</i> , 11.2, 11.2, 5.6)	47.6	2.80 ( <i>m</i> )	47.5
20		149.8		149.7
21		29.9		29.8
22		33.2		33.2
23	0.92 ( <i>s</i> )	28.0	0.84 ( <i>s</i> )	27.9
24	0.76 ( <i>s</i> )	15.4	0.68 ( <i>s</i> )	15.3
25	0.84 ( <i>s</i> )	15.9	0.75 ( <i>s</i> )	15.8

**Table 16.**  $^1\text{H}$  (400 MHz) and  $^{13}\text{C}$  (100 MHz) NMR assignments of compound DG06 and betulinaldehyde (in  $\text{CDCl}_3$ ) (continued)

Position	Compound DG06		Betulinaldehyde*	
	$\delta_{\text{H}}$ (ppm), (mult., $J$ in Hz)	$\delta_{\text{C}}$ (ppm)	$\delta_{\text{H}}$ (ppm), (mult., $J$ in Hz)	$\delta_{\text{C}}$ (ppm)
26	0.97 (s)	16.2	0.90 (s)	16.1
27	1.26 (s)	14.3	1.19 (s)	14.2
28	9.69 (s)	206.8	9.60 (s)	206.7
29	4.64 (br s), 4.76 (br s)	110.2	4.56 (d, 2.0), 4.69 (d, 2.0)	110.1
30	1.70 (s)	19.0	1.62 (s)	19.0

\*  $^1\text{H}$  (400 MHz) and  $^{13}\text{C}$  (100 MHz); Theerachayanan *et al.*, 2007.

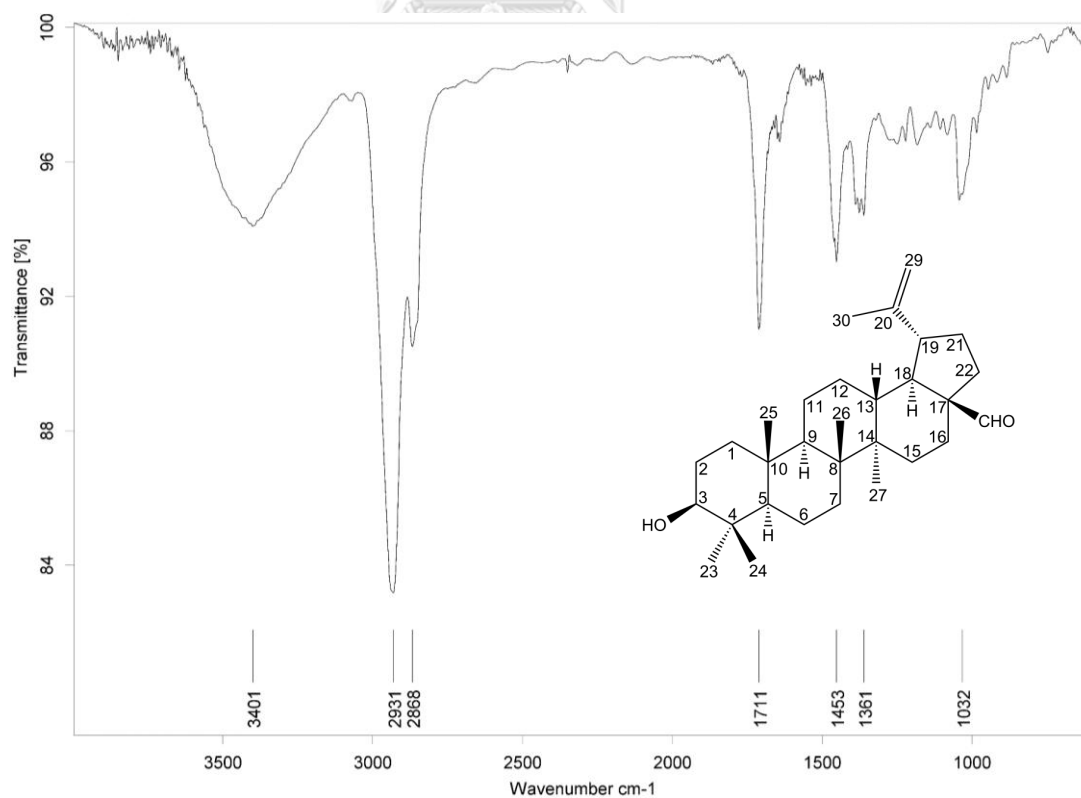


**Figure 26.** IR spectrum of compound DG06

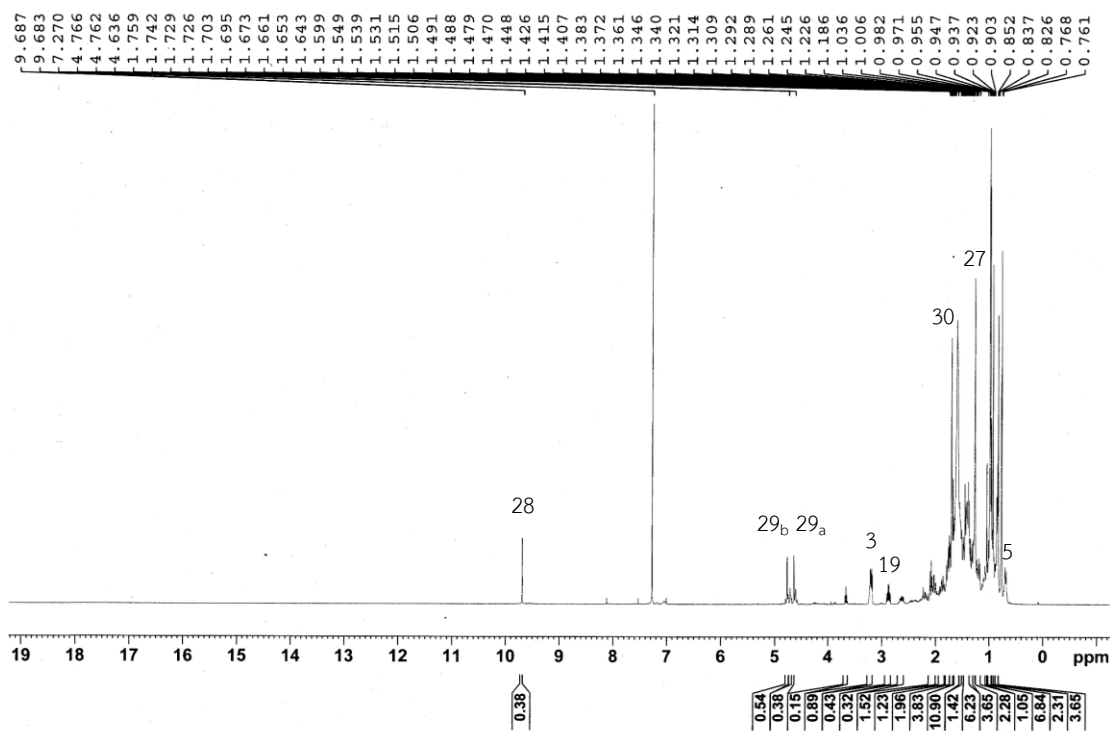


Figure 27a.  $^1\text{H}$  NMR (400 MHz) spectrum of compound DG06 (in  $\text{CDCl}_3$ )

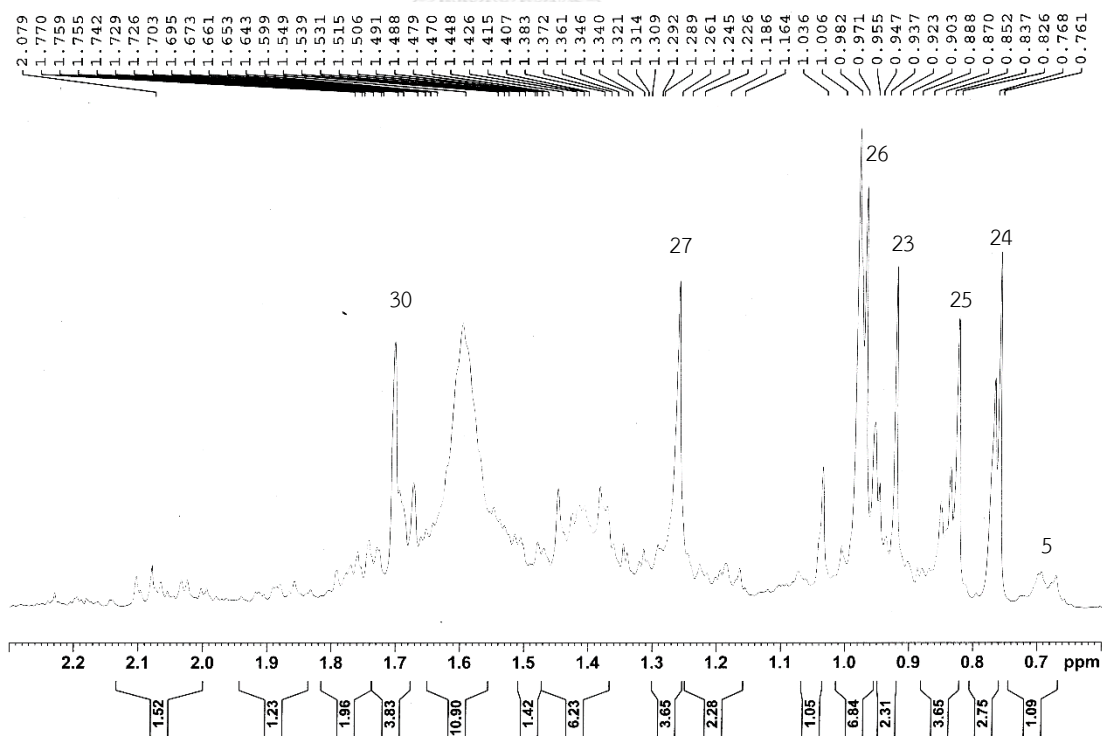


Figure 27b.  $^1\text{H}$  NMR (400 MHz) spectrum of compound DG06 (in  $\text{CDCl}_3$ ) (expanded)





Betulinaldehyde has been found in *Diospyros* plants including *D. anisandra*, *D. carbonaria*, *D. discolor*, *D. glans*, and *D. virginiana* (Fareed *et al.*, 2022). It has been reported to exhibit various biological activities such as antimycobacterial activity against *Mycobacterium tuberculosis* and *Plasmodium falciparum* (Amiri *et al.*, 2020).



## 2. Biological Activities of Isolated Compounds

The isolated compounds DG01-DG05 were investigated for their biological activities. Owing to the limited quantity obtained, DG06 was not included in this study. The results and detailed discussion are given below.

### 2.1 Cytotoxic Activity

Cytotoxicity of compound DG01-DG05 against two human cancer cell lines, U87 (glioblastoma) and MDA-MB231 (breast cancer), and a normal human cell line, EA.hy926 (endothelial cells) were evaluated by using MTT assay with doxorubicin as the positive control. All experiments were performed in triplicate except for those dealing with DG04, which were not repeated, because of insufficient quantity of the compound. The results represented by graphs plotted between the percentage of cell viability and logarithm of the concentration, are shown in **Figures 29-31**.  $IC_{50}$  values of the compounds for each of the tested cells, extrapolated from the graphs, are shown in **Table 17**.

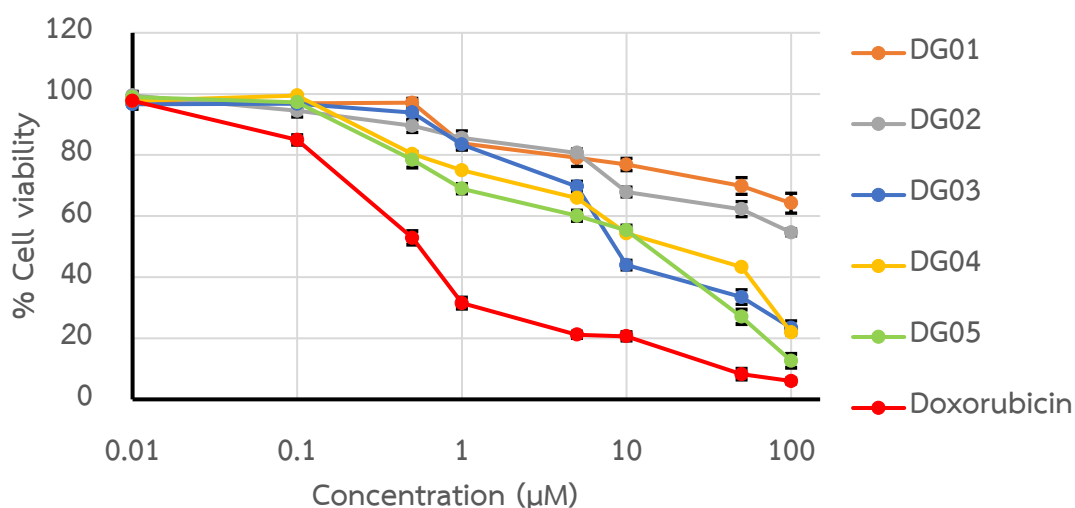


**Figure 29.** Cytotoxicity of tested compounds on glioblastoma U87 cells

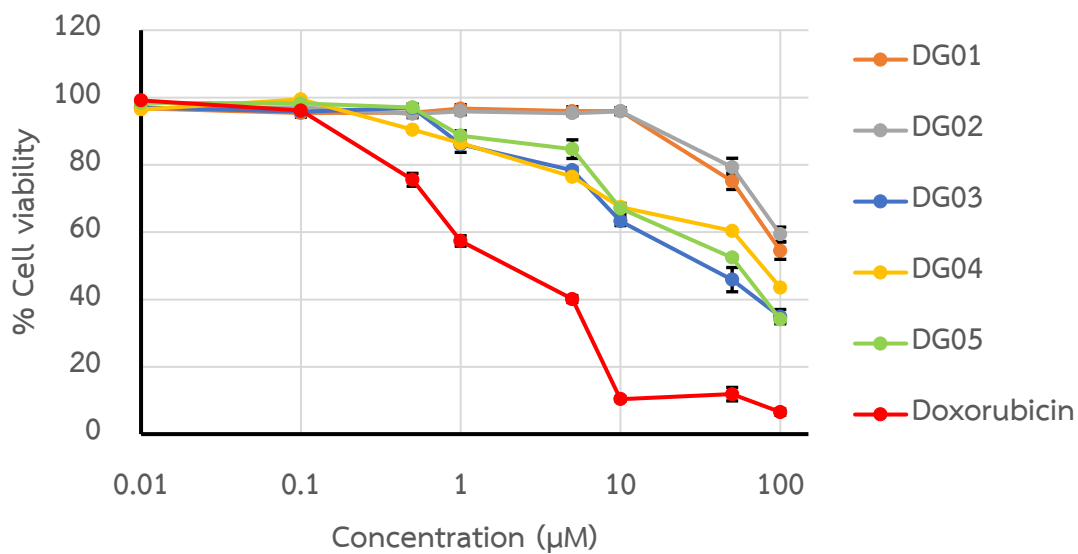


Figure 30. Cytotoxicity of tested compounds on breast cancer MDA-MB231 cells

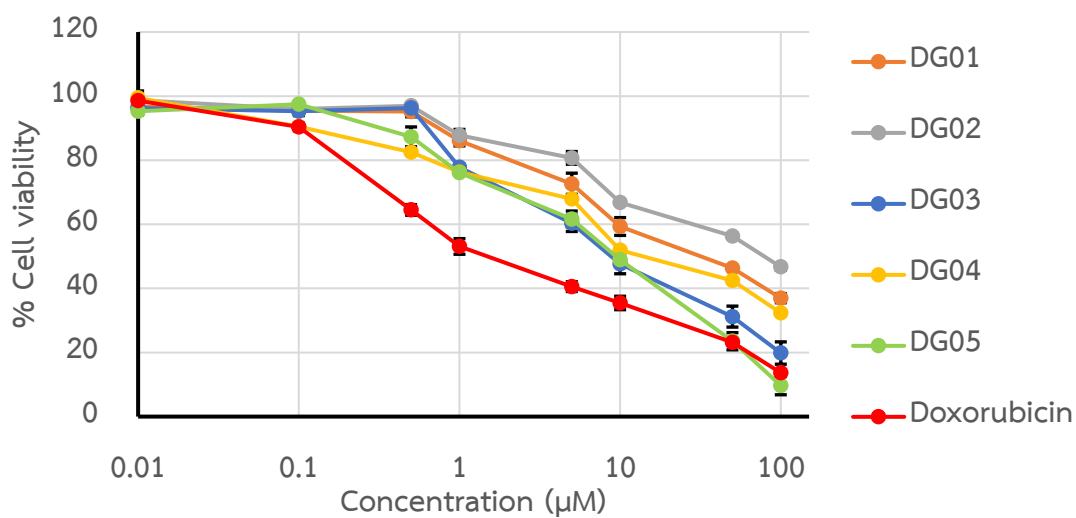


Figure 31. Cytotoxicity of tested compounds on normal endothelial EA.hy926 cells

**Table 17.** Cytotoxic activity of compounds DG01-DG05

Compound	IC <sub>50</sub> (μM)		
	U87	MDA-MB231	EA.hy926
DG01 (friedelin)	>100 (~533.2) *	>100 (~118.5) *	32.44
DG02 (epifriedelanol)	>100 (~160.3) *	>100 (~144.2) *	72.78
DG03 (lupeol)	13.16	34.41	10.67
DG04 (betulin)	15.39	74.49	19.08
DG05 (betulinic acid)	8.31	43.88	8.29
Doxorubicin	0.63	1.89	2.38

\* Extrapolated IC<sub>50</sub> (maximum tested concentration = 100 μM).

The isolated compounds used for the study could be classified into 2 groups: the friedelane-type triterpenoids, including DG01 and DG02, and the lupane-type triterpenoids, including DG03, DG04 and DG05. The data presented in **Table 17** indicated that cytotoxicity against the cancer and normal cells of the three lupane-type triterpenoids was stronger than that of the two friedelane-type triterpenoids. Compounds DG01 and DG02 exhibited no significant cytotoxic activity against both cancer cell lines but were cytotoxic to some extent against the normal cell line. All the lupane-type triterpenoids were more cytotoxic against glioblastoma U87 cells than breast cancer MDA-MB231 cells. The cytotoxicity against both the cancer cell lines of these compounds was not comparable to that of doxorubicin. Furthermore, their IC<sub>50</sub> values for these cell lines were higher or close to those for the normal cell lines, indicating the lack of selectivity which was a drawback for drug development.

## 2.2 Inhibitory Activity on T Cell Activation

Compounds DG01, DG02, DG03 and DG05 were investigated for their inhibitory activity on T cell activation mediated by CD3 and CD28, using Jurkat T cells. CD3 and CD28 are receptors on the surface of T cells. In our body, the stimulation of CD3 by MHC (major histocompatibility complex) together with that of CD28 by CD80 results in T cell activation. Overstimulation of CD3/CD28 signaling is the cause of overactive

T cells which can lead to autoimmune diseases. Suppression of stimulated CD3/CD28 signaling is considered as a strategy for the treatment of these diseases. Therefore, searching for compounds that exhibit an inhibitory effect on T cell activation mediated by CD3/CD38 can provide useful information for research and drug development in this therapeutic area.

In the assay, Jurkat T cells, pre-treated with the tested compounds, were stimulated with anti-CD3 and anti-CD28 antibodies, and the level of Interleukin 2 (IL-2) produced by the T cells was determined. The cytotoxicity of the tested compounds on Jurkat T cells was evaluated, and the results obtained are shown in **Figure 32**. The effects of the tested compound on Jurkat T cells stimulated with anti CD3/CD28 antibodies are shown in **Figure 33**.

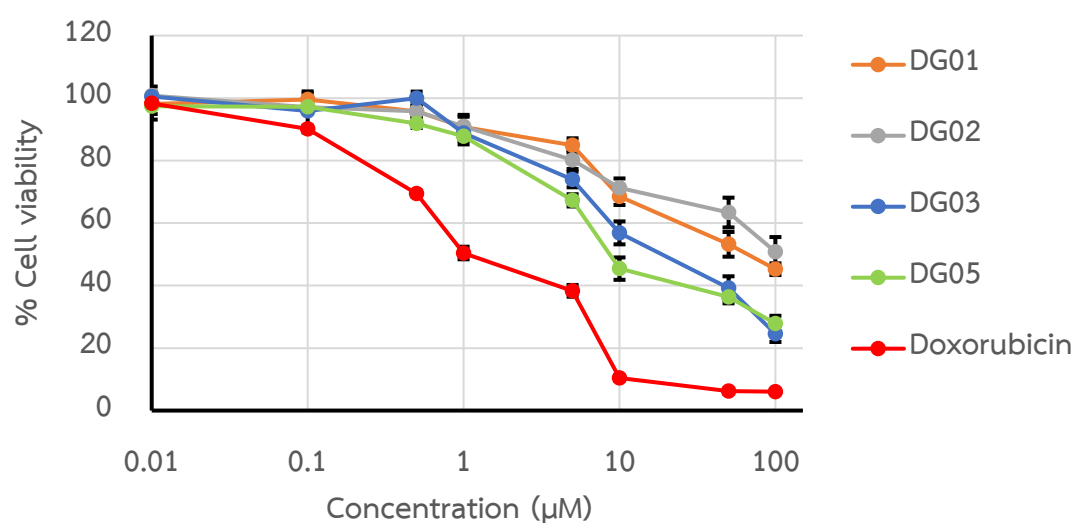


**Figure 32.** Cytotoxicity of tested compounds on Jurkat T cells

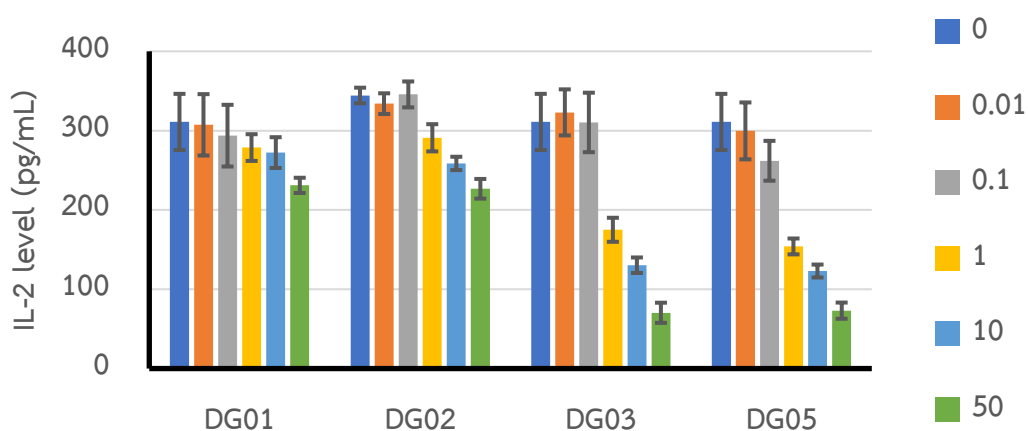


**Figure 33.** Effects of tested compounds on Jurkat T cells stimulated with anti-CD3/CD28 antibodies

All the tested compounds did not exhibit significant cytotoxicity on Jurkat T cells at a concentration range of 0-1  $\mu\text{M}$ . A decrease in the IL-2 level observed in this range was possibly due to direct inhibitory effect of the compounds, while that observed at a concentration more than 1  $\mu\text{M}$  could be a result of the cytotoxicity. At a concentration of 1  $\mu\text{M}$ , the lupane-type triterpenoids, DG03 and DG05, exhibited noticeably greater effects than the friedelane-type triterpenoids, DG01 and DG02, suggesting the possible relationship between the structural type of triterpenoids and the activity.

## CHAPTER V

### CONCLUSION

Investigation on chemical constituents of *Diospyros gracilis* stem has revealed six pentacyclic triterpenoids. These triterpenoids were identified to be friedelin and epifriedelanol, classified under the friedelane type, and lupeol, betulin, betulinic acid, and betulinaldehyde of the lupane type. The occurrence of the six compounds in *Diospyros* genus and their biological activities have been well-documented in the scientific literature. Nonetheless, this is the first report on phytochemical constituents of *D. gracilis*.

Friedelin, epifriedelanol, lupeol, betulin, and betulinic acid were investigated for cytotoxic activity on glioblastoma U87 cells and breast cancer MDA-MB231 cells. The lupane-type triterpenoids exhibited greater effects than the friedelane-type triterpenoids, especially on the glioblastoma U87 cells for which their significant effects were demonstrated. However, this activity of all the compounds was not selective as their IC<sub>50</sub> values for glioblastoma U87 cells were very close to those for the normal cells.

Friedelin, epifriedelanol, lupeol, and betulinic acid were evaluated for inhibitory activity on T cell activation, mediated by CD3 and CD28, in Jurkat T cells. The results indicated that the lupane-type triterpenoids exhibited greater inhibitory effects on IL-2 production in activated T cells than the friedelane-type triterpenoids at a concentration of 1  $\mu$ M, which was a non-cytotoxic concentration.



## REFERENCES

- Adu, O. T., Naidoo, Y., Lin, J., Adu, T. S., Sivaram, V., Dewir, Y. H., and El-Banna, A. N. (2022). Phytochemical Screening and Biological Activities of *Diospyros villosa* (L.) De Winter Leaf and Stem-Bark Extracts. *Horticulturae*, 8(10), 945.
- Akihisa, T., Yamamoto, K., Tamura, T., Kimura, Y., Iida, T., Nambara, T., and Chang, F. C. (1992). Triterpenoid Ketones from *Lingnania chungii* McClure : Arborinone, Friedelin and Glutinone. *CHEMICAL & PHARMACEUTICAL BULLETIN*, 40(3), 789-791. <https://doi.org/10.1248/cpb.40.789>
- Ali-Seyed, M., Jantan, I., Vijayaraghavan, K., and Bukhari, S. N. A. (2016). Betulinic Acid: Recent Advances in Chemical Modifications, Effective Delivery, and Molecular Mechanisms of a Promising Anticancer Therapy. *Chemical Biology & Drug Design*, 87(4), 517-536. <https://doi.org/10.1111/cbdd.12682>
- Aljohny, B. O., Rauf, A., Anwar, Y., Naz, S., and Wadood, A. (2021). Antibacterial, Antifungal, Antioxidant, and Docking Studies of Potential Dinaphthodiospyrols from *Diospyros lotus* Linn. Roots. *ACS Omega*, 6(8), 5878-5885. <https://doi.org/10.1021/acsomega.0c06297>
- Aminin, D., and Polonik, S. (2020). 1,4-Naphthoquinones: Some Biological Properties and Application. *Chemical and Pharmaceutical Bulletin*, 68(1), 46-57. <https://doi.org/10.1248/cpb.c19-00911>
- Amiri, S., Dastghaib, S., Ahmadi, M., Mehrbod, P., Khadem, F., Behrouj, H., Aghanoori, M.-R., Machaj, F., Ghamsari, M., Rosik, J., Hudecki, A., Afkhami, A., Hashemi, M., Los, M. J., Mokarram, P., Madrakian, T., and Ghavami, S. (2020). Betulin and its derivatives as novel compounds with different pharmacological effects. *Biotechnology Advances*, 38, 107409. <https://doi.org/10.1016/j.biotechadv.2019.06.008>
- Aronsson, P., Munissi, J. J. E., Gruhonjic, A., Fitzpatrick, P. A., Landberg, G., Nyandoro, S. S., and Erdelyi, M. (2016). Phytoconstituents with Radical Scavenging and Cytotoxic Activities from *Diospyros shimbaensis*. *Diseases*, 4(1), 3.
- Bae, K. J., Lee, Y., Kim, S. A., and Kim, J. (2016). Plumbagin exerts an immunosuppressive

effect on human T-cell acute lymphoblastic leukemia MOLT-4 cells.

*Biochemical and Biophysical Research Communications*, 473(1), 272-277.

<https://doi.org/10.1016/j.bbrc.2016.03.092>

Bawazeer, S., and Rauf, A. (2021). In vitro antiglycation and lipoxygenase inhibition of naphthoquinones isolated from *Diospyros lotus* Linn. *South African Journal of Botany*, 143, 406-409. <https://doi.org/10.1016/j.sajb.2021.03.014>

Blanchard, B., Faustin, K., Yapi, T., Mathias, K., Tomi, F., and Félix, T. (2018). <sup>13</sup>C NMR Analysis: Terpenoids, Steroids and Carotenoid from *Diospyros soubreana* (Ebenaceae). 26, 1-7. <https://doi.org/10.9734/EJMP/2018/45230>

Boué, G. B., Kabran, F. A., Tomi, F., and Tonzibo, Z. F. (2018). A New Naphthalene Derivative with Unusual Furanose Sugar from the Leaves of *Diospyros soubreana* (Ebenaceae). *International Journal of Pharmaceutical Sciences Review and Research*, 49(1), 138-142. <https://hal.science/hal-02126827>

Bumroong, B., and Thanakijcharoenpath, W. (2016). Stilbenoids from the stem of *Diospyros collinsae*, the first evidence for the production of stilbene derivatives in ebenaceous plants. *Thai Journal of Pharmaceutical Sciences*, 40, 185-189.

Cesari, I., Hoerle, M., Simoes-Pires, C., Grisoli, P., Queiroz, E. F., Dacarro, C., Marcourt, L., Moundipa, P. F., Carrupt, P. A., Cuendet, M., Caccialanza, G., Wolfender, J. L., and Brusotti, G. (2013). Anti-inflammatory, antimicrobial and antioxidant activities of *Diospyros bipindensis* (Gurke) extracts and its main constituents. *J Ethnopharmacol*, 146(1), 264-270. <https://doi.org/10.1016/j.jep.2012.12.041>

Choi, J., Cho, J. Y., Kim, Y. D., Htwe, K. M., Lee, W. S., Lee, J. C., Kim, J., and Yoon, K. D. (2015). Phenolic compounds and triterpenes from the barks of *Diospyros burmanica*. *Natural Product Sciences*, 21, 76-81.

Deng, Z.-T., Yang, T.-H., Huang, X.-Y., Chen, X.-L., Zhang, J.-G., Zhang, X.-M., Chen, J.-J., and Geng, C.-A. (2017). UFLC-MS-IT-TOF and Bioassay Guided Isolation of Flavonoids as Xanthine Oxidase Inhibitors from *Diospyros dumetorum*. *Natural Product Communications*, 12, 1713-1715. <https://doi.org/10.1177/1934578X1701201113>

Dev, M. J., and Rajarajeshwari, N. (2013). Phytoconstituents isolated from *Diospyros oocarpa* Thwaitist. *Asian Journal of Biomedical and Pharmaceutical Sciences*, 3,

50-54.

- Dongmo, J. d. d., Akak, C. M., Tala, M. F., Kedi, P. B. E., Azebaze, A. G. B., Vardamides, J. C., and Laatsch, H. (2018). Longiflorol, a bergenin  $\alpha$ -D-apioside from the stem bark of *Diospyros longiflora*, and its antioxidant activity. *Zeitschrift für Naturforschung B*, 73(8), 539-543. <https://doi.org/doi:10.1515/znb-2018-0019>
- Dzubak, P., Hajdich, M., Vydra, D., Hustova, A., Kvasnica, M., Biedermann, D., Markova, L., Urban, M., and Sarek, J. (2006). Pharmacological activities of natural triterpenoids and their therapeutic implications. *Natural Product Reports*, 23(3), 394-411. <https://doi.org/10.1039/B515312N>
- Fareed, N., El-Kersh, D. M., Youssef, F. S., and Labib, R. M. (2022). Unveiling major ethnopharmacological aspects of genus *Diospyros* in context to its chemical diversity: A comprehensive overview. *Journal of Food Biochemistry*, 46(12), e14413. <https://doi.org/10.1111/jfbc.14413>
- Feng, A., Yang, S., Sun, Y., Zhang, L., Bo, F., and Li, L. (2020). Development and Evaluation of Oleanolic Acid Dosage Forms and Its Derivatives. *BioMed Research International*, 2020, 1308749. <https://doi.org/10.1155/2020/1308749>
- Feusso, H. M. F., Akak, C. M., Tala, M. F., Azebaze, A. G. B., Tsabang, N., Vardamides, J. C., and Laatsch, H. (2016). Conocarpol, a new cycloartane triterpenoid from *Diospyros conocarpa*. *Zeitschrift für Naturforschung B*, 71(9), 935-940. <https://doi.org/10.1515/znb-2016-0059>
- Feusso, H. M. F., Dongmo, J. d. D., Akak, C. M., Lateef, M., Ahmed, A., Azebaze, A. G. B., Waffo, A. F. K., Ali, M. S., and Vardamides, J. C. (2019). Biological activities of the methanolic extracts and compounds from leaves and twigs of *Diospyros zenkeri* (Gürke) F. White (Ebenaceae). *Trends in Phytochemical Research*, 3(2), 117-122.
- Feusso, H. M. F., Dongmo, J. d. D., Djomkam, H. L. M., Akak, C. M., Lateef, M., Ahmed, A., Azebaze, A. G. B., Waffo, A. F. K., Ali, M. S., and Vardamides, J. C. (2020). Chemicals constituents from leaves of *Diospyros iturensis* (Gurke) Letouzey & F. White and their biological activities. *Natural Product Sciences*, 26(4), 311-362.
- Feusso, H. M. F., Mvot Akak, C., Feussi Tala, M., Azebaze, A. G. B., Vardamides, J. C., and Laatsch, H. (2017). Mannic acid, a new *ent*-kaurane dimer diterpenoid and other chemical constituents from different parts of *Diospyros mannii*. *Biochemical*

- Systematics and Ecology*, 74, 51-56. <https://doi.org/10.1016/j.bse.2017.09.001>
- Gallo, M. B. C., and Sarachine, M. J. (2009). Biological Activities of Lupeol. *Int. J. Biomed. Pharm. Sci*, 3(1), 46-66.
- Ha, N. T. T., Cuong, P. V., Tra, N. T., Tuyen, N. V., Anh, L. T. T., Cham, B. T., and Son, N. T. (2020). Cytotoxic naphthoquinones from *Diospyros fleuryana* leaves. *Discovery Phytomedicine - Journal of Natural Products Research and Ethnopharmacology*, 7(1), 42-46. <https://doi.org/10.15562/phytomedicine.2020.117>
- Higa, M., Takashima, Y., Yokaryo, H., Harie, Y., Suzuka, T., and Ogihara, K. (2017). Naphthoquinone Derivatives from *Diospyros maritima*. *Chemical and Pharmaceutical Bulletin*, 65(8), 739-745. <https://doi.org/10.1248/cpb.c17-00178>
- Hordyjewska, A., Ostapiuk, A., Horecka, A., and Kurzepa, J. (2019). Betulin and betulinic acid: triterpenoids derivatives with a powerful biological potential. *Phytochemistry Reviews*, 18(3), 929-951. <https://doi.org/10.1007/s11101-019-09623-1>
- Jiang, W., Li, X., Dong, S., and Zhou, W. (2021). Betulinic acid in the treatment of tumour diseases: Application and research progress. *Biomedicine & Pharmacotherapy*, 142, 111990. <https://doi.org/10.1016/j.biopha.2021.111990>
- Kim, K. S., Lee, D. S., Kim, D. C., Yoon, C. S., Ko, W., Oh, H., and Kim, Y. C. (2016). Anti-Inflammatory Effects and Mechanisms of Action of Coussaric and Betulinic Acids Isolated from *Diospyros kaki* in Lipopolysaccharide-Stimulated RAW 264.7 Macrophages. *Molecules*, 21(9), 1206.
- Lenta, B., Ngamgwe, R., Kamdem, L., Ngatchou, J., Tantangmo, F., Antheaume, C., Kaiser, M., Silvere, N., Tsamo, E., and Sewald, N. (2015). Compounds from *Diospyros canaliculata* (Ebenaceae) and their Antiparasitic Activities. *International Research Journal of Pure and Applied Chemistry*, 6, 56-65. <https://doi.org/10.9734/IRJPAC/2015/15267>
- Li, H., Webster, D., Johnson, J. A., and Gray, C. A. (2015). Anti-mycobacterial triterpenes from the Canadian medicinal plant *Alnus incana*. *Journal of Ethnopharmacology*, 165, 148-151. <https://doi.org/10.1016/j.jep.2015.02.042>
- Mori-Yasumoto, K., Izumoto, R., Fuchino, H., Ooi, T., Agatsuma, Y., Kusumi, T., Satake, M.,

- and Sekita, S. (2012). Leishmanicidal activities and cytotoxicities of bisnaphthoquinone analogues and naphthol derivatives from Burman *Diospyros burmanica*. *Bioorganic & Medicinal Chemistry*, 20(17), 5215-5219.  
<https://doi.org/10.1016/j.bmc.2012.06.055>
- Mullauer, F. B., Kessler, J. H., and Medema, J. P. (2010). Betulinic acid, a natural compound with potent anticancer effects. *Anti-Cancer Drugs*, 21(3), 215-227.  
<https://doi.org/10.1097/CAD.0b013e3283357c62>
- Njanpa, C. A. N., Wouamba, S. C. N., Yamthe, L. R. T., Dize, D., Tchatat, B. M. T., Tsouh, P. V. F., Poufofo, M. N., Jouda, J. B., Ndjakou, B. L., Sewald, N., Kouam, S. F., and Boyom, F. F. (2021). Bio-guided isolation of anti-leishmanial natural products from *Diospyros gracilescens* L. (Ebenaceae). *BMC Complementary Medicine and Therapies*, 21(1), 106. <https://doi.org/10.1186/s12906-021-03279-1>
- Peyrat, L.-A., Eparvier, V., Eydoux, C., Guillemot, J.-C., Litaudon, M., and Stien, D. (2017). Betulinic Acid, The First Lupane-Type Triterpenoid Isolated from Both a *Phomopsis* sp. and Its Host Plant *Diospyros carbonaria* Benoist. *Chemistry & Biodiversity*, 14(1), e1600171. <https://doi.org/10.1002/cbdv.201600171>
- Peyrat, L.-A., Eparvier, V., Eydoux, C., Guillemot, J.-C., Stien, D., and Litaudon, M. (2016). Chemical diversity and antiviral potential in the pantropical *Diospyros* genus. *Fitoterapia*, 112, 9-15. <https://doi.org/10.1016/j.fitote.2016.04.017>
- Phengklai, C. (1981). Ebenaceae. In T. Smitinand & K. Larsen (Eds.), *Flora of Thailand* (Vol. 2, pp. 281-392). Tistr press.
- Pironi, A. M., de Araújo, P. R., Fernandes, M. A., Salgado, H. R. N., and Chorilli, M. (2018). Characteristics, Biological Properties and Analytical Methods of Ursolic Acid: A Review. *Critical Reviews in Analytical Chemistry*, 48(1), 86-93.  
<https://doi.org/10.1080/10408347.2017.1390425>
- Pooma, R., and Suddee, S. (2014). *Thai plant names Tem Smitinand revised* (2014 ed.).  
<https://botany.dnp.go.th/mplant/index.html>
- POWO. (2023). *Diospyros* L. | *Plants of the World Online* | Kew Science.  
<http://powo.science.kew.org/taxon/urn:lsid:ipni.org:names:326017-2>
- Priya, S., Nethaji, S., and Sindhuja, B. (2014). GC-MS analysis of some bioactive constituents of *Diospyros virginiana*. *Research Journal of Pharmacy and*

*Technology*, 7, 429-432.

- Radi, M. H., El-Shiekh, R. A., El-Halawany, A. M., and Abdel-Sattar, E. (2023). Friedelin and 3 $\beta$ -Friedelinol: Pharmacological Activities. *Revista Brasileira de Farmacognosia*, 33(5), 886-900. <https://doi.org/10.1007/s43450-023-00415-5>
- Rahman, M. M., Islam, M. R., Akash, S., Shohag, S., Ahmed, L., Supti, F. A., Rauf, A., Aljohani, A. S. M., Al Abdulmonem, W., Khalil, A. A., Sharma, R., and Thiruvengadam, M. (2022). Naphthoquinones and derivatives as potential anticancer agents: An updated review. *Chemico-Biological Interactions*, 368, 110198. <https://doi.org/10.1016/j.cbi.2022.110198>
- Rasamison, V. E., Rakotondraibe, H. L., Razafintsalama, V. E., Rakotonandrasana, S. R., Rakotondrafara, A., Ratsimbason, M. A., and Rafidinarivo, E. (2016). Chemical constituents from stems and leaves of *Diospyros gracilipes* Hiern and the antimicrobial and cytotoxic principles. *Journal of Pharmacognosy and Phytochemistry*, 5, 109-113.
- Rashed, K., Ćirić, A., Glamočlija, J., and Soković, M. (2014). Antibacterial and antifungal activities of methanol extract and phenolic compounds from *Diospyros virginiana* L. *Industrial Crops and Products*, 59, 210-215. <https://doi.org/10.1016/j.indcrop.2014.05.021>
- Rauf, A., Abu-Izneid, T., Rashid, U., Alhumaydhi, F. A., Bawazeer, S., Khalil, A. A., Aljohani, A. S. M., Abdallah, E. M., Al-Tawaha, A. R., Mabkhot, Y. N., Shariati, M. A., Plygun, S., Uddin, M. S., and Ntsefong, G. N. (2020). Anti-inflammatory, Antibacterial, Toxicological Profile, and *In Silico* Studies of Dimeric Naphthoquinones from *Diospyros lotus*. *BioMed Research International*, 2020, 7942549. <https://doi.org/10.1155/2020/7942549>
- Rauf, A., Uddin, G., Patel, S., Khan, A., Halim, S. A., Bawazeer, S., Ahmad, K., Muhammad, N., and Mubarak, M. S. (2017). *Diospyros*, an under-utilized, multi-purpose plant genus: A review. *Biomedicine & Pharmacotherapy*, 91, 714-730. <https://doi.org/10.1016/j.biopha.2017.05.012>
- Rauf, A., Uddin, G., Siddiqui, B. S., Molnár, J., Csonka, Á., Ahmad, B., Szabó, D., Farooq, U., and Khan, A. (2015). A Rare Class of New Dimeric Naphthoquinones from *Diospyros lotus* have Multidrug Reversal and Antiproliferative Effects. *Frontiers in*



*Pharmacology*, 6. <https://doi.org/10.3389/fphar.2015.00293>

- Reynolds, W. F., McLean, S., Poplawski, J., Enriquez, R. G., Escobar, L. I., and Leon, I. (1986). Total assignment of  $^{13}\text{C}$  and  $^1\text{H}$  spectra of three isomeric triterpenol derivatives by 2D NMR: an investigation of the potential utility of  $^1\text{H}$  chemical shifts in structural investigations of complex natural products. *Tetrahedron*, 42(13), 3419-3428. [https://doi.org/10.1016/S0040-4020\(01\)87309-9](https://doi.org/10.1016/S0040-4020(01)87309-9)
- Ribeiro, A., Serrano, R., da Silva, I. B. M., Gomes, E. T., Pinto, J. F., and Silva, O. (2023). The Genus *Diospyros*: A Review of Novel Insights into the Biological Activity and Species of Mozambican Flora. *Plants*, 12(15), 2833.
- Salazar, G. M., Silva, G. D. F., Duarte, L. P., Vieira Filho, S. A., and Lula, I. S. (2000). Two epimeric friedelane triterpenes isolated from *Maytenus truncata* Reiss:  $^1\text{H}$  and  $^{13}\text{C}$  chemical shift assignments. *Magnetic Resonance in Chemistry*, 38, 977-980.
- Sharma, A., Sharma, T., Singh, R., Payal, P., Gupta, R., and Sharma, M. (2018). A novel compound Lup-20 (29)-ene-3 $\alpha$ ,6 $\beta$ -diol identified in petroleum ether extract of *Diospyros melanoxylon* Roxb. leaves and to reveal its antidiabetic activity in rats. *Pharmacognosy Magazine*, 14(55), S245-S248. [https://doi.org/10.4103/pm.pm\\_429\\_17](https://doi.org/10.4103/pm.pm_429_17)
- Sharma, V. (2017). *Diospyros montana* Roxb.: A source of 1,4-naphthoquinone dimers counting diospyrin esters. *IOSR Journal of Applied Chemistry*, 10, 25-26. <https://doi.org/10.9790/5736-1001012526>
- Siddiqui, S., Hafeez, F., Begum, S., and Siddiqui, B. S. (1988). Oleanderol, a New Pentacyclic Triterpene from the Leaves of *Nerium oleander*. *Journal of Natural Products*, 51(2), 229-233. <https://doi.org/10.1021/np50056a006>
- Somat, N. A., Yusoff, Z., and Osman, C. P. (2020). Chemical Constituents from *Diospyros discolor* Willd. and their Acetylcholinesterase Inhibitory Activity. *Pharmacognosy Journal*, 12(6s), 1547-1551. <https://doi.org/10.5530/pj.2020.12.212>
- Suchaichit, N., Suchaichit, N. P., Kanokmedhakul, K., Boottanun, P., Sermswan, R. W., Moosophon, P., and Kanokmedhakul, S. (2021). A new cytotoxic plumbagin derivative from roots of *Diospyros undulata*. *Natural Product Research*, 35(10), 1605-1612. <https://doi.org/10.1080/14786419.2019.1630120>
- Suchaichit, N. P., Suchaichit, N., Kanokmedhakul, K., Poopasit, K., Moosophon, P., and

- Kanokmedhakul, S. (2018). Two new naphthalenones from *Diospyros undulata* stem bark and their cytotoxic activity. *Phytochemistry Letters*, 24, 132-135. <https://doi.org/10.1016/j.phytol.2018.02.008>
- Suwama, T., Watanabe, K., Monthakantirat, O., Luecha, P., Noguchi, H., Watanabe, K., and Umehara, K. (2018). Naphthalene glycosides in the Thai medicinal plant *Diospyros mollis*. *Journal of Natural Medicines*, 72(1), 220-229. <https://doi.org/10.1007/s11418-017-1134-1>
- Tameye, N. S. J., Akak, C. M., Happi, G. M., Frese, M., Stammler, H. G., Neumann, B., Lenta, B. N., Sewald, N., and Nkengfack, A. E. (2020). Antioxidant norbergenin derivatives from the leaves of *Diospyros gilletii* De Wild (Ebenaceae). *Phytochemistry Letters*, 36, 63-67. <https://doi.org/10.1016/j.phytol.2020.01.012>
- Tameye, N. S. J., Akak, C. M., Tabekoueng, G. B., Mkounga, P., Bitchagno, G. T. M., Lenta, B. N., Sewald, N., and Nkengfack, A. E. (2022). Chemical constituents from *Diospyros fragrans* Gürke (Ebenaceae). *Biochemical Systematics and Ecology*, 100, 104373. <https://doi.org/10.1016/j.bse.2021.104373>
- Thanakijcharoenpath, W., and Theanphong, O. (2007). Triterpenoids from the stem of *Diospyros glandulosa*. *The Thai Journal of Pharmaceutical Sciences*, 31(1), 1-8.
- Theerachayanan, T., Sirithunyalug, B., and Piyamongkol, S. (2007). Antimalarial and antimycobacterial activities of dimeric Naphthoquinone from *Diospyros glandulosa* and *Diospyros rhodocalyx*. 6(2), 253-259.
- Uc-Cachón, A. H., Borges-Argáez, R., Said-Fernández, S., Vargas-Villarreal, J., González-Salazar, F., Méndez-González, M., Cáceres-Farfán, M., and Molina-Salinas, G. M. (2014). Naphthoquinones isolated from *Diospyros anisandra* exhibit potent activity against pan-resistant first-line drugs *Mycobacterium tuberculosis* strains. *Pulmonary Pharmacology & Therapeutics*, 27(1), 114-120. <https://doi.org/10.1016/j.pupt.2013.08.001>
- Uddin, G., Rauf, A., Siddiqui, B. S., Muhammad, N., Khan, A., and Shah, S. U. A. (2014). Anti-nociceptive, anti-inflammatory and sedative activities of the extracts and chemical constituents of *Diospyros lotus* L. *Phytomedicine*, 21(7), 954-959. <https://doi.org/10.1016/j.phymed.2014.03.001>
- Utsunomiya, N., Subhadrabandhu, S., Yonemori, K., Oshida, M., Kanzaki, S., Nakatsubo,



F., and Sugiura, A. (1998). *Diospyros* species in Thailand: Their distribution, fruit morphology and uses. *Economic Botany*, 52(4), 343-351.

<https://doi.org/10.1007/BF02862064>

Wisetsai, A., Schevenels, F. T., and Lekphrom, R. (2021). Chemical constituents and their biological activities from the roots of *Diospyros filipendula*. *Natural Product Research*, 35(16), 2739-2743. <https://doi.org/10.1080/14786419.2019.1656630>

Wosawat, P., Senawong, T., Suchaichit, N., Suchaichit, N. P., Kanokmedhakul, K., Kanokmedhakul, S., and Moosophon, P. (2021). Cytotoxic compounds from the stems of *Diospyros ehretioides* and their bioactivity. *Natural Product Research*, 35(23), 4922-4929. <https://doi.org/10.1080/14786419.2020.1749610>

Zhang, Y., Zhao, L., Huang, S.-W., Wang, W., and Song, S.-J. (2018). Triterpene saponins with neuroprotective effects from the leaves of *Diospyros kaki* Thunb. *Fitoterapia*, 129, 138-144. <https://doi.org/10.1016/j.fitote.2018.06.023>





จุฬาลงกรณ์มหาวิทยาลัย  
**CHULALONGKORN UNIVERSITY**

## VITA

**NAME** Somnathakit Wuttikit

**DATE OF BIRTH** 3 October 1996

**PLACE OF BIRTH** Chanthaburi, Thailand

**INSTITUTIONS ATTENDED** Bachelor of Science (Botany), Faculty of Science, Kasetsart University

**HOME ADDRESS** Chanthaburi, Thailand

**PUBLICATION** Wuttikit, S. and Thanakijcharoenpath, W. Isolation and Characterization of Triterpenoids from the Stem of *Diospyros gracilis*. IOP Conference Series: Earth and Environmental Science, 1139(1), 012001.